2005

Electromechanical Characterization of Poly(Dimethyl Siloxane) Based Electroactive Polymers

Wrutu Deepak Parulkar
Virginia Commonwealth University

TO MY LOVING SISTER

LATE MRS.SHILPA S MUTHA

ELECTROMECHANICAL CHARACTERISATION OF POLY (DIMETHYL SILOXANE) BASED ELECTROACTIVE POLYMER

A Dissertation submitted in partial fulfillment of the requirements for the degree of Masters of Engineering at Virginia Commonwealth University.

by

WRUTU DEEPAK PARULKAR
Bachelors of Engineering, Cummins College of Engineering for Women, India, 2002
Master's of Engineering, Virginia Commonwealth University, 2005

Director: DR. ZOUBEIDA OUNAIES
ASSISTANT PROFESSOR, MECHANICAL ENGINEERING

Virginia Commonwealth University
Richmond, Virginia
December 2005

Acknowledgement

I would like to thank my advisor Dr. Zoubeida Ounaies for the many productive discussions and continuous support financially as well as professionally. I would like to extend my thanks to Dr. Karla Mossi for the encouragement and help she rendered to me. I would like to thank Dr. Daniel Resseler for sparing his valuable time and assessing my work.

Special thanks to five most important persons of my life, without whom I would have never reached the stage of successful completion of my Masters. Firstly my loving parents Mrs. Disha Parulkar and Mr. Deepak Parulkar who have been my guru as well as a strong supportive power behind me. Secondly I would like to acknowledge my two adoring sisters Purva and Megha, who have been very enthusiastic and caring in every decision I made. And last but not the least I am immensely grateful to my fiancé Harshad Shanbhag, who has been so kind and given me the encouragement and new perspective of life.

Finally I would like to thank all my laboratory friends and colleagues, who have been so kind to me, during difficulties. A special thanks to Sumanth to be my guide and tolerating me during my final semester. I would be always thankful to Ihab and Qiao, who have been so kind and helping to me during my two years away from home.

Table of Contents

Page

List of Tables

Page

List of Figures

Page

Abstract

ELECTROMECHNICAL CHARACTERISATION OF POLY (DIMETHYL SILOXANE)

BASED ELECTROACTIVE POLYMER

By Wrutu Deepak Parulkar, ME

A Dissertation submitted in partial fulfillment of the requirements for the degree of Masters of Engineering at Virginia Commonwealth University.

Virginia Commonwealth University, 2005

Major Director: Dr. Zoubeida Ounaies
Assistant Professor, Mechanical Engineering

The main objectives of this thesis are 1) to evaluate the effect of cross-linking polar cyano phenyl (CN) groups on poly (dimethyl siloxane) (PDMS) and 2) to characterize the electromechanical properties of the resulting CN-PDMS blend as an electroactive actuator. Materials responding to an external stimulus are referred to as electroactive materials. There are several phenomena, which govern the mechanism in these materials, such as piezoelectricity, Maxwell's effect, ferroelectricity, electrostriction to name a few. These electroactive materials can be employed in several applications such as biomedical devices,

robots, MEMs, aerospace vehicles, where the application is governed by the specific mechanism. However in order for the materials to be used effectively, they need to be thoroughly characterized to understand their behavior under factors like electric field, temperature, frequency and time.

The present work focuses on developing an electroactive actuator, which has tailorable properties, allowing a wide operational temperature window from -100 °C to 200 °C and stability in harsh conditions.

The characterization of the CN-PDMS polymer blend is done in two folds. First the physical properties of the polymer system are characterized by performing tests such as Dielectric Spectroscopy, Differential Scanning Calorimetery and Thermally Stimulated Current measurement. These techniques offer complete understanding of the structure-property relationship and effects of the functional groups on the dielectric and relaxation behavior of the polymer. The Dielectric Spectroscopy and the Thermally Stimulated Current analysis are used to elucidate the primary and the secondary relaxations, such as molecular mobility, interfacial polarization and dipolar relaxation.

Dielectric Spectroscopy reveals that the molecular weight of PDMS does not affect the dielectric permittivity of the polymer blend. Also, Dielectric Spectroscopy clarifies the role of the CN polar group in the polarization of the CN-PDMS blend, inducing electromechanical strain in the polymer blend through electrostriction.

The Differential Scanning Calorimetery is used to quantify the thermal behavior of the CN-PDMS polymer blend by quantifying properties such as melting temperature (T_m) and re-crystallization temperature of the PDMS polymer cross-linked with CN functional

group. Results reveal that the thermal characteristics of the blend are not affected when PDMS is cross-linked with the functional CN moieties, meaning CN-PDMS maintains the advantages of PDMS in terms of stability towards harsh conditions, wide operating temperature and resistance to ultraviolet radiations.

Following the physical characterization, electromechanical characterization of the CN-PDMS polymer blend is done to assess the electromechanical strain induced in the blend in response to electric field. The electromechanical strain is studied in two configurations; the electromechanical strain induced along the length of the polymer blend and induced through the thickness of the blend. These strain measurements are performed by applying both direct current as well as alternating current electric fields, and the induced electromechanical strain is studied as a function of amplitude and frequency of the electric field as well as the time of application of the electric field.

The mechanism behind the development of the electromechanical strain and the nature of the strain under electric field is elucidated. The performance of the electroactive polymer is compared with several other polymeric actuators such as PVDF and PVDF-TrFE, polyurethane based actuators and ionomers. Comparison gives favorable results in terms of strains. In addition, CN-PDMS polymer system has the advantage of allowing control of processing of the blend, which is not present in all the other commercial electroactive polymers. The maximum electromechanical strain yielded along the length of the CN-PDMS polymer blend is 1.74 % when an electric field of 0.2MV/m is applied along the length of the polymer. Through the thickness, the maximum induced strain is 0.12 % for an electric field of 0.8 MV/m. Based on the nature of the strain yielded it is

observed that the strain induced in the CN-PDMS blend is consistently proportional to the square of the electric field (E^2). Moreover, the strain is driven by the concentration of the dipolar moieties (CN) present in the polymer blend.

All the above-mentioned techniques used for thermal and electromechanical characterization of the CN-PDMS polymer blend illustrate the electrostrictive nature of the polymer under the study.

CHAPTER 1 INTRODUCTION

1.1 Electroactive Polymers And Their Applications

This thesis entails the physical understanding and the electromechanical characterization of electrostrictive polymeric actuators. The polymers considered in this work are insulating, rubber-like structures which respond to electric stimuli by undergoing mechanical deformation at microscopic as well as macroscopic level.

New avenues in engineering and science need novel materials that provide maneuverability in applications ranging from biomedical to MEMS to aerospace. Ability of these new materials to have structural integrity and at the same time offer features such as sensing and actuation make these materials multifunctional. Some electroactive polymers fit the mold of multifunctionality. However multifunctionality offered by the materials is not the only important factor; at the same time the materials should be coupled with other factors like ease in processing, efficient availability, and physical stability.

Electroactive polymers (EAPs) are polymeric materials, which respond to electric stimuli by undergoing change in one or more properties. EAPs have attracted attention due to their excellent functionalities and mechanical properties, which are key factors in almost all fields ranging from space applications to the commercial world spanning from biomedical applications to telecommunication.

Nature is the greatest source of inspiration in engineering and science, one of the paradigms being the electroactive materials, whose applications are greatly inspired by nature. The natural muscle is a phenomenal example of engineering. The movement of blood within the body triggers the contraction/expansion of muscles to generate energy. This principle is exploited to develop artificial muscles. The EAPs are referred by many researchers in the field of active materials as the artificial muscles. This is due to the functional similarity between the EAP and the natural muscles, whereby the polymeric actuator mimics the natural muscle by providing linear motion similar to that seen in the latter. Thus the introduction of new polymeric materials that are more supple and responsive, or materials that offer tremendous performance yet require little energy, have the ability to duplicate the function of natural muscles. Though natural muscle surpasses the artificial muscles in many aspects, several other features of the natural muscles like controlled motion and adaptable stiffness to suit the applications can be emulated in order to reinforce the artificial muscle/EAP designing and applications.

Fundamentally, EAPs are characterized by several mechanisms such as piezoelectricity, ferroelectricity, pyroelectricity or electrostriction. These mechanisms govern the behavior and nature of response of every EAP material. It is these phenomena, which result into the actuating and/or the sensing capability of the polymer materials. Thus the electroactive response can take one or more of several forms, such as physical deformation under applied voltage as in case of piezoelectric and electrostrictive materials, or a change in optical properties as seen in electroluminescent or photo luminescent materials where the applied stimulus is electric field and the response is in the form of light

emission, or a change in magnetic properties in material such as seen in magnetostrictive EAPs[1]. The EAPs, which respond by showing a change at the molecular level of the material or by mechanical response such as bending or expanding, can be divided into two categories: electronic EAPs and ionic EAPs. Examples of ionic EAPs are ionomers, conductive polymers, and carbon nanotubes while EAPs, which fall under the category of electronic EAPs, are dielectric elastomers, ferroelectric polymers, and electrostrictive polymers. The working principle common to all these EAPs briefly follows.

1.2 Current Trends In EAP

EAPs are not a recent discovery; in fact several reports on EAPs are available from early 1800[2]. The start of this field can be trailed back to 1880 when Roentgen conducted an experiment on a rubber band with one end fixed and a mass attached to the free-end. The rubber band was studied as it was loaded and unloaded resulting into charging and discharging of the rubber band. The same experiment was further followed by another study in 1899 by Sacerdote, where he studied the strain response of rubber-band to an electric field[3]. Another report on the polarizability of materials was done in 1892 when Heaviside postulated that certain waxes have the ability to form permanently polarized dielectrics, when they are allowed to solidify from the molten stage in the presence of electric field[4]. Around the same era, the Curie brothers conducted an experiment on crystals of quartz, Rochelle salt and tourmaline, where they measured charge developed on the surface of these crystals when these crystals were subjected to mechanical stress. This phenomenon was named ‘piezoelectricity’ meaning Pressure-electricity. They observed

that mechanical stress was converted into electricity and referred it as the 'direct effect'. The 'converse effect' manifests when the application of electricity yields mechanical stress; it was introduced by Lippman in 1881, when he mathematically deduced this property using thermodynamics fundamentals[5].

In early 1900, Fukada recorded another phenomenon of EAP. By applying an electric field of about 1.5 MV/m to a molten mixture of carnauba wax, resin and bee wax at about 130°C and further analyzing the behavior, he discovered that permanently charged dielectrics had developed. This was the first report of piezoelectricity in polymers in 1924[6]. Thus by the mid 1900s, it was well established that molecules containing permanent dipole moments orient in the direction of the electric field when the dipoles have maximum mobility in the liquid state. Upon solidification of the material, the dipoles lose mobility and are then frozen in this orientation. The net dipole orientation is related to a phenomenon called Polarization[4]. In parallel with the detection of polarizability of waxes, polarizability was also reported in biopolymers. In 1950, Bazhenov observed piezoelectric effect in wood, where both the inverse as well as the direct piezoelectric effects were studied and reported. In 1953, an experiment carried out by Yasuda discovered that bending of bones produces electricity. The compressed and the elongated regions of the bone carry opposite charges, thus forming a callus in the vivo state[6]. This physiological significance of polarization of biopolymers was further enhanced when another phenomenon shown in collagen, again a biopolymer, was reported in early 1900s when electro-chemically coupled collagen filaments seemed to show deformation when placed in acidic solutions.

EAPs have opened a complete new arena for biomimetics and in the artificial intelligence stream. Recently an article titled "Biologically inspired Robots"[3] suggests biomimetic robots, which mimic the biological structures and inherently need muscle-like actuators for optimal functioning. The article also highlights that the EAP-based actuators may be used to eliminate the need for gears, bearings, and other components that complicate the construction of robots and are responsible to high costs, weight and premature failures. Most of the EAP materials show a viscoelastic behavior, which can potentially provide more lifelike aesthetics, vibration and shock dampening, and more flexible actuator configurations. Exploiting such properties of EAP materials may enable a conformably morphing skin to define the character of the robots and provide expressions, thus developing androids. In fact, several reports on employing EAP as a material to develop a human android have been presented by researchers at University of Pisa, Italy[7]. Another field in which EAPs have recently been employed is Bio-MEMS, where engineering is coupled with medical science to achieve micromanipulations of biological entities[8]. Recently EAPs have been preferred over other electroactive materials such as piezo- ceramics and magnetrostrictive materials usually found in MEMs devices. This is because EAPs offer high strain, lightweight, flexibility, and low cost. Also, they have good tolerance towards impact and due to their pliable nature, are resistant to fracture[9].This would make an all-polymer MEMs, having advantages such as flexibility, lightweight and avoiding the need for mechanical parts[10].

The working principle of each of the ionic as well as electronic EAP needs to be well understood and characterized as per the application requirements. Each of the

applications from robots to aerospace is EAP selective, i.e. every application exploits the principle on which a particular EAP works. For instance, owing to the structural and functional capability of conducting polymers, they are employed for several biomedical applications[11] such as drug-delivery systems and micro valves. Biomedical devices have certain specific requirements that pose constraints on the type of EAP that can be used to build the device. Devices like artificial sphincters and microsurgical instruments need to be very compact while at the same time need precision positioning in the body. They should have reasonably fast response time and should be damage–tolerant and most importantly should be biocompatible or else they may result into series of inflammatory reactions. Since these and similar other factors are present in each of the applications from medical sciences to electronics to aerospace, it becomes important to characterize the material to be employed.

1.3 Working Principles Of Ionic And Electronic EAPs

1.3.1 Ionic EAPs

Ionic EAPs are a branch of EAPs studied extensively for actuation as well as sensing since the 1900s[12]. The working principle of Ionic EAPs is ion transfer related. An initial report shows tests performed on commercially available Nafion material, which is a polymer made by DuPont and is a poly (tetrafluoroethylene) based ionomer. These first transducers, reported by Oguro (1992) and Segalman (1992) showed that mechanical deformation is produced when an electric field is applied across the thickness of a Nafion

membrane based transducer, thus demonstrating an ionic polymer actuator (See Figure 1.1). Ionic EAPs show deformation at very low voltage, on the order of 1-2 volts[13].

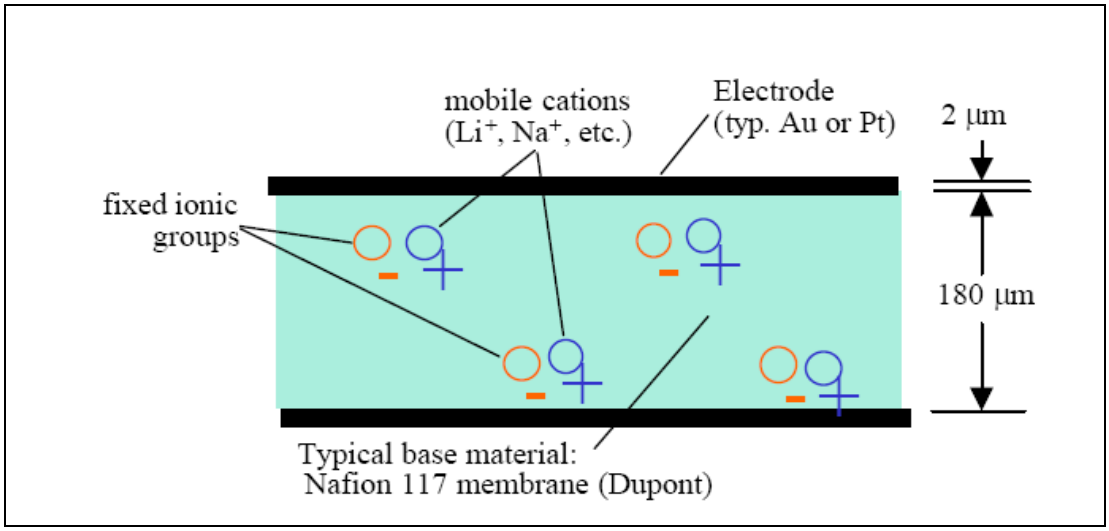

Figure 1.1: Cross-sectional view of a typical ionomers. (From refrence[12])

Ionomers are a subset of ionic EAPs, also known as Ionic Polymer Metal Composites (IPMC). They are ion-containing polymers sandwiched between metal plates. The most commonly studied ionic polymers are perfluorsulfonate polymers that contain small proportions of sulfonic or carboxylic ionic functional groups, for instance Nafion. Another perflournated polymer being used as ionomer is Flemion. In order to use ionomer as an artificial muscle, Nafion and/or Flemion can be produced in sheet geometry with positive counter ion (e.g., Na+ or Li+) contained in the matrix. Thus ionic polymer actuators are a class of electroactive polymers that can be formulated to have a range of electrical properties through the chemical composition and structure of the polymers. By

variations in the base matrix as well as by changing the mobile cationic groups in the base material, the actuation direction can be controlled.

In polymer gel, for instance in the case of a Nafion membrane based transducer, the membrane is sandwiched between two metal electrodes, and an electric field is applied to these metal electrodes as seen in Figure 1.1. Owing to the selective permeable nature of the ionomers, it allows only one-polarity ions to pass through while blocking others; this results into the bending/deformation of the ionomer.

These ionomers have an electro-chemical-mechanical coupling[14], which transduces the electrical energy into mechanical energy due to the ion transfer mechanism. This electro-chemical-mechanical coupling factor in ionomers is dependent on several aspects such as the morphology of the electrodes, water of diffusion, electrolyte used in the transducer configuration, level of hydration and to some extent electrostatic forces[15]. Substituting various alkali-metal like NA+, Li+ and alkyl-ammonium cations can enhance the actuation of these polymers[16]. Desirable magnitude of actuation can be obtained by incorporating various cations into the ionomers. By controlling the amount and type of the cations in the ionomers, various characteristics like response time, direction of bend, duration of displacement and magnitude of the displacement can be controlled. Recently there has been extensive research done by Donald Leo et al (2000) to get a mathematical model of the ionomers where they act as sensors as well as actuators. The actuation system utilizing ionic polymers have certain constrains such as slow response time, limited actuation and settling time varying from 5 to 30 seconds. In spite of certain excellent features shown by ionomers such as actuation under very low voltages, their major

drawback is that these ionic EAPs need to be constantly hydrated in order for efficient actuation. The material properties are also affected by factors like ionic constituents, temperature, wettablility which significantly obstruct the actuation mechanism of the inomers[17]. Also it is seen that although ionomers require very small amount of voltage for their actuation, these EAPs fail to sustain the induced strain under direct current electric field. Also the ionomers tend to be permanently damaged when they are exposed to a voltage beyond 5V. Electroding ionomers is another critical issue, as the ionomer is a very soft material with low compliance. Generally the material used for electroding tends to increase the stiffness of the over all actuator and reduces the induced strain. Further the response time of these polymers is low on the order of 5-20 seconds when a step field is applied[18], thus restricting the degree of actuation in the transducer.

Another ionic EAP, which is supposed to closely resemble natural muscle, is conducting polymer. In early 1976 it was discovered that polyacetylene, which is intrinsically a wide band-gap semi-conductor, achieved high conductivity to the order of 10^3 $ohm^{-1}cm^{-1}$ when doped with iodine[19]. Further it was realized that every conducting polymer contains an extended pi conjugated systems, formed by alternating single and double bonds along the polymer backbone. This pi bond could be delocalized by chemical oxidation or reduction process called doping, thus resulting into formation of a positive charge, which further makes the polymer conductive. For instance, in case of polypyrrole based EAP, when a positive potential is applied across the polymer membrane, the electrons are removed and the polymer undergoes oxidation. This introduction of positive

charge carriers make the polymer electrically conducting, which can be better understood from Figure 1.2[11].

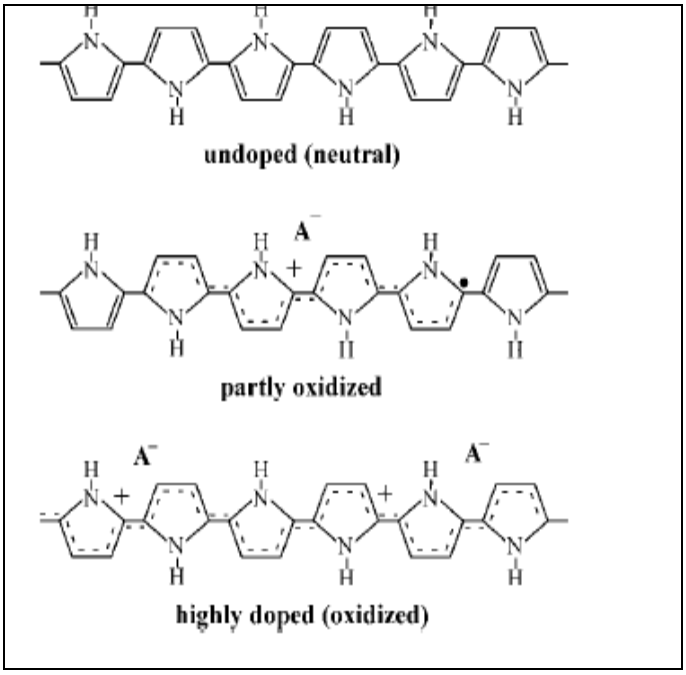

Figure 1.2: Polypyrrole at different oxidation state. (From reference[11])

In Figure 1.2, the A^- helps to maintain the charge neutrality in the oxidized state of this conducting polymer. The functioning of these polymers depends on the large electrochemical changes that take place from the electrochemical doping of various conducting polymers, most common being polypyrroles, polyanilines, polythiophenes and their derivatives. The polymer backbone loses or gains charge during the electrochemical oxidation reaction, which also forms a flux of ions to balance a charge[20] as seen in Figure 1.2. Thus the functioning of conducting polymers can be said to be analogous to the conducting polymer batteries where the electromechanical cycle of the polymer

corresponds to the charge-discharge-charge of these batteries. The oxidation and extraction of electrons from the polymer chains along with the new positive charges in near chains promotes high electrostatic repulsions. The chains move with conformational changes, the structure opens and the counter ions come into the polymer from the solution to maintain the electro-neutrality. Solvent molecules come in with ions too and the expansion of the polymer occurs. Both the amount of counter ions and the volume variation are controlled by the oxidation charge, which further controls the volume change, which can be stopped or inverted at any moment. This feature coupled with other operating factors like high tensile strength, large stresses and low operating voltages have made this EAP attractive[21] amongst other EAP materials. However despite of having many attractive features, conducting polymers have some flaws, which cannot be over looked. For instance, in case of polypyrrole, a commonly used polymer for making conductive actuators, in its oxidation state, it has a higher concentration of dopants, which affects the properties of the base polymer. Also the solvent current density and other polymerization conditions indirectly affect the life cycle of the actuator[21]. Similarly in case of polyaniline, the electroactivity is seen only in acids below pH 4 at which it can undergo oxidation/reduction, thus electro-chemical coupling in polyaniline is more complex compared to polypyrrole thereby accounting as polyaniline's drawback[11]. In more than 90% applications, when conducting polymer is used for actuation technology, they need an aqueous media as an electrolyte for actuation, thus leading to difficulty in employing these polymers in completely dry environments[22]. Further, the ion intercalation process on which the conducting polymers

depend limits the actuator life as well as the rate of actuation[23]. Also, increasing the electromechanical coupling is not easy, and moreover high strains cannot be yielded.

The most recent advancement in the field of active materials is the exploration of carbon nanotubes, which falls under the category of ionic electroactive polymer. These are rolled sheets of graphene with typically 1.2nm diameter[23] as seen in Figure 1.3. Their few nanometers diameter shows that they are not thicker than the typical molecule and their length can be several micrometers to even millimeters. These tubes are conductive or semi-conductive in nature. Structural analysis like X-ray of graphene shows that its honeycomb lattice structure expands if the graphene sheets are charged electrically. Since carbon nanotubes are nothing but rolled graphite sheets, quantum chemical calculations predict increase in the length of the carbon nanotube on application of electric field.

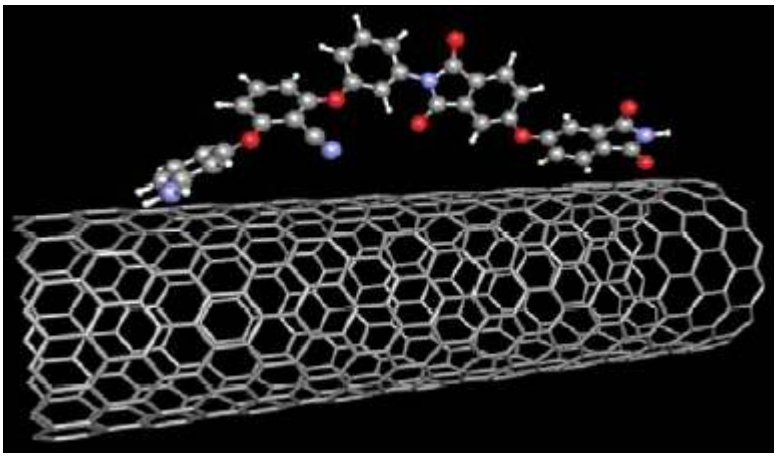

Figure 1.3: Graphical presentation of Carbon nanotube. (From reference[24])

Owing to the curvature and cylindrical symmetry of the carbon nanotubes they cause important modifications compared to planar graphite structures[25]. The single wall carbon nanotubes are capacitive in nature. Principle of actuation in single wall carbon

nanotube is similar to an electrochemical cell, where the porous sheet of SWNT forms the primary electrode. When an electric field is applied to the carbon nano tube, an electrical double layer is formed at the electrode/ electrolyte interface. Ions get attracted towards the nanotubes and are stored onto the surface of the nanotube. This ionic charge accumulation at the surface of the carbon nanotube is balanced by the electronic charges within the tube walls. This charging results in the rearrangement of the electronic structure of the nanotubes. The length of the C-C bond tends to increase during this process of electron injection. This rate at which the bond length undergoes change is related to the rate of charge injection and thus even the rate of actuation is related to the rate of charge injection[26, 27].

However CNT based actuators have certain drawbacks such as low strain rate as well as the need for an electrolyte for their actuation. Also the CNT actuators yield small to moderate strains of about 0.2 to 1% and in order for them to be employed, they need mechanical amplification[26]. This is paralleled with the relatively higher cost of the carbon nanotubes making the overall technology costly.

1.3.2 Electronic EAPs

Dielectric elastomers actuators (DEA) are a fairly new class of electronic EAP exhibiting excellent mechanical as well as electromechanical properties as actuators. Typically DEA technology uses thermoplastic polymers such as polyurethane elastomeric films; this is due to their pliable and good mechanical properties. Owing to their thermoplastic nature, these polymers have the ability to regain their structure after the

stress is removed. So far, research has been presented on elastomers wherein the mechanical strain developed in them, on application of electric field, is believed to be contributed by Coloumbic forces of attraction known as the Maxwell's effect[28]. In this technology, the elastomer is analyzed to relate the strain developed in it due to the application of electric field with the segmental motion of the soft segments at the molecular level of the elastomer. The study shows the relation between Maxwell's stresses, temperature, and elastic properties of the elastomer, and at the same time, the contribution of the electrostrictive effect towards the total strain induced. The DEA functions like a capacitor whereby the polymer is sandwiched between the two conducting electrodes as seen in Figure 1.4.

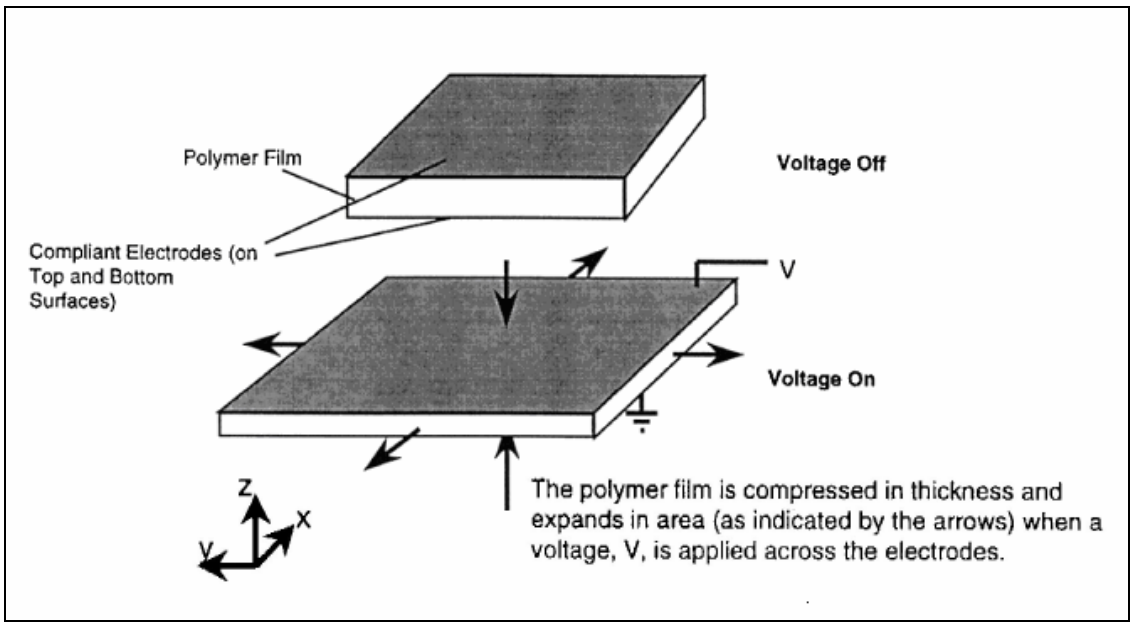

Figure 1.4: Principle of operation of DEA. (From reference[29])

When an electric field is applied to the two electrodes, this capacitor configuration is charged with positive charge on one electrode and balanced by negative charges on the other[30]. Since the dielectric elastomer is very pliable with a low compliance, the charges cause the material to be squeezed. Owing to the constant volume of the DEA, when one dimension of the elastomer reduces, the other increases, as can be seen in Figure1.4. Due to this increase, the charges on one electrode get a chance to move further away from each other and thus conserve the internal energy[31]. Since the spacing between the two conducting layers is very small, on the order of millimeters, though the strains are large, the displacement of the polymer is small, on the order of millimeters to centimeters. In most of the reports presented on DEA, the strain perpendicular to the direction of the applied field is reported; this is because, due to the configuration of the DEA, the length of the polymer expands more in length in comparison to the thickness. Thus, several articles report strain obtained in polyurethanes after they are pre strained along one of the two axes, thereby directing maximum strain along the pre-strained axis [29].

Kornbluh et al[31] have reported on dielectric elastomers deforming (expanding or contracting) in the direction perpendicular to the applied electric field. The phenomenon is related to the electrostatic force of attraction between the conductive layers on the two surfaces of the elastomer as seen in Figure 1.4. The effective actuation pressure or the effective compressive stress is given by the following equation,

$$p = \varepsilon' \cdot \varepsilon_0 \left(\frac{V}{z} \right)^2 \tag{1.1}$$

Where p is the compressive stress, ε' is the dielectric constant of the material, ε_0 is the dielectric permittivity of vacuum, V is the voltage applied against the thickness z of the polymer. The elastomer is quite compliant and results in large strains with efficient coupling between the electrical energy and the mechanical output; it can be seen from equation 1.1 that the compressive stress value is greater by a factor of 2, than that arising from the commonly used Maxwell's stress in a dielectric of a rigid plate capacitor[28, 32]. The greater pressure is due to the compliance of the electrodes, which allows both the forces of attraction between the oppositely charged electrodes and the forces tending to separate the charges on the electrode to couple into effective pressure normal to the plane of the DEA. Several polymers such as silicone, polyurethane, and acrylic have been explored as dielectric EAP; of which silicone seems to yield maximum strain of around 35%[33]. In the field of robots and android applications, DEA elastomer is the most commonly used EAP material, as the cross-linked structure of the elastomers allows the entanglement of the soft segments and the hard segments to loosen up on application of electric field and absorb massive strain, and then release it with little energy loss. This strain leads to the physical change, and when elongated, the elastomer transduces physical stress into strain spring tension by pulling the disordered polymer molecules into alignment, in effect very efficiently removing entropy and adding order. This energy will remain stored as function of stress and the strain in the material until it can be returned by doing work[34]. Recently, a report has been presented whereby a joystick configuration was developed, where DEA polymers drive the motion in all axes by bending and contracting. However, there are complications like compliant electrodes, dependence of strain on the elastic modulus of the

polymer and boundary conditions of the overall system. The high dielectric breakdown rate of the DEA owing to the pre-straining is also an important issue, when yielding high strain values. The problem relating to developing compliant electrodes is very crucial as the magnitude of the strain developed in the DEA depends upon the nature of the electrodes. If the electrode is not compliant and is unable to stretch in at least one planar direction of the film while its thickness contracts, the actuation is damped drastically, i.e. its bulk modulus appears to be more than the elastic modulus of the polymer and misguides the measurement of the induced strain. Several approaches of obtaining compliant electrodes are reported, varying from use of carbon grease, carbon black, powdered graphite, as well as gold sputtering. However, each has some restrictions. For instance, in case of gold electroding, the electrodes tend to crack quickly under actuation. While electrodes made of carbon grease are cumbersome, they also do not seem to be highly conducting. Moreover, in case of grease or carbon black, it becomes difficult to get a uniform smooth coat of the conducting layer on the polymer surface to form electrodes.

Another electronic EAP extensively studied is the ferroelectric polymer. In 1969, Kawai reported unusually large piezoelectric response from drawn and poled synthetic organic material namely PVDF [poly (vinylidene fluoride)][35]. It is the most common ferroelectric polymer under study followed by its copolymer poly (vinyl fluoride-trifluoroethylene) PVDF-TrFE. PVDF has been shown to exhibit at least four polymorphic crystal forms (α, β, γ, δ) of which at least 3 are polar (β, γ, δ). The most commonly studied forms are the non polar α form and the polar β form, of which β is the most desirable form taking polarizability of PVDF into consideration. In the β form, the Carbon-Carbon chain

is in all-trans form while the carbon- fluorine bonds are perpendicular to the chain backbone as seen in Figure 1.5 b. This polar phase can be obtained by melt cooling, stretching or rolling the film in α phase.

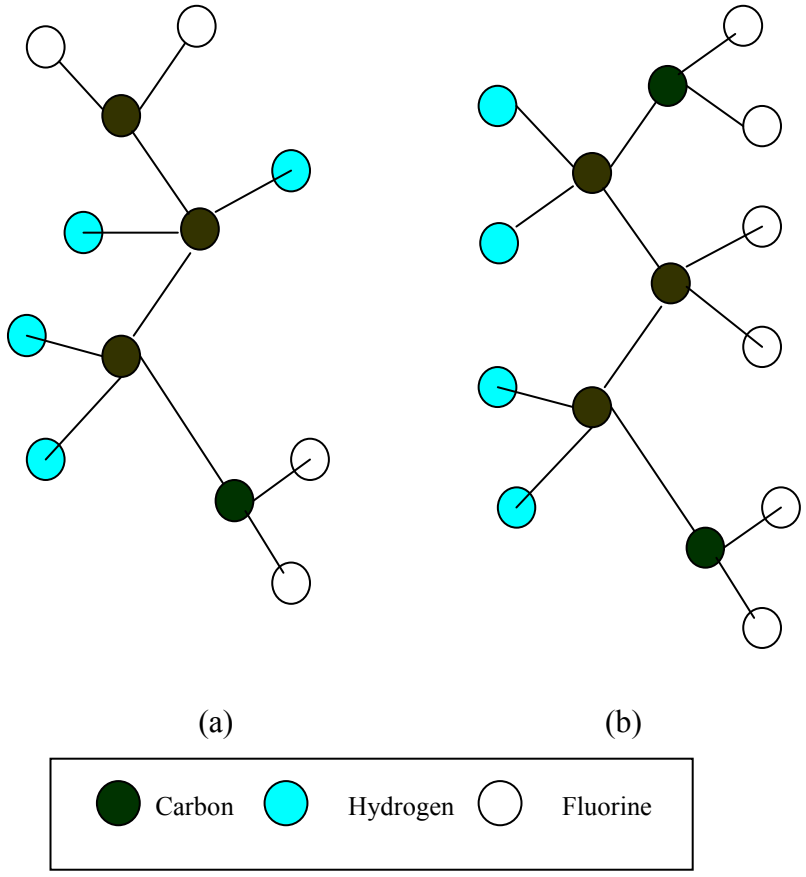

Figure 1.5: Structure of PVDF (a) The non polar α phase. (b) The polar β phase.

(Adapted from reference[24])

This procedure results into orientation of the molecular chain along the direction of the deformation or stretching, thus giving a polar phase. The explanations of these forms, the inter-conversions among structures, the influence of the co-monomers and their effects on the electric properties of PVDF are of great interest in order to make use of this polymer

as an actuator and sensor. A wealth of information related to investigating PVDF can be found in the literature[4, 36-38].

PVDF functions similar to ferromagnets, whereby the application of electric field aligns the polarized domains within the material. The response of PVDF is linear to the applied electric fields and thus is piezoelectric, however the polarization in PVDF becomes non linear for high electric field. This non-linearity in polarization is defined as the hysteresis effect. The molecular chains in the PVDF start aligning as the field is applied. However, when the field is made zero, the polarization does not become zero but shows a permanent polarization. This is referred to as the remnant polarization (P_r)[6]. The existence of the hysteresis loop showing the spontaneous polarization (P_s) along with polarization reversal is indicative of ferroelectricity in the polymers (See Figure 1.6).

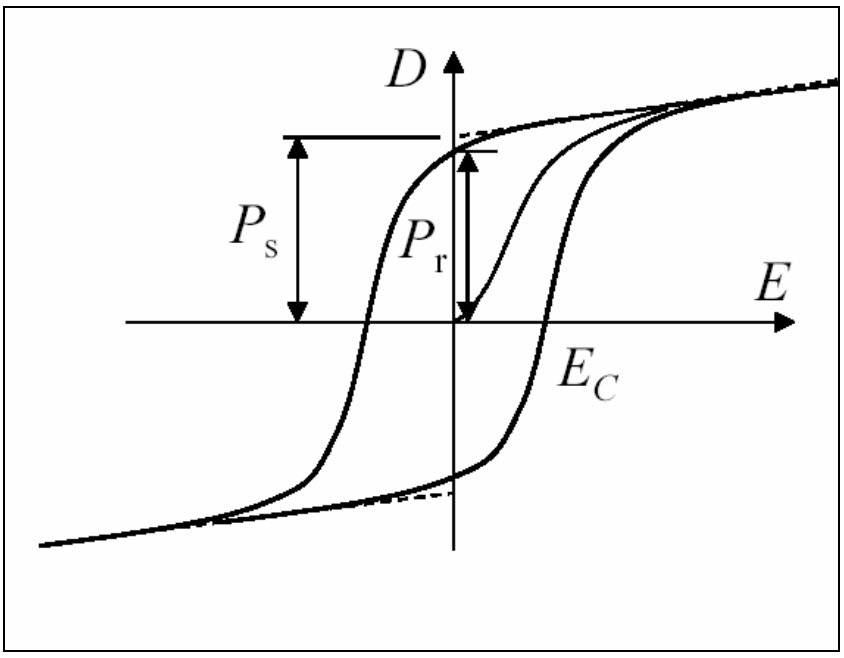

Figure 1.6: Hysteresis loop showing the spontaneous polarization (P_s), remnant polarization (P_r) and the coercive field (E_c). (From refernce[24])

When dealing with ferroelectric polymers, there are two factors which play an important role; the coercive field (E_c), which marks the reversal of the polarization and the remnant polarization, which shows the presence of oriented molecular chains even when the field is removed[39]. The values of these two factors depend on the temperature and the frequency of the measurement. It is seen that ferroelectric polymers lose their polarization below a particular temperature and this temperature is referred to as the Curie temperature T_c. Similar behavior is observed in PVDF-TrFE, which is a copolymer of PVDF. The copolymers differ from PVDF in that they have the ability to force the polymer in an all-trans state, which is a polar crystalline phase, and thus eliminating the need for melt cooling and stretching process. Though ferroelectric polymers can generate high stresses, moderate strain responses and decent frequency responses, their usage is often limited as they result in large hysteresis as well as high heat dissipation[26, 40], which constrains their application as actuators. Also, these EAPs require higher voltages for actuation.

Electrostrictive polymers are a class of electronic EAPs. Electrostriction is the basis of electromechanical coupling in all the insulators[41] and is discussed in detail in subsection 1.4. One of the most commonly studied elastomer for electrostriction is Polyurethane. Several reports on electrostriction in polyurethanes have been presented by Watanabe and group[2, 42, 43] where polyurethane is studied in the cantilever beam configuration. The induced strain reported in polyurethane is along the length of the polymer and is analyzed as function of changing field polarity, frequency and field application time. Their study shows the relation between the space charge accumulation

and the induced strain[43]. It is seen that owing to the repulsive forces between the space charges, the polymer tends to displace / deform thus yielding strain. As it is observed that electrostriction is independent of the electric field polarity, studies of this elastomer by applying reversed electric field show that the direction of the bend of the polymer is not a function of the field direction, which further confirms the electrostriction phenomenon. The polyurethane elastomer, when seen at a molecular level, is composed of small crystallites which act as cross-links, while the hard and soft segments endow the elastomer with its mechanical and dielectric properties[44] as seen in Figure 1.7. It is seen that the higher the dielectric constant of the polymer, the more is the polarizability, and thus the higher is the strain rate[45]. Upon variation of the hard and soft segments, the dielectric constant may reach values as high as 7, for which a strain of 1.34% at an electric field of 0.25 MV/m has been observed[46].

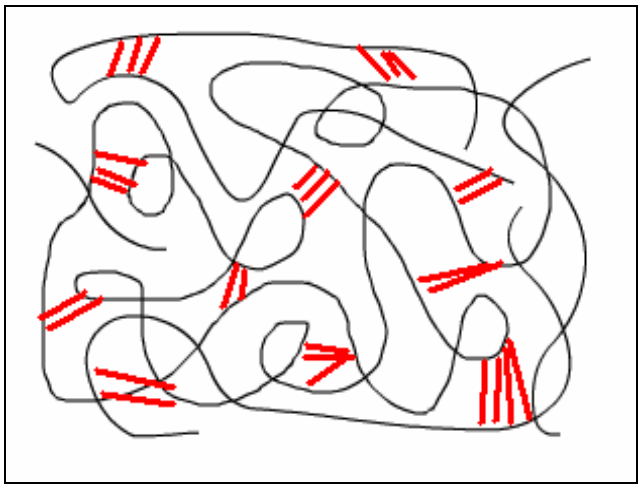

Figure 1.7: Graphical presentation of molecular structure of polyurethane.

(The solid red lines indicate the crystallites while the black lines represent the amorphous soft segment of polyurethane.)

Factors such as temperature and applied frequency of the electric field are strongly related to the induced strain in the polyurethane elastomer. Reports on theoretical as well as experimental evaluation of the electrostrictive and Maxwell contributions of the strain coefficient have been presented previously by Kornbluh et al and Zhang et al [28, 33, 47] as well as is done in this work to analyze the cause of the induced strain in the polymers. The Maxwell contribution can comprise from 10% to 60%, depending upon temperature, the higher value observed near the glass transition temperature[41, 47, 48].

Another polymer recognized as electrostrictive in nature is poly (vinylideneflouride) PVDF, poly (vinylideneflouride-triflouroethylene) (P (VDF-TrFE)). One of the very first reports on electrostrictive strain of about 3% was presented in PVDF in 1994[2]. Further, by co-polymerizing PVDF, moderate to high strains were achieved by application of very high electric fields[49].

However, in most of the above-mentioned EAP technologies, the polymer materials used are obtained commercially from vendors, thus offering very little or no tailorability and limiting the analysis of the polymer with variation at the material level. In this work, the aim is to relate variations at the molecular level to performance at the macroscale. Scientists at Langley Research center synthesized the polymer under study, allowing variations in the polymer system's structure. Poly (dimethyl Siloxane) (PDMS) is used as the base polymer, with cyano phenyl CN) functional groups forming a unique polymer blend.

1.4 Electrostriction In Polymers

Electrostriction refers to the strain induced in a dielectric material by electric polarization. The electromechanical interaction seen in the electrostrictive polymers depends quadratically on the polarization and can be expressed;

$$S_{ij} = Q_{ijab} \cdot P_a \cdot P_b \tag{1.2}$$

Where S_{ij} is the induced strain tensor and Q_{ijab} is fourth ranked electrostrictive coefficient tensor of the material. This tensor Q_{ijab} is charge related and thus is associated with polarization. In linear dielectric material, the following relation relates the polarization to the applied electric field,

$$P_i = \left(\varepsilon_{ij}^{'} - 1\right) \cdot \varepsilon_0 \cdot E_j \tag{1.3}$$

Where P_i is the tensor notation for the polarization caused due to the electric displacement of the dipoles in the polymer, ε_{ij}' is the dielectric constant of the polymer material, ε_0 is the permittivity of the free space and E_j is the applied electric field[45]. The factor $[(\varepsilon_{ij}'-1)\varepsilon_0]$ is called as the dielectric susceptibility and is denoted as χ_{ij}.

For linear dielectrics, the electrostrictive strain can be similarly related to electric field through another electric field related tensor M_{ijab} as follows;

$$S_{ij} = M_{ijab} \cdot E_a E_b \tag{1.4}$$

Where M_{ijab} is the fourth ranked electric field related vector and a strain S_{ij} is induced when an electric field E_i is applied to the polymer.

From Equations 1.2-1.4, the two electrostrictive coefficients Q and M are related by the following relationship:

$$M_{ijmn} = \left(\varepsilon_{ij}'-1\right)^2 \varepsilon^2{}_0 \cdot Q_{ijab} \quad (1.5)$$

Where M_{ijmn} is the electric field related fourth order tensor while Q_{ijab} is the polarization related quadratic tensor and $[(\varepsilon_{ij}'-1)\varepsilon_0$ is the dielectric susceptibility.

Thus the electrostrictive mechanism in linear dielectric materials is governed by the nonlinearly coupled electromechanical constitutive equations[50].

$$S_{ij} = s_{ijab}T_{ijab} + M_{ijab}E_aE_b \quad (1.6)$$

$$D_{ij} = \varepsilon'_{ijab}E_j + 2M_{abij}T_{ab}E_j \quad (1.7)$$

Where S_{ij} is the strain induced in the polymer T_{ijab} is the stress, s_{ijab} is the elastic compliance, ε'_{ijab} is the dielectric permittivity of the polymer under stress, M_{ijab} is the electrostrictive coefficient while D_{ij} is the electric displacement when an electric field E_j is applied to the polymer.

The electrostrictive effect is present in all materials, regardless of the symmetry[51]. Further it is seen that due to the quadratic nature of the electrostrictive effect, the strain induced due to electrostriction is independent of the electric field polarity, which is not the case in linear piezoelectric materials, where the strain depends on the field polarity.

Also another feature of the electrostriction is that the induced strain has twice the applied field frequency; in case of alternating current field application[52].

1.5 Advantages Of Poly (Dimethyl Siloxane) Based Electroactive Polymers

PDMS, a fairly transparent polymer having high elasticity and low stiffness, is a polymer composed of an alternating backbone of silicon and oxygen atoms with two

organic functionalities attached to each silicon atom. The absence of a chromophore within alkyl-substituted polysiloxanes results in a polymer with high stability towards ultraviolet radiation. Also, the silicon-oxygen backbone gives polysiloxanes high resistance towards oxidation and chemical attack. The high torsional mobility about the silicon-oxygen bond results in the dimethyl substituted polysiloxane having one of the lowest glass transition temperatures of any polymer (-123 °C), thus allowing a large temperature window from -100°C to over 200 °C of operation and showing stable behavior even for harsh environments. Owing to the combination of these properties with its adaptable molecular composition and excellent process-ability, PDMS systems attract attention for a variety of actuation applications like robotics, android heads, MEMS. Moreover, PDMS is used as a base polymer because a stable electroactive blend can be obtained by attaching not only cyanophenyl as the dipolar moiety but several other functional groups like nitro, flouro or other group that have either a permanent or induced dipole moment and can be cross-linked to the poly (dimethyl siloxane) oligomer. Thus, making PDMS the base of the electrostrictive EAP and tailoring it with dipolar entities is a step towards implementation of the applications. Figure 1.8 below shows the graphical representation of the CN-PDMS blend, where the polar pendants are attached to the functional component, which is crosslinked with the PDMS strands.

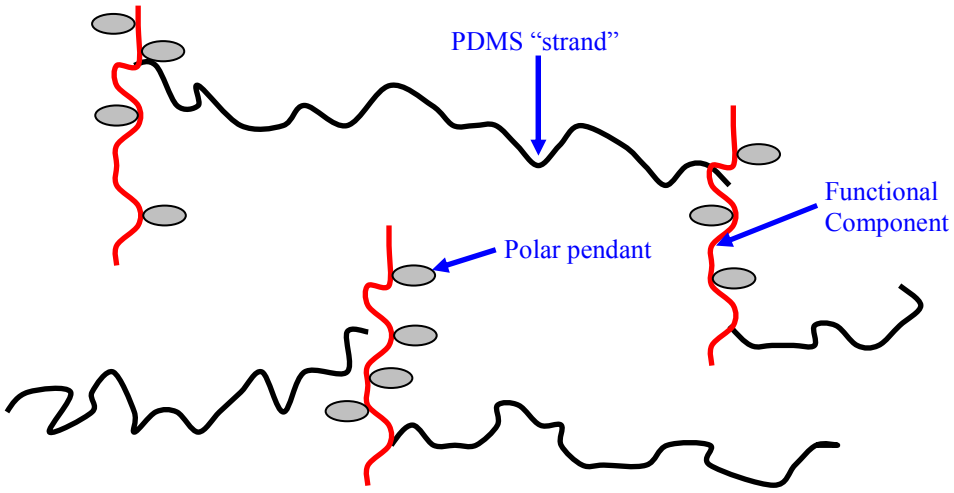

Figure 1.8: CN-PDMS system.

CHAPTER 2 SCOPE OF THESIS

2.1 Problem Statement

Growth in technology and material science has opened new avenues in every field; from robotics to telecommunication. New avenues in the design of future applications such as biomimetic devices, nanoscale technology, and animatronics can be made possible by developing new active materials, possessing more than one functionality. Such multifunctional polymer materials can be attained by amalgamation of the structural functionality at the material level and sensing and /or actuation capabilities at the practical level. Owing to several excellent functional and structural properties of polymers, they promise to increase the intelligence of aerospace applications and biomedical devices, thus offering optimization and increased efficiency in the overall system. In all of these applications, polymers need to be lightweight, flexible and able to sustain extreme environmental conditions. To meet these requirements, a polymer blend is proposed in the current study, which can offer these characteristics along with actuation.

This work describes a method of taking advantage of the unique combination of properties offered by the hybridization of organic and inorganic components in a PDMS based system. PDMS is crosslinked with cyano phenyl (CN-phenyl) dipolar groups. The resulting CN-PDMS polymer system is analyzed to evaluate its potential as an electroactive polymer.

The objectives of this study are: (1) To obtain a stable, tailorable, lightweight polymer blend of CN-PDMS; (2) To analyze the dielectric behavior of the polymer having a varying content of CN-phenyl dipoles as a function of the dipole content with regard to frequency and temperature; (3) To analyze the strain induced in the polymer blend as a function of applied electric field and CN-phenyl dipole content; (4) To assess the nature of actuation and its dependence on the applied electric field; (5) To study the actuation load current drawn by the polymer in order to evaluate the energy density of CN-PDMS system.

2.2 Thesis Organization

This study of the characterization of cross-linked poly (dimethyl-siloxane) containing CN-phenyl functional groups is comprised of five chapters. Chapter 1 introduces electroactive polymers and their associated mechanisms, and current research status and trends. The chapter gives a background on characterization techniques of electroactive polymers and their applications. This is followed by a detailed description on the phenomenon of electrostriction, which governs the mechanism of the polymer blend in this study. Chapter 1 ends with a discussion of the advantages of poly (dimethyl siloxane).

Chapter 2 is the problem statement and the scope of this study. Chapter 3 presents the experimental details of the CN-PDMS system. It outlines the processing of the polymer followed by its electromechanical characterization. It describes the dielectric spectroscopy done on the polymer system further analyzing the electromechanical strain induced in the polymer. The strain is measured in the parallel (i.e. through the thickness of the polymer) as well as perpendicular (i.e. along the length of the polymer sample) direction. Chapter 3

also presents other measurements such as Differential Scanning Calorimetery, Thermally Stimulated Current measurement, and Load current measurement. Chapter 4 is the results section, which presents a detailed analysis and discussion of the data obtained. This is followed by the conclusion in Chapter 5, which also makes recommendations for future work.

CHAPTER 3 EXPERIMENTAL

3.1 Synthesis Of The Poly (Dimethyl Siloxane) Polymer With CN-phenyl Dipoles

The CN-PDMS polymer blends are synthesized by researchers at NASA Langley Research Center (LaRC). The synthesis of this polymer is done by cross-linking of vinyl terminated Poly (dimethyl siloxane) with methyl (3-(4'-cyanophenoxy) propyl) siloxane-methylhydrosiloxane-dimethylsiloxane copolymer in the presence of platinum as the catalyst. This copolymer itself is prepared from the platinum catalyzed hydrosilylation reaction of allyl 4-cyanophenyl ether with methylhydrosiloxane-dimethylsiloxane copolymer (see Figure 3.1). Vinyl terminated poly (dimethyl siloxane) (*DMS-V22*, *DMS-V25*, and *DMS-V31*, M_w = 9400, 17,200, and 28,000, respectively) and methylhydrosiloxane-dimethylsiloxane copolymers (*HMS-301* and *HMS-151* containing 25-30 and 15-18 mol % MeHSiO, respectively; M_w = 1900-2000) are purchased from Gelest, Inc. Chloroplatinic acid (hydrogen hexachloroplatinate (IV) hydrate, $H_2PtCl_6 \cdot xH_2O$) is purchased from Aldrich in 99.995% purity. Allyl 4-cyanophenyl ether is prepared by the general procedure of Lasek and Makosza in good yield[53, 54]. NMR spectra are recorded on a Bruker Advancer 300 spectrometer at 300 MHz with tetramethylsilane (TMS) as internal standard at 0.00 ppm.

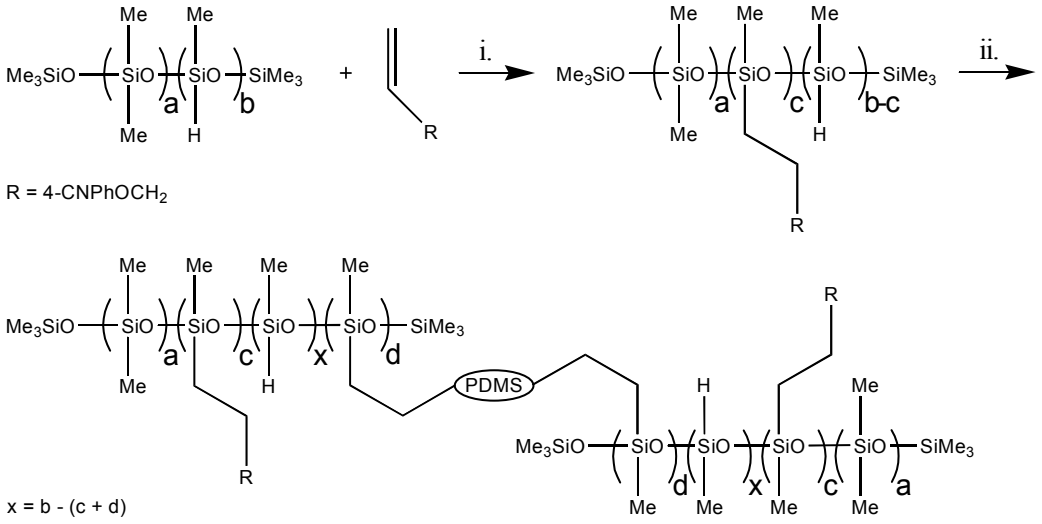

Figure 3.1: Synthetic Strategy. (i.) "Pt"/Δ. (ii.) vinyl terminated PDMS/"Pt"/Δ.

Methylhydrosiloxane-dimethylsiloxane copolymer (*HMS-301*: 0.9709 g, 0.4978 mmol, 3.5 mmol of MeHSiO), allyl 4-cyanophenyl ether (0.3083 g, 1.94 mmol), and Chloroplatinic acid (0.30 mL of a 0.12 M solution in THF, 0.036 mmol) are stirred in toluene (5 mL) at 80 °C for 4-8 h, the reaction monitored by TLC for consumption of allyl 4-cyanophenyl ether. Elimination of vinyl signals (5.20-6.20 ppm) in the ^{1}H-NMR spectrum of the modified copolymer is taken as proof of complete hydrosilylation. Vinyl terminated polydimethylsiloxane (*DMS-V22*: 2.8087 g, 0.2987 mmol, 0.5974 mmol of vinyl) and Chloroplatinic acid (0.30 mL of a 0.12 M solution in THF, 0.036 mmol) are then added to the methyl (3-(4'-cyanophenoxy) propyl) siloxane-methylhydrosiloxane-dimethylsiloxane copolymer with toluene (5 mL), mixed thoroughly, and the mixture poured into a PFA-Teflon® (perfluoroalkoxy-PTFE) dish to be cured at 80 °C for 24-48 h under constant nitrogen flow.

3.2 Differential Scanning Calorimetery

The CN-PDMS polymers are characterized using Differential Scanning Calorimetery, commonly known as DSC. It is a powerful tool that measures temperatures and heat flows associated with the thermal transitions in the material. DSC provides information regarding properties of the polymer under study such as the glass transitions (T_g), "cold" crystallization, phase changes, melting (T_m), crystallization, product stability, cure / cure kinetics, and oxidative stability [54]. Figure 3.2 shows the pictorial representation of the DSC used to perform the analysis on the polymer samples. The principle of operation of DSC is based on comparing the amount of heat taken by the polymer under study and a reference pan.

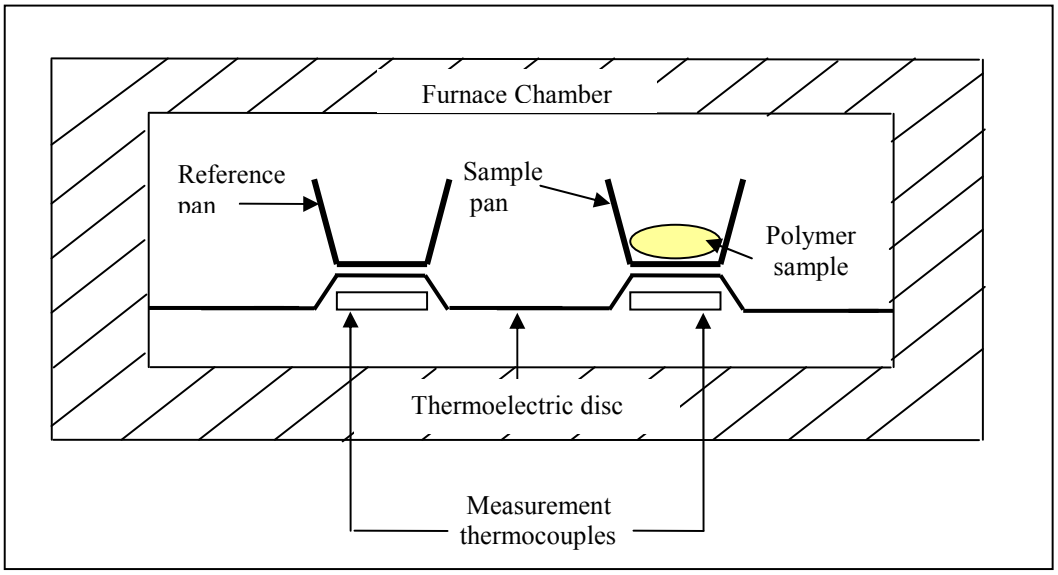

Figure 3.2: DSC measurement set-up. (Adapted from reference[56])

In this measurement, the samples with varying CN-phenyl content are weighed and enclosed in the pans. After the samples are prepared, they are placed in the sample holder, which has capacity to hold 50 samples at a time. The DSC machine has two pans, a sample pan and a reference pan. Both pans are placed on two identically positioned platforms as seen in Figure 3.2. These platforms are further connected to a furnace by a common heat flow path. Both the sample as well as the reference pan are heated at the same rate, with a constant heating rate throughout the experiment. However since the sample pan contains the polymer, it will take up more heat in order to maintain an equilibrium and keep the sample pan at the same temperature as that of the reference. This machine is connected to the computer from which a plot for the difference in the heat flow as a function of temperature is obtained. This plot gives us information regarding the phase changes in the polymer, the glass transition temperature of the polymer, and other transitions such as melting and crystallization. The DSC machine used in this study is a TA instruments make model Q1000. It is a DSC machine with high baseline stability, sensitivity and resolution.

3.3 Dielectric Spectroscopy

Measurement of Dielectric Properties

Dielectric spectroscopy probes the molecular motion and electrical properties of materials. While performing dielectric analysis of an insulating material it can be modeled as a material composed of small dipoles, which are electrically neutral, and are separated from each other by an internal charge. When such a material is exposed to an external electric field, the tendency of a single dipole is to align itself with the electric field, such

that the positive end points toward lower potential, and the negative end points toward the higher potential[57]. When all the dipoles in a material align in this way to an applied electric field, the material forms a *dielectric*. Such model can be better understood from Figure 3.3[31].

Figure 3.3 is a graphical representation of a parallel plate capacitor describing three situations when a constant electric field is applied between its two capacitor plates separated partially by a vacuum as seen in part (a). Part (b) illustrates when a dielectric material is introduced between the parallel plates. This model also has a part of the dielectric material, which is not under the influence of applied constant voltage as seen in part (c) of Figure 3.3. In case of part (b) owing to the applied electric field, a charge is developed on the surface of the capacitor plates. This building of the charge continues until the voltage drop across the capacitor plates equals the applied voltage.

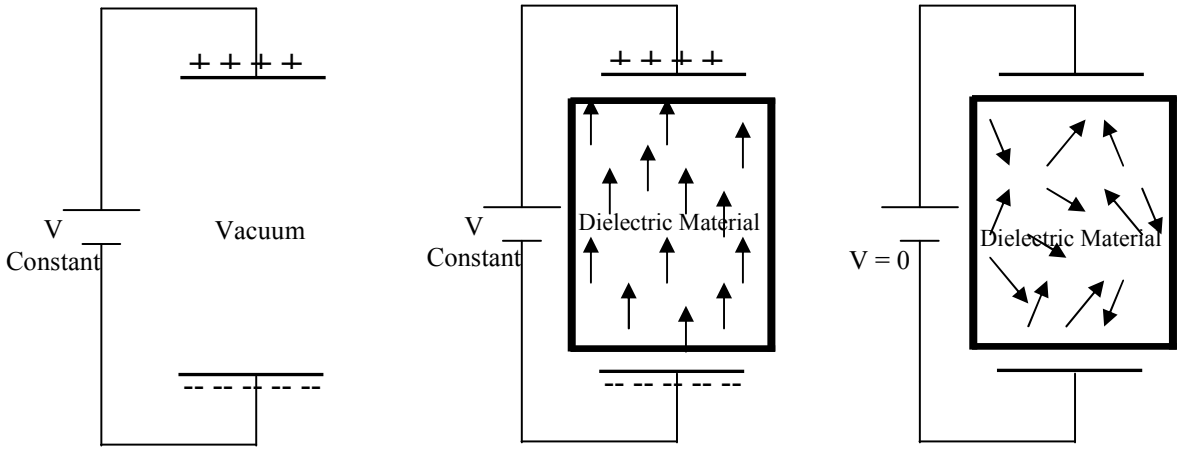

Figure 3.3: Dielectric susceptibility. (a) Vacuum capacitor. (b) Polarized dipoles in the dielectric inserted between the two-capacitor plates. (c) Random dipoles when no electric field is applied. (Adapted from Reference[31])

This build up charge Q is related to the applied voltage by the following relationship:

$$Q = C \cdot V \tag{3.1}$$

Where C is the capacitance of the dielectric material. Capacitance is the ability of the polymer to build up energy in the form of charge. The dielectric constant, ε', is related to C by equation 3.2 below (A is the area of the polymer, d is the thickness of the polymer and ε_0 is the dielectric permittivity of free space = 8.85 x 10^{-12} F/m).

$$\varepsilon' = \frac{C \cdot d}{A \cdot \varepsilon_0} \tag{3.2}$$

When a dielectric material is inserted between two capacitor plates, the dielectric constant of the material between the capacitor plates and the dielectric permittivity of free space are related by relative dielectric constant, which is a ratio of dielectric constant and the vacuum permittivity. It is given by equation 3.3.

$$\varepsilon_r = \frac{\varepsilon'}{\varepsilon_0} \tag{3.3}$$

In the case of part b of Figure 3.3, the dipoles in the dielectric material start aligning along the electric field by reorientation, thereby posing a net charge on the capacitor plates. In this case, the electric field flux due to polarization in the material D_p is given as:

$$D_p = \varepsilon_0 \varepsilon' \cdot E \tag{3.4}$$

This flux density of the material is also a measure of the electric displacement caused due to the reorientation of the dipoles under the influence of the electric field. This displacement of the charges under the electric field known as Polarization (P) arises due to actual polarization of the dielectric material as well as due to the vacuum electric displacement. Thus Polarization is given as:

$$P = D_p - \varepsilon_0 E \tag{3.5}$$

After substituting for D_p in equation 3.5 we get the Polarization given as in equation 3.6,

$$P = (\varepsilon' - 1)\varepsilon_0 E \tag{3.6}$$

The factor (ε' - 1) in equation 3.6 gives the electric susceptibility of the dielectric material denoted as χ.

Polarization in dielectric material develops from a range of mechanism, where occurrence of each type of polarization is frequency and response time related. Also each polarization differs in strength. Understanding the polarization mechanisms in dielectric material is very important. Each polarization mechanism affects the dielectric constant and the dielectric loss of the material. The cause of polarization plays a crucial role in strains

caused by linear as well as non-linear electromechanical interactions as seen in some of the electrostrictive polymers such as PVDF and it co-polymers like (PVDF-TrFE)[45]. There are different types of polarization mechanisms: electronic polarization, atomic polarization, dipolar polarization and interfacial polarization. In a given dielectric material, the total polarization is a sum of all the polarizations resulting from each one of them. In this study the most closely associated polarization mechanism is dipolar polarization (through the addition of CN-phenyl dipoles to PDMS). Figure 3.4 is an illustration of electronic polarization. This polarization occurs at the molecular level. When electric field is applied, there is a displacement of the center of mass of the negative electron charge cloud surrounding the positive atomic nucleus. This charge displacement acts to neutralize part of the applied field.

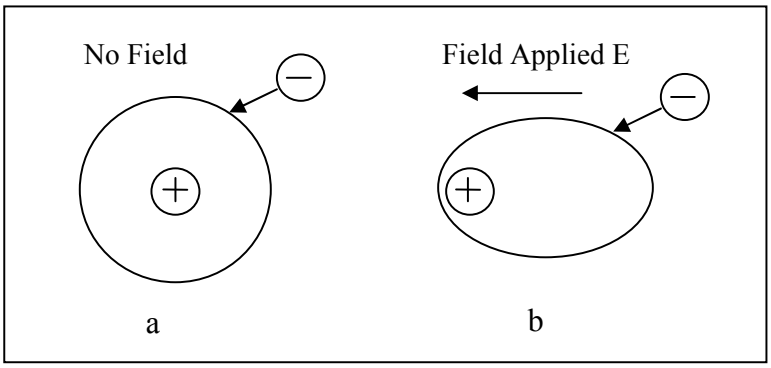

Figure 3.4: Electronic Polarization. (a) No electric field. (b) In the presence of electric field E. (Adapted from Reference [30])

This occurs in materials where the structure is formed from the molecules of different atoms with different electro-negativities. When a molecule is formed of different atoms, there is a tendency of the electron clouds to move towards the strongly binding

atom. This shift of the electron cloud results in a change of polarity of the atoms, whose equilibrium position is further changed when electric field is applied. Electronic polarization occurs in almost all materials and typically the time required for this polarization to occur is around 10^{-15} s, thus it is apparent only at higher frequencies[30].

In case of the atomic polarization, there is a relative shift of the atoms, as seen in Figure 3.5. The movement of the atom with heavy nuclei is slower as compared to that of the electron clouds, thus atomic polarization occurs at higher frequencies than electronic polarization. Basically, atomic polarization results from the bending and twisting motions of the molecules.

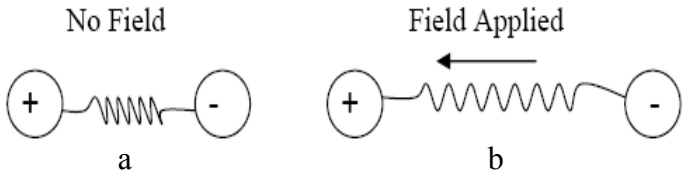

Figure 3.5: Atomic Polarization (a) In the absence of electric field. (b) In the presence of electric field. (Adapted from Reference [30])

As seen in Figure 3.5 b, on application of electric field, there is a relative motion of the atoms with respect to the electric field. Both electronic as well as atomic polarization cause molecular distortion and thereby produce a dipole moment, which is known as the induced dipole moment[30].

Another contribution towards dielectric properties of a material, which is significant only at lower frequencies, is the interfacial polarization. This polarization is seen for heterogeneous dielectrics where each constituent of the matrix has a different

dielectric constant as well as different electrical conductivities[58]. Interfacial polarization which occurs at frequencies below 10 Hz is basically due to the charge pile up inside the dielectric when the charge carriers face physical obstruction to their movement. In this case, it is seen that if the relative motion of the charge occurs easily through one phase, it might face an obstruction near the phase boundaries. The motion of these charges can be impeded either by getting trapped in the material or may be due to the failure to be freely discharged, which results into space charges and a macroscopic distortion occurs.

Dipolar polarization, which is associated closest with this study, occurs when an electric field is applied to a randomly oriented dipolar material, and the dipoles start aligning in the direction of the applied field. A net charge develops, which tries to cancel out a part of the applied field in order to attain equilibrium. This is seen in polymer molecules already possessing permanent dipole moment; these moments tend to align by the applied field to give rise to a net dipolar polarization. It is illustrated in Figure 3.6b where random dipoles start to orient themselves along the field direction.

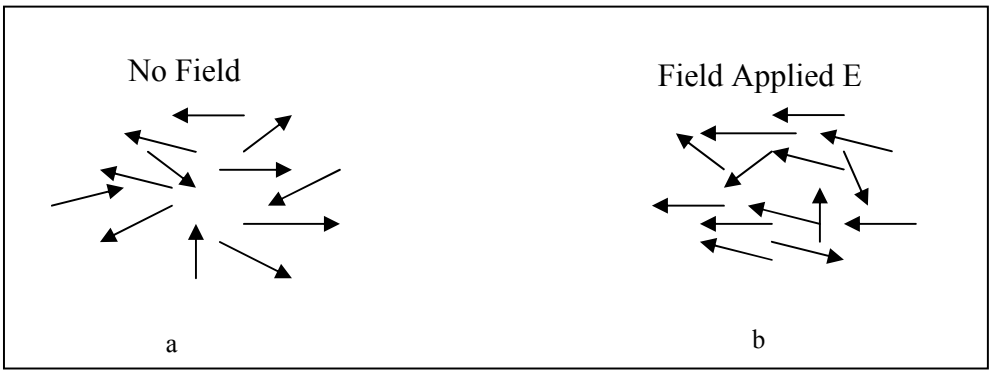

Figure 3.6: Dipolar Polarization. (a) Random dipoles in absence of field. (b) Aligning of dipoles in the direction of field. (Adapted from Reference [30])

All these polarization mechanisms occurring in dielectric materials are frequency and temperature dependent. They also depend largely on the composition of the dielectric material under investigation. It is seen that in the case of electronic and atomic polarization due to the inertia of the orbiting electrons, the observed polarization is very small and is seen only at lower frequencies[59]. Electronic polarization occurs at a characteristic frequency of about 10^{15} Hz and atomic polarization occurs at about 10^{13} Hz. The reorientation of dipoles in the field depends upon factors like barriers from the neighboring parts of the molecules, electrostatic interactions or forms of restrains. In order for the polymer molecules to overcome these barriers they should possess sufficient energy. This dipolar polarization depends upon the frequency of measurement relative to the reorientation time. Lower frequencies of measurement at a given temperature will allow dipoles to reorient and contribute to dipolar polarization, whereas higher frequencies will not induce as large a dipolar polarization. This occurs at about 10^{7} to 10^{9} Hz, depending on factors which affect mobility of the charge carriers. Interfacial polarization occurs at frequencies below 10 Hz but, and is generally observed in polymers having structural inhomogeneities. Interfacial polarization is seen to decrease with increase in frequency. Since no polymer system is 100% homogeneous, dielectric constants obtained at very low frequency are much higher than dielectric constants obtained at intermediate or higher frequencies.

Dielectric properties of a material are highly dependent on temperature as there is a major effect of temperature on polarization mechanisms. Electronic polarization is not dependent on temperature, as the shift of mass of the negative electron charge cloud

around the nucleus is not affected. Dipolar polarization is highly dependent on temperature as the ability to rotate a dipole is temperature dependent. At a given temperature above the T_g, the dipoles start to reorient, which results in an increase in dipolar polarization. Interfacial polarization is temperature dependent because charge mobility is temperature dependent.

Dielectric spectroscopy provides information regarding the segmental mobility of a polymer. This measurement is done in order to measure the charge storing capacity of the polymer and its dependence on the weight % of CN-phenyl in the polymer. Dielectric properties, such as dielectric constant ε' and dielectric loss ε'', are measured by scanning samples using a Hewlett Packard 4284A Precision LCR meter.

The relative permittivity (ε_r) of each sample is obtained from the relationship between the dielectric constant (real part) and the dielectric loss (imaginary part).

$$\varepsilon_r = \varepsilon' + i\varepsilon'' \tag{3.7}$$

In equation 3.7, the imaginary part is the heat related loss of the polymer material and is denoted a refers to as dielectric loss, while 'i' in the equation shows the complex dielectric constant relation, 'i'= $(-1)^{1/2}$ .The ε'' and the ε' are related by the factor tan δ by the following relation,

$$\varepsilon'' = \varepsilon' \tan\delta \tag{3.8}$$

A polymer sample of known thickness is electroded on both sides using high purity silver paint and the electroded area is measured. This electroded sample is clamped between the two electrodes of a circular Teflon holder as shown in Figure 3.7.

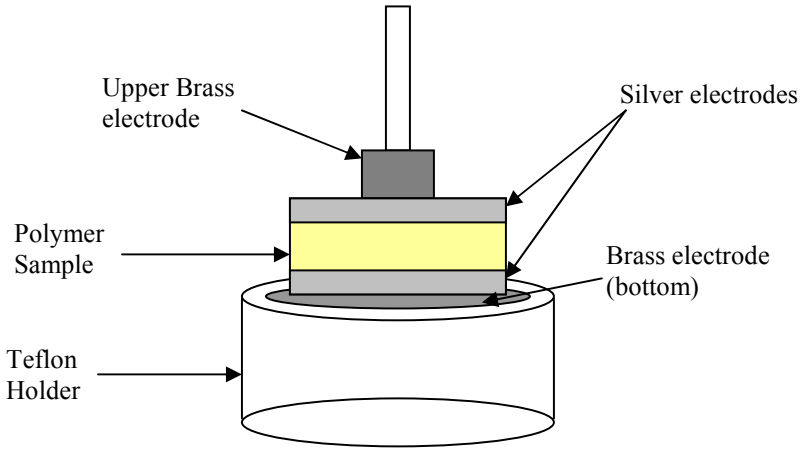

Figure 3.7: Electroded CN-PDMS sample clamped in the holder.

The dielectric properties of the sample are measured using Labview software, which is interfaced with the Hewlett Packard 4284 A LCR meter. The software converts the raw data in the form of capacitance C and tan δ into dielectric constant ε' and dielectric loss ε''. This measurement is performed by scanning the samples over a frequency range of 20 Hz to 1 Mhz.

3.4 Measurement Of The Electromechanical Strain Induced In The CN-PDMS Polymer System

The CN-PDMS polymer blend is studied to measure the strain developed when electric field is applied to the polymer samples. The strain induced in the polymer blend samples are analyzed in two configurations; strain induced along the length and strain induced through the thickness. The induced strain is referred to as electromechanical strain

because there is an electromechanical coupling between the applied signal, which is electric field, and the mechanical response of the polymer sample, which is bending deformation and expansion in the sample thickness. In the first configuration, the polymer samples are analyzed for the strain induced along the length of the sample when an electric field is applied across the thickness of the sample as seen in Figure 3.8 a. Similarly, in the second configuration, the field is applied across the thickness of the sample and the strain developed through the thickness of the sample is analyzed, as seen in Figure 3.8 b.

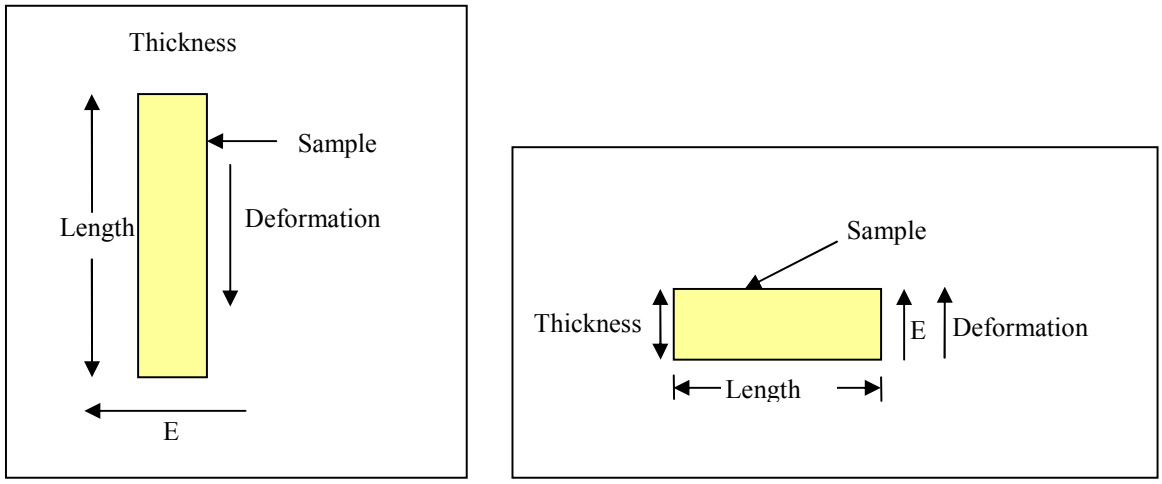

Figure 3.8: Strain measured in the two configurations. (a) Strain measured is perpendicular to the applied field. (b) Strain measured is parallel to the direction of the field.

3.4.a Experimental Measurements Of Strain Induced Along The Length Of The Polymer

This experiment is conducted on polymer films about 4-5 cm long, 0.8-1.5 mm thick, and 0.5 cm wide. These measurements are carried out by placing the sample between two rectangular electrodes spaced 2-4 cm apart (see Figure 3.9). The setup is comprised of

an oil bath as dielectric medium to prevent arcing under high field. The oil used for the oil-bath is a low viscosity silicone oil having high dielectric breakdown. An Instek programmable power supply PSH 6400 series is used for the direct current measurements while the Hewlett Packard signal generator model 33120A is used for the alternating current measurements. Further a Trek amplifier having gain of 1000V/V±20 is used to amplify the signal from the signal generator. Starting from 0 kV/cm, the electric field is increased to about 4 kV/cm. The deformation of the polymer is studied under both alternating current and direct current electric fields. The frequency of the alternating current field is in the range of 100-350 mHz.

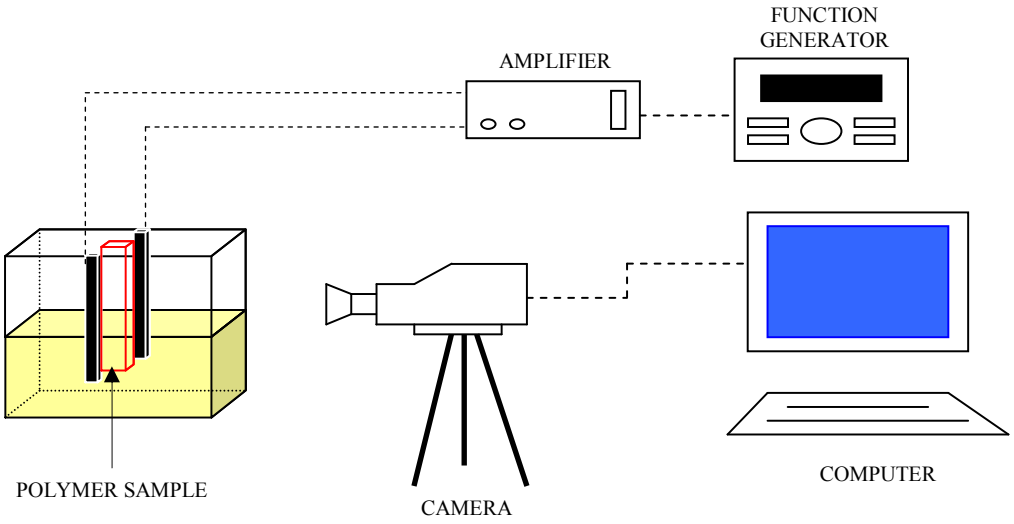

Figure 3.9: Oil bath displacement setup of PDMS polymer experiment.

The polymer is held static at one end, while the free end is allowed to undergo bending deformation, which is captured using a fast motion capture camera from Photron tools, model PCI-R2. The camera software enables several measurements along with capturing the motion of the polymer, such as velocity measurement, tracking displacement

of the polymer bender for each pixel, and displacement of the polymer free end along two axes, horizontal, i.e., x-direction as well as vertical, i.e., y-direction. Total displacement, velocity of displacement, actuation time, and relaxation time of the polymer can be gathered from these measurements.

The direct current measurements are done by gradually increasing the electric field and recording the resultant displacement. Figure 3.10 is a representation of the polymer sample in a deformed state, showing the angle of deflection and the deformed length of the polymer under electric field.

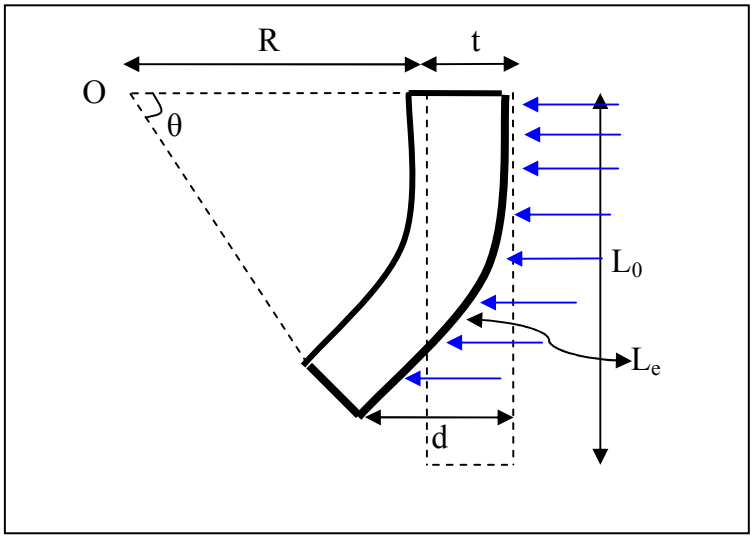

Figure 3.10: Graphical representation of the polymer sample under constant uniform force. The blue colored arrowheads represent the force.

The strain equation used for relating the displacement obtained can be derived from the model of a simple cantilever beam having uniform loading. There are some assumptions made while developing the relationship:

(a) The polymer under stress does not yield.

(b) The polymer undergoes elastic deformation.

(c) The polymer sample is a cantilever beam supported only at one end.

(d) The cantilever beam is uniformly loaded.

There is a linear relationship between the force experienced by the beam and the deflection of the beam. In Figure 3.10 the beam of length L_0 experiences a total force F shown by the blue arrowheads, producing a deflection at the free end of the beam is d.

The force F is related to the deflection d by a linear relationship (see equation 3.9)

$$d = \frac{F \cdot L_0^{\,4}}{8 \cdot E \cdot I} \tag{3.9}$$

Thus the total force F can be obtained from equation 3.9 as

$$F = \frac{8 \cdot E_m \cdot I}{L_0^{\,4}} \cdot d \tag{3.10}$$

Where E_m is the elastic modulus of the polymer and I is the moment of inertia of the beam cross section. The stress distribution in the beam generated by the given deflection is an important factor contributing towards the strain induced along the beam length. The amount of stress acting on the beam depends on the bending moment M, which is equal to the product of the force acting on the beam and the distance between the point of application of force and the free end. Thus in this case the force exerted at the tip is zero while maximum force is exerted at the fixed held end. The equation for stress developed at any point along the beam is given as follows:

$$\sigma = \frac{M \cdot y}{I} \tag{3.11}$$

$$\sigma = \frac{F \cdot x \cdot y}{I} \tag{3.12}$$

Where σ is the stress developed, y is the distance from the neutral axis, F is the force exerted, x is the distance at which force is applied and I is the moment of inertia. Since in a uniformly loaded cantilever beam, the maximum force exerted is at the center of the beam length, x is equal to $L_0/2$ while the y equals half of the beam thickness. Substituting for the force and the distance in equation 3.12 we get a relationship between the stress developed per unit length of the beam and the deflection of the free end of the beam (d) as follows:

$$\sigma = \frac{2 \cdot E \cdot t \cdot d}{L_0^{\,2}} \tag{3.13}$$

Since strain is related to stress and the elastic modulus of the material by the following relation (assuming elastic deformation),

$$S = \frac{\sigma}{E_m} \tag{3.14}$$

From equation 3.13 and 3.14, we get the induced percent strain in the beam as a function of beam length, beam thickness and the deflection of the free end.

$$S = \frac{2 \cdot t \cdot d}{L_0^{\,2}} \cdot 100 \tag{3.15}$$

This relationship of strain and deflection is used in the present study to measure the strain developed in the CN-PDMS polymer system, when it is analyzed in the configuration shown in Figure 3.11.

The relation of strain and the deflection obtained in equation 18 can also be validated by geometrical calculations as follows: In Figure 3.10, L_0 is the length of active

side of the polymer sample and L_e is the non-active side of the polymer sample, t is the thickness of the polymer and d is the displacement of the free end of the polymer. O is the center of the constant radius arc, while θ is the angle of deflection. The radius R of the arc is given as [60, 61].

$$R = \frac{L_0^{\ 2} + d^2}{2 \cdot d} \tag{3.16}$$

Now the displacement of the free tip d can be given in the terms of deflection angle θ and sample thickness as,

$$d = (R + t) - (R + t)Cos\theta \tag{3.17}$$

$$d = (R + t)Sin^2\theta / 2 \tag{3.18}$$

The length of the arc formed by the angle θ is given by,

$$L_c = \theta(R + t) \tag{3.19}$$

The strain developed in the polymer sample is the ratio of the elongation to the original length and thus is given by equation 3.20 as,

$$S = \frac{(L_e - L_o)}{L_o} \tag{3.20}$$

From equations 3.17 - 3.20 the displacement d is derived as,

$$d = \frac{2(S+1)L_0}{2} \cdot \frac{Sin^2\theta/2}{\theta/2} \tag{3.21}$$

Since θ is small, $(Sin^2\theta/2)/\ \theta/2$ term reduces to θ/2.

Thus giving the displacement as,

$$d = (S+1)L_0 \cdot \frac{\theta}{2} \tag{3.22}$$

Thus for smaller strains, (S+1) ~ 1, displacement reduces to,

$$d = L_0 \cdot \frac{\theta}{2} \tag{3.23}$$

Now from equation 3.20, 3.21 and 3.23 we get the strain relationship as follows,

$$S = \frac{(R+t)\theta - R \cdot \theta}{L_0} \tag{3.24}$$

$$S = \frac{2t \cdot d}{L^2_0} \tag{3.25}$$

Thus the amount of electromechanical strain induced in the polymer is calculated from the geometrical analysis of the cantilever beam model above, where the expansion ratio of the polymer, i.e., the strain S induced in the polymer, is given in terms of the displacement of the free tip d, the thickness of the polymer t across which the electric field is applied and the original length of the polymer L.

In order to study the hysteresis effect of these polymers, an electric field is applied in sequence with a small time interval of about 150-200 sec between consecutive field applications. The first field is applied to yield the optimum displacement of the polymer film. Once the polymer sample is displaced with no further deformation, the field is zeroed. The next field is then reapplied once the actuated polymer relaxes back to the original, or zeroth, position. Figure 3.11 shows the zeroth and actuated positions of the polymer film upon applied electric field.

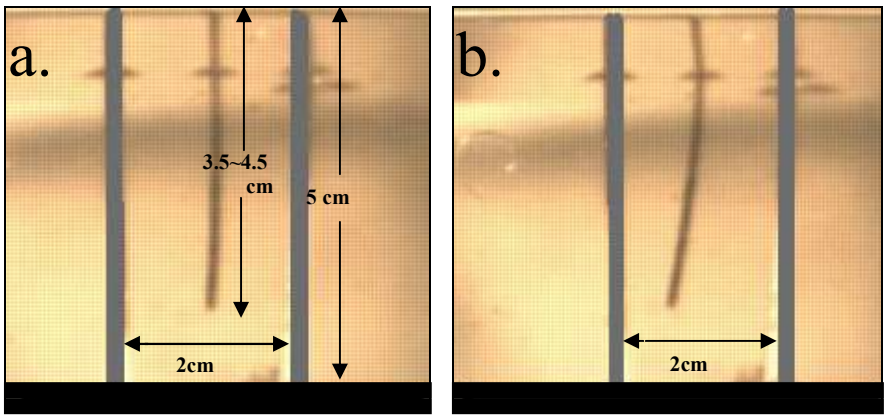

Figure 3.11: Polymer film displacement upon applied field: (a) electric field is zero, film at position zero; (b) electric field applied film displays actuation.

3.4.b Experimental Measurement Of Strain Induced Through The Thickness Of The Polymer

In section 3.4.a, the polymer is characterized for the strain yielded along the length of the polymer. The strain obtained in this case is along the length of the polymer and is referred to as the bending strain. In this section the polymer is characterized for the strain induced in the polymer through its thickness. In this case the electric field is applied parallel to the thickness of the polymer. The strain is induced through the thickness of the sample is also parallel to the applied field. Figure 3.12 shows the experimental set-up.

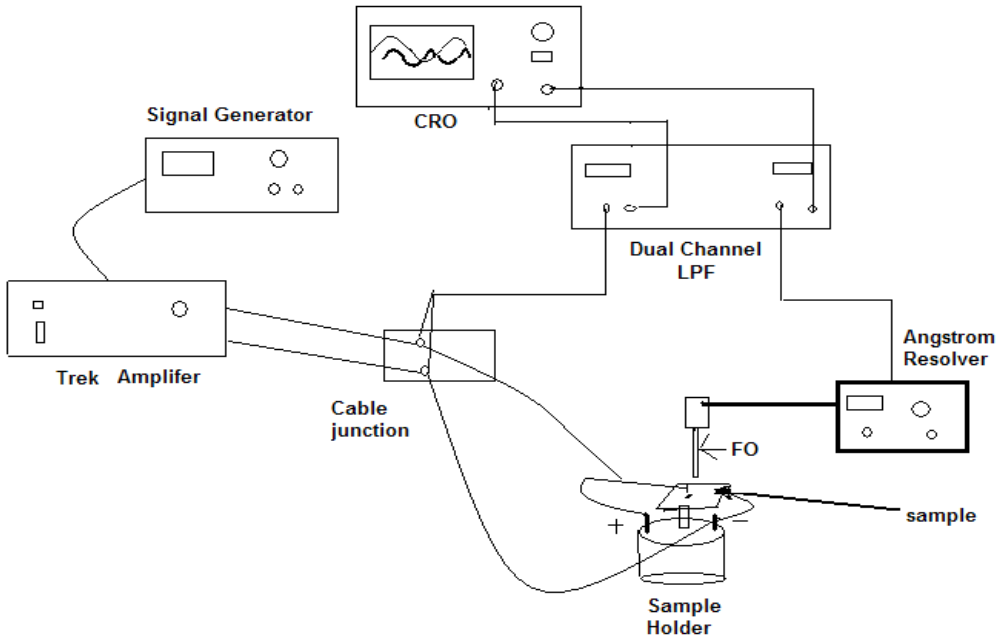

Figure 3.12: Experimental set-up for the strain through thickness measurement

The CN-PDMS polymer sample of about 1.5cm x 2cm is cut and the sample thickness is noted for each case (1.2mm to 1.5 mm). Further they are electroded on both sides by painting a very thin coat of high purity silver paint. The sample is then placed on a wooden sample holder using a thin double-sided tape as shown in Figure 3.13 below.

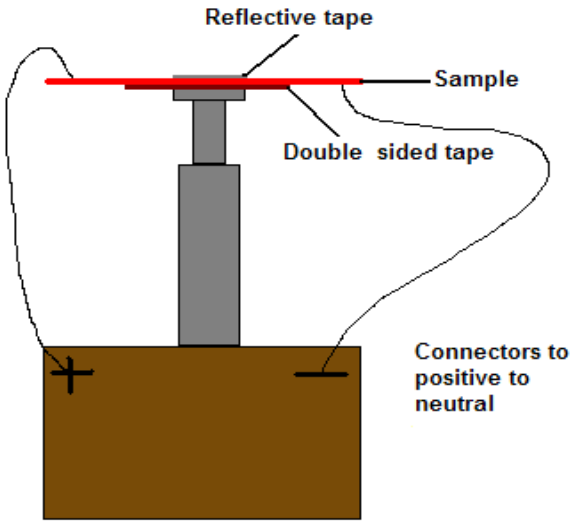

Figure 3.13: Electroded sample and holder

A very small piece of mirror tape is placed on the top surface of the sample. A Hewlett Packard signal generator model 33120 A is plugged to a Trek amplifier of gain 1000±20 V/V and further is an alternating current electric field from a range of 0.05 MV/m to 1.1MV/m is applied for a constant frequency of 1Hz is applied across the thickness of the polymer sample. The fiber optic probe of the Angstrom resolver series dual channel model 201 monitors the output of the sample. The output is measured on a Tektronix TDS 2024 oscilloscope. The input, i.e., the electric field, as well as the output of the polymer both are filtered before being monitored on the oscilloscope. The filter used in this measurement is a SRS 640 dual channel low pass filter from Stanford Research System, with a variable input and output gain. The filter adds the same phase lags to both signals, thereby giving the true phase difference between the signals. When an electric field is

applied to the polymer sample, the sample undergoes deformation in the form of change in thickness. The mirror reflects the deformation into the fiber optic sensor probe. The fiber optic probe of this resolver has two slopes, the front slope, which is for fairly small displacements with a linear range of ± 8.75x10^{-6} m; and the back slope, which is used in case of intermediate to large displacements (millimeter to centimeter) and has a linear range of ± 273.5 x10^{-6} m. In the present study, the front slope is used due to its higher sensitivity.

The strain induced in the thickness of the sample is obtained from the following equation,

$$S_t = \frac{D_t \cdot Scopesensi\ tivity}{A \cdot t} \tag{3.26}$$

Where S_t is the strain through the thickness of the polymer, D_t is the deformation of the polymer (output of the polymer in V) scope sensitivity is 0.196x10^{-3} m/V, A is the amplification factor in db and t is the thickness of the polymer sample in millimeter.

3.5 Charge /Current Measurement of CN-PDMS polymer system

Electrical properties such as load current, power consumption and capacitive behavior of the polymer material are necessary for the optimization of the system configuration and the design of efficient driving electronics. This becomes a crucial factor when developing biomedical applications, which demand compactness and lightweight.

Power consumed by the CN-PDMS polymer system as an actuator is the rate of energy required to excite the whole actuator system. It is a function of the peak applied voltage and the frequency of the applied signal[62]. In this measurement, the CN-PDMS

polymer is employed in the configuration shown in Figure 3.9. The sample is set to actuation by applying alternating electric field using a Hewlett Packard function generator model 33120 A and a Trek amplifier whose gain is1000± 20 V/V. The Trek amplifier has a current monitoring node, which is connected to a computer through a SRS Dual pass filter, which cancels the noise and amplifies the signal. This is further connected, to an oscilloscope where both the applied signal as well as the output of the load is read. Using Labview software, the current drawn by the load while being actuated is computed as a function of frequency and amplitude of the applied signal. The set-up of this measurement is shown in Figure 3.14 below.

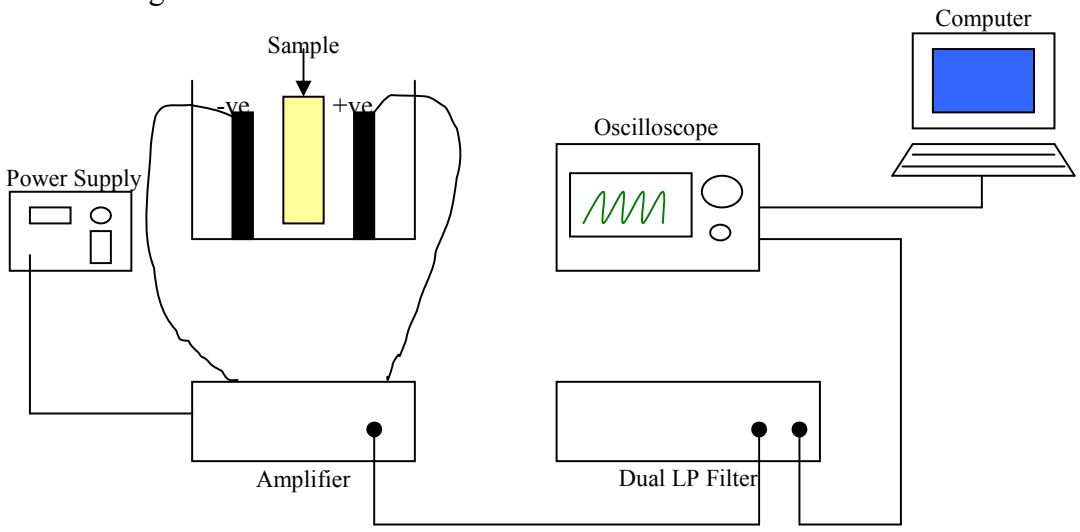

Figure 3.14: Load current measurement set-up

The frequency of the applied electric signal is maintained constant and the voltage is increased from 0 to 6 kV_{pp}.

3.6 Thermally Stimulated Current

Thermally stimulated current, commonly referred to as TSC, is one of the thermal analysis tests performed on the polymeric materials in order to obtain their structural information at the molecular level. It is also referred to as Thermally Stimulated Discharge (TSD) or thermally stimulated depolarization current (TSDC). It is a powerful tool for measuring the release of stored dielectric polarization in the form of charge or current. The charge in a dielectric polymer may be generated by various mechanisms, such as orientation of permanent dipoles, trapping of real charges by structural defects or impurities, or ionic or electronic build-up near inhomogeneities such as amorphous-crystalline interfaces in semi-crystalline polymers. The measurement of this charge is done by making use of the molecular mobility of the polymer under study. This analysis can be divided into three steps; in the first step the polymer sample is placed between two electrodes and a static electric field E_p is applied for a set amount of time t_p at a particular temperature T_p. This time t_p is called the poling time and the temperature T_p is known as the poling temperature. The poling time should be long enough for all the dipoles in the polymer sample to orient. In the second step, the sample is cooled at a very rapid rate while E_p is on, thereby freezing in the oriented dipoles. At the lower temperature, there is no or very little dipolar mobility. The electric field E_p is removed at this temperature and the sample is short circuited. This is done in order to eliminate any free electrical surface charge if any are present[63]. Such programmed and sequential relaxation or orientation of the dipoles in the polymer sample can be observed during the final step by linearly increase the temperature of the sample. The depolarization current is then measured as a function of

temperature. The spectra thus obtained show peaks, which are associated with characteristics features of the polymer, such as dipolar moments, glass transition temperature and melting temperature of the polymer. Figure 3.15 shows a cross section view of TSC machine. A SETARAM TSC 3000, automated TSC equipment, is used to track the relaxation processes in the dielectric polymers. The apparatus has a temperature range from -180°C to 400°C, and a voltage up to 500V. The sample is inserted in between two electrodes as shown in Figure 3.15 and Figure 3.16, and polarized by applying a voltage at a known temperature for a fixed time. The sample is then cooled with the electric field still on. In the next step, the sample is reheated at a constant rate (1 to 2°C/min), and the current is monitored. Heating of the sample at a constant rate accelerates the real charge decay, which can be observed as a current release. Current is monitored as a series of peaks, the shape and location of which can be related to dipole orientation and charge migration.

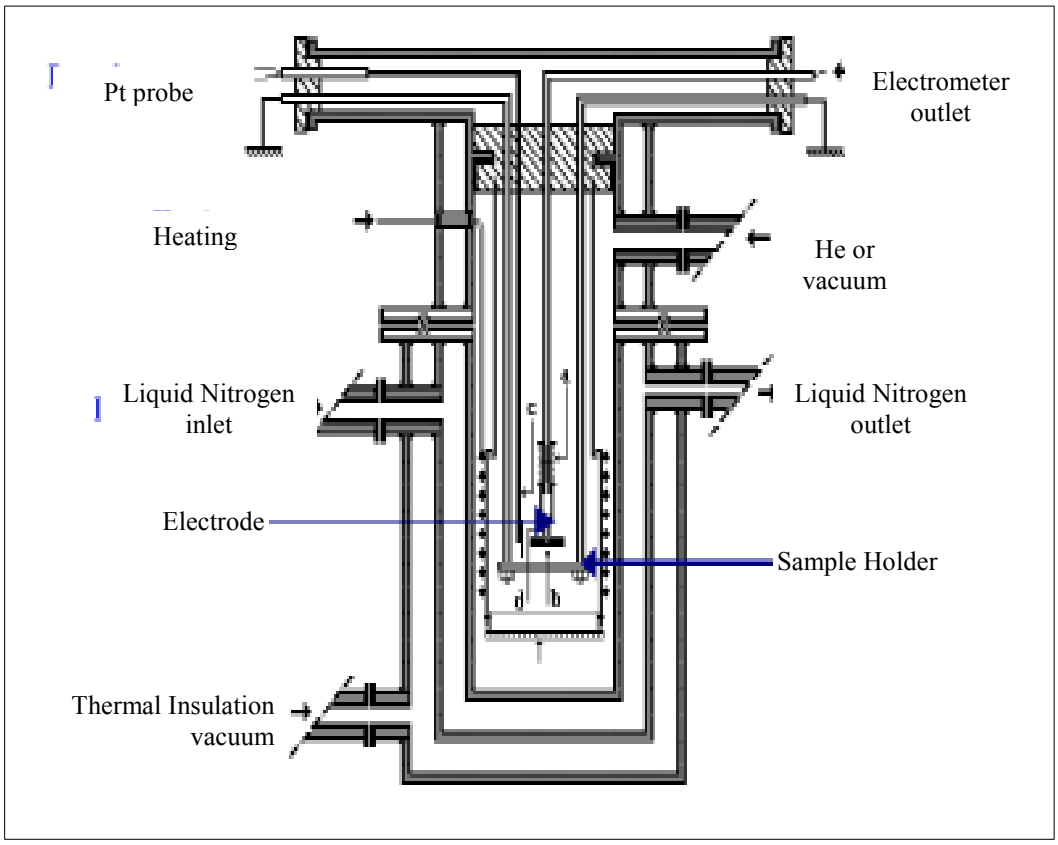

Figure 3.15: Cross-sectional view of the TSC machine. (Adapted from Reference [63])

Figure 3.16 is a magnified view of the electrodes between which the polymer sample is placed to perform the analysis.

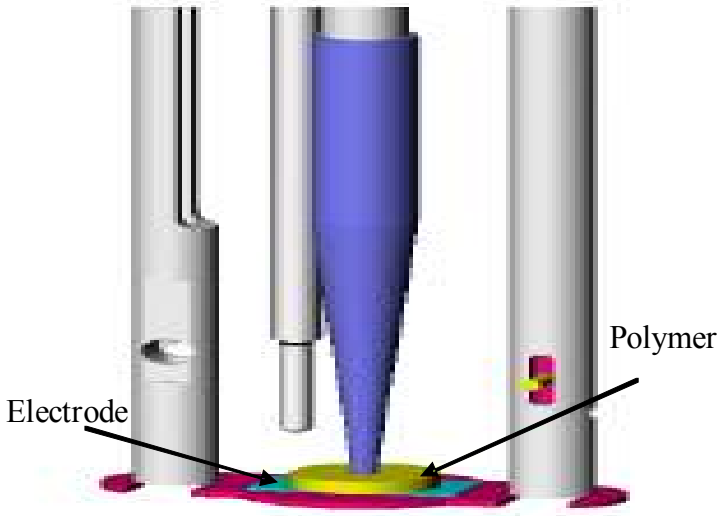

Figure 3.16: Electrode arrangement for the TSC (Adapted from Reference [63])

In the TSC analysis of the CN-PDMS polymer samples, the first heat or background run is done by starting at –70° C and heating to 80° C with a heating rate of 4°C/min. The second heat or the poling of the sample is done at a poling temperature of 80°C for a t_p of 5 min and poling field calculated depending upon the thickness of the polymer, as the ratio of maximum voltage across the electrodes and polymer sample thickness.

Then, as a third step, the spectra for the depolarization current as a function of temperature are obtained for each CN-PDMS samples and analyzed.

CHAPTER 4 RESULTS AND DISCUSSION

This chapter presents the results for the experimental tests conducted on the CN-PDMS polymer blend. It discusses each of the measurements presented in Chapter 3. The Differential Scanning Calorimetry and Thermally Stimulated Current measurements are performed on the polymer blend to analyze polymer properties such as the melting temperature of the polymer blend and its re-crystallization temperature. These tests also reveal the effect of polar CN functional pendant group on the PDMS polymer. Dielectric Spectroscopy is performed to obtain information about the segmental mobility of the polymer blend.

A dielectric theory is employed to validate the experimental dielectric data obtained from the CN-PDMS polymer blend. The electromechanical strain experiments are performed to evaluate the mechanism governing the actuation performance of the polymer.

4.1 Processing Of The Poly (Dimethyl Siloxane) Polymer With CN-Phenyl Cross Linkages

A series of CN-PDMS polymer blends are obtained with varying molecular weight PDMS base polymer. The resulting polymer contains various weight % of polar CN moieties cross-linked to PDMS. The resulting polymer blends are cast and thermally cured as mentioned in the processing section of Chapter 3. In order to check the completion of hydrosilylation in the polymer processing, H-NMR spectrum of the modified copolymer is

obtained where the spectrum showed no vinyl signals at 5.20- 6.20 ppm thus showing successful hydrosilylation. This test is performed at NASA Larc by Dr. Jason Rouse. This Vinyl eliminated copolymer is further cross-linked with CN-phenyl copolymer, which is the functional moiety of the polymer blend. The processing of the CN-PDMS blend is shown by the reactions of Figure3.1 in Chapter 3.This CN-PDMS blend is poured onto the PFA-Teflon dish and cured at 80 º C for a day or two. It is observed from the electromechanical strain measurements that although the polar elements are crosslinked to the poly (dimethyl siloxane), the blend may not have uniform distribution of dipolar elements. This is because when the polymer blend is poured into the Teflon dish and thermally cured; the curing being a surface reaction; possibly results into a concentration gradient across the polymer blend. Thus the side exposed to air may be less polar and the side of the polymer on the Teflon dish more polar. This observation during electromechanical strain measurements and telephonic discussions with Dr. Belcher, show that the CN-PDMS blend may possibly have the structure as seen in Figure 4.1.

Figure 4.2 shows the air side (non active side) and the non-airside (active side) of the CN-PDMS sample as discussed in this section. The electromechanical strain measurements are performed with keeping the side into consideration.

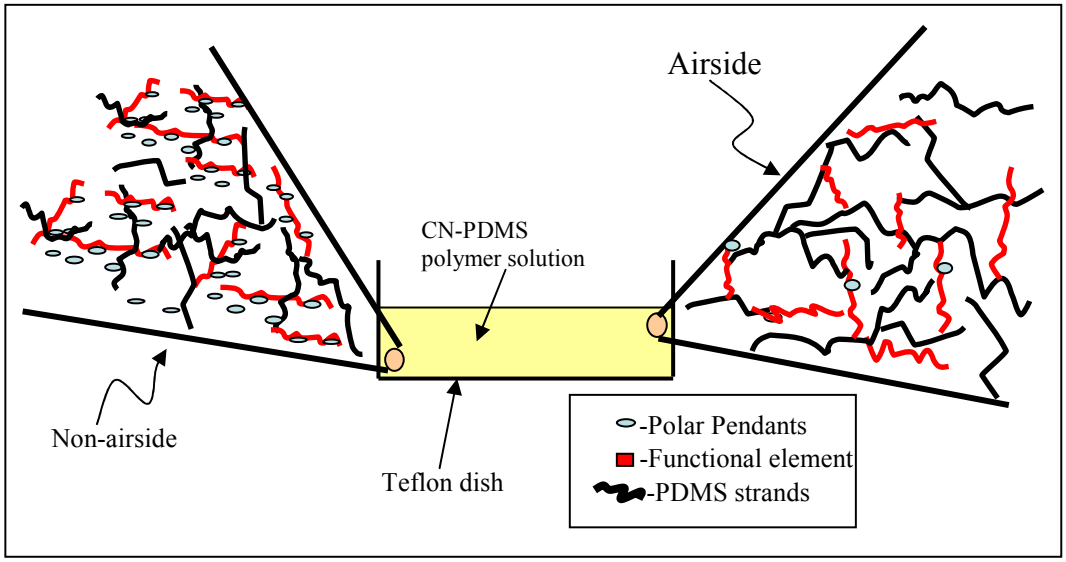

Figure 4.1: Settling of the functional elements when the CN-PDMS polymer blend solution is cured in a Teflon dish. (The magnified view of the polymer blend shows concentration of dipolar moieties at airside and non-airside of the dish.)

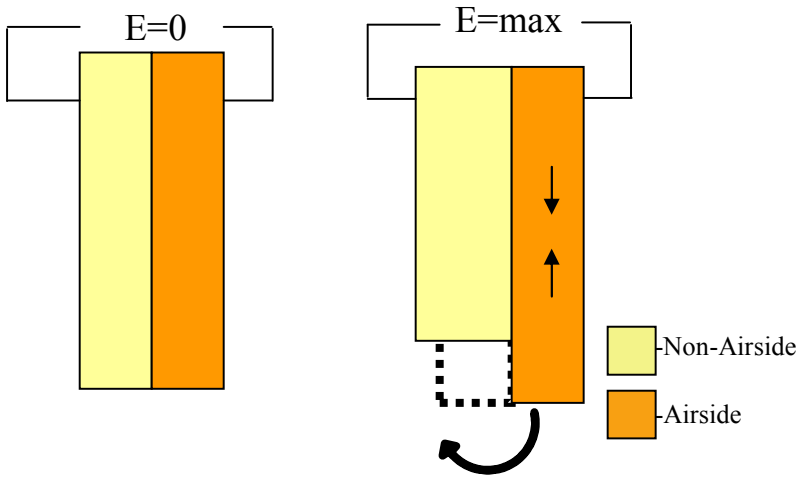

Figure 4.2: Airside and Non-airside of the CN-PDMS polymer blend.

(The arrows indicate the force of tension on the airside.)

4.2 Differential Scanning Calorimetry Analysis

Thermal characteristics of CN-PDMS polymer samples are evaluated, such as the melting temperature of the blend and re-crystallization of the polymer. Influence of factors such as molecular weight of the base polymer PDMS and of CN-phenyl element groups on the overall polymer blend are also assessed. The Differential Scanning Calorimetry is performed as discussed in section 3.2 of Chapter 3. A total of six samples are used for the analysis having different CN-phenyl content 3.1 to 8.6 % and different molecular weight from 9.4 to 28 k. A sample with no CN-phenyl group crosslinked to PDMS is tested as a control sample. The maximum dipolar content sample having 8.6 weight % of CN- phenyl gives a calorimetry plot as seen in Figure 4.3.The experiment is started from a low temperature of –80 º C, the sample is heated at a constant rate of 10 º C/ min. Figure 4.3 shows that CN-PDMS blend starts melting at ~ -50 º C. However on further heating the polymer sample, a sharp decrease in the heat capacity of blend is seen, indicative of an endothermic reaction-taking place. This reaction relates to the melting of the crystalline part of the CN-PDMS blend. When the first heat is applied to the 8.6 weight % sample, the endothermic peak is obtained at –44.23 º C. Cooling of the sample results into re-crystallization of the melted polymer. This is seen from the increase in the heat capacity of the sample shown by the exothermic peak in Figure 4.4, and this re-crystallization is observed at ~ - 73 º C. The melting point of the 8.6 % CN sample is further confirmed by the second heating cycle where the sample melted at –44.11 º C. Thus the 8.6 weight % CN sample shows a melting temperature of ~ -44.23 º C to ~ -44.11º C. This experimental melting temperature range is very much similar to the theoretical melting temperature for

pure poly (dimethyl siloxane) polymer i.e. – 44 ° C to – 22 ° C[64]. The sharp nature of the endothermic peak with absence of any minor peaks confirmed that CN-PDMS blend is processed to obtain uniform and stable blend avoiding formation of any unstable crystals. Generally, the unstable crystals are formed in poly (dimethyl siloxane) at low temperature during quenching of the polymer[64].

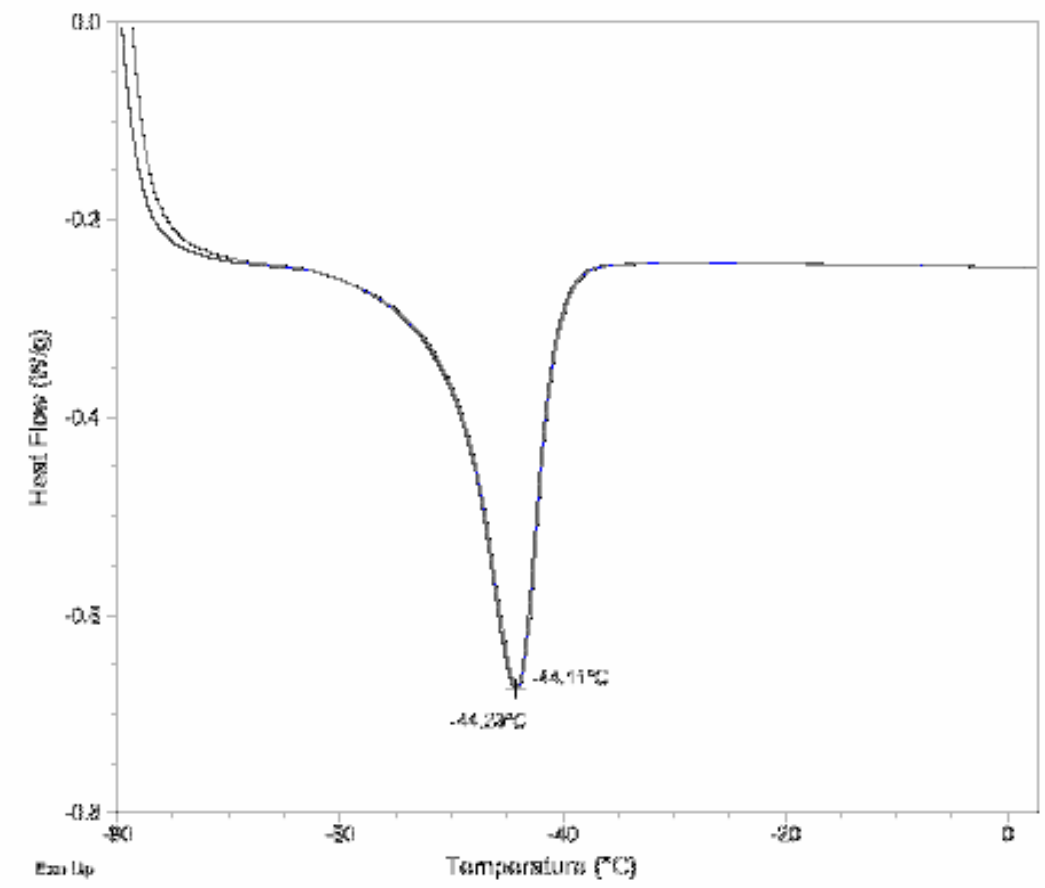

Figure 4.3: Differential Scanning Calorimetery done on 8.6 weight % CN sample.

The thermal characteristic for all the six samples with 3.3 weight %, 5.7 weight %, 6.1 weight %, 7.8 weight % and zero weight % (control sample) of the CN-PDMS samples found to be similar as shown by DSC.

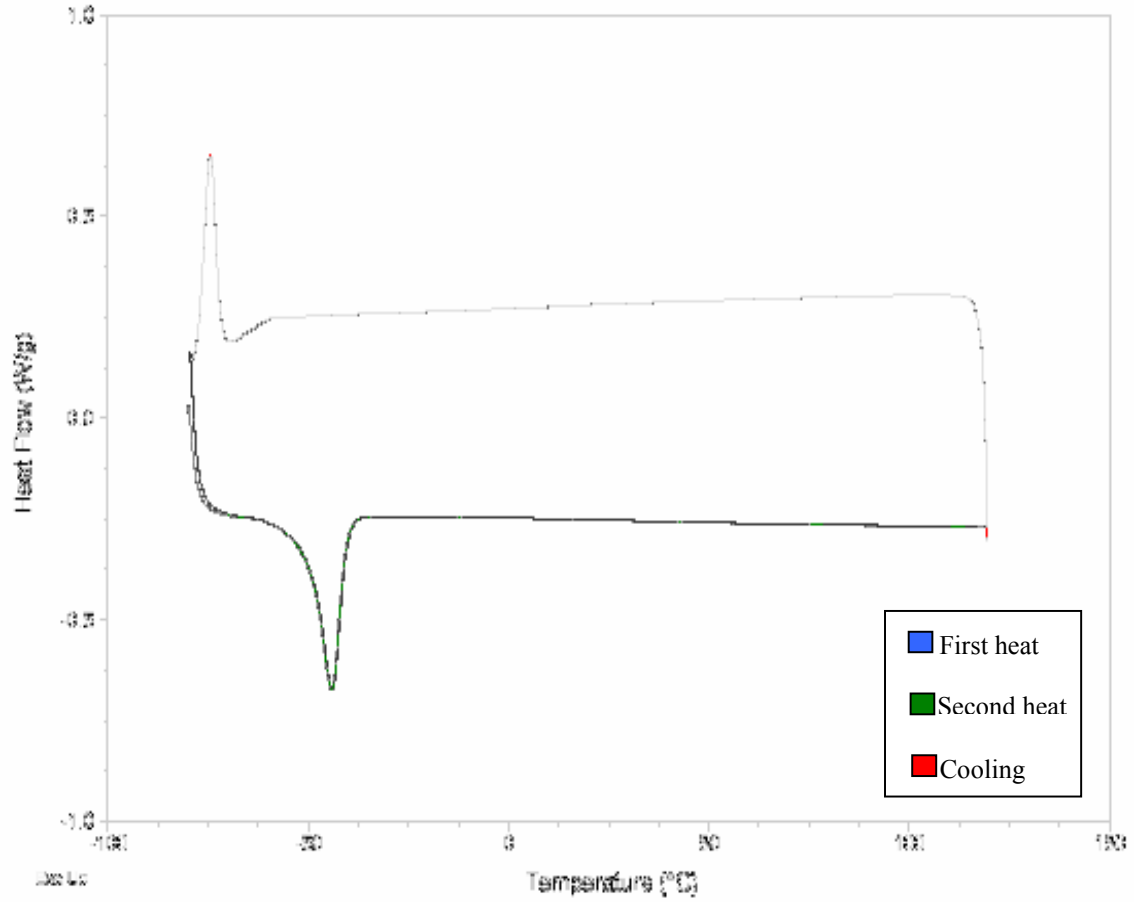

Figure 4.4: DSC plot of 8.6 weight % CN-PDMS sample showing the melting temperature as well as the re-crystallization.

Relatively similar range for the melting point is seen in the DSC of the control sample about – 46.46 ° C to – 46.23 ° C (Figure 4.5). The Table 1 below states the melting temperature range observed for each of the six samples on which the DSC is performed.

Thus, DSC can be taken as a proof that presence of CN-phenyl group does not alter the thermal properties of the PDMS blends.

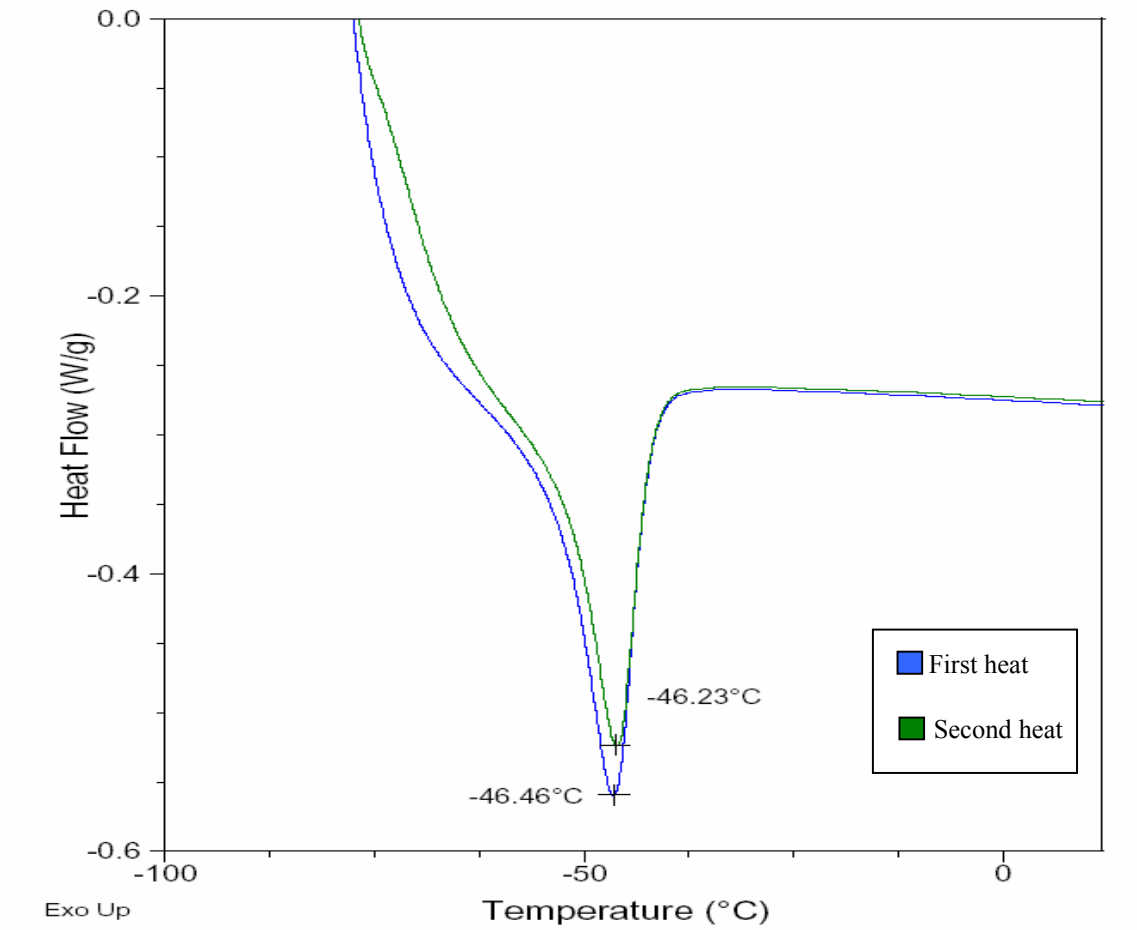

Figure 4.5: DSC done on the control sample.

Table 1: Melting range of the six CN-PDMS samples with varying weight % of dipolar content.

Sample Information	Melting Temperature Range (º C)
Control Sample (0 weight % CN-phenyl)	-46.44 to – 44.23
3.3 weight % CN-phenyl	-47.13 to – 46.49
5.7 weight % CN-phenyl	-47.50 to –46.93
6.1 weight % CN-phenyl	-46.36 to – 46.26
7.8 weight % CN-phenyl	-44.91 to –44.91
8.6 weight % CN-phenyl	-44.23 to –44.11

4.3 Dielectric Measurements

The dielectric properties of the CN-phenyl functionalized poly (dimethyl siloxane) polymer blend are measured, to establish a point of reference on the performance of the polar component of the CN-PDMS blend. The dielectric spectroscopy is performed on the CN-PDMS polymer blend having varying molecular weight and varying weight % CN-phenyl moieties cross-linked to the polymer. These tests are performed as discussed in section 3.3 of Chapter 3. The dielectric constant for CN-PDMS samples having weight % CN-phenyl from zero to 8.6 % is plotted over a frequency range of 20 Hz to 1 MHz, for the samples having molecular weight of 28 k (Figure 4.6). It is seen from the plot that for 20 Hz, the dielectric constant observed is higher (10.0 ~ 21.5) as compared to that at 1kHz or 1MHz where the dielectric values stabilize to values around 4.0~9.0. The dielectric properties at lower frequencies have contributions from the dipolar polarization as discussed in Chapter 3. Since the frequency is low, the dipolar polarization which is a

slower mechanism gets sufficient time to take place and contribute significantly towards the dielectric value (Figure 4.6). At the same time, as the frequency of the measurement is increased it is observed that the dielectric value drops considerably and stays relatively constant, thus showing that at higher frequency the slower mechanism drops out leaving only faster mechanism i.e. atomic and electronic polarization to persist. Thus at 1 kHz frequency which is regarded as the standard frequency for dielectric constant, it is the dipolar functional moieties present in the polymer blend which contribute towards the dielectric value.

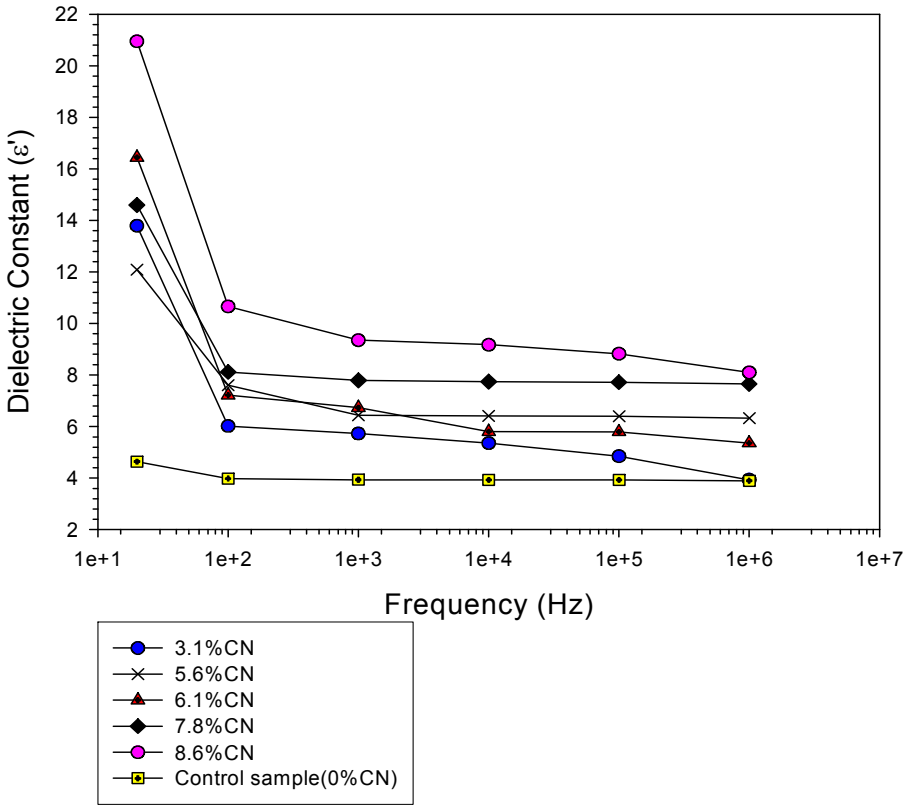

Figure 4.6: Comparative plot of CN-PDMS samples having varying weight % concentration of the functional moieties.

This is also confirmed from Figure 4.6, as the weight % of the polar functional component is increased there is an increase in the dielectric constant of the CN-PDMS samples, thus supporting the dielectric spectroscopy theory discussed in Chapter 3. It is observed that the dielectric constant of the control sample remains fairly constant as expected varying from 4.6 to 4.0 over a frequency range of 20 Hz to 1MHz. The value for the dielectric constants for other non zero weight % CN samples are well above the control samples varying from ~10.5 to ~5.0 over the same frequency range of 20 Hz to 1 MHz. Owing to the wide frequency range for which the dielectric measurements are done, the dielectric spectroscopy shows that the varying molecular weight of the base polymer which is poly (dimethyl siloxane) from 9.4 k to 28 k does not have any contribution towards the dielectric properties of the over all CN-PDMS polymer blend. This can be seen from Figure 4.7, here the dielectric constant of CN-PDMS samples for varying molecular weights of 9.4 k, 17.2 k and 28 k as well as varying CN content from zero weight % to 8.6 weight % are plotted for 1 kHz frequency, giving a linear trend. These measurements show that the control sample, a pure PDMS has relatively constant dielectric value for all the three molecular weights mentioned above. And as the weight % of the CN-phenyl pendants is increased the dielectric value shows relative increase, irrespective of the molecular weight of the sample.

The samples having ~8.0~8.6 weight % CN-phenyl content show fairly similar dielectric constant of ~9.6 to ~ 7.0 for the 9.4 k, 17.2 k and 28 k molecular weight of the blends. Similarly for the samples with ~ 5.0 to ~ 6.2 weight % CN-phenyl but different molecular weights, the dielectric values are in the range of 7.0 to ~ 5.5.

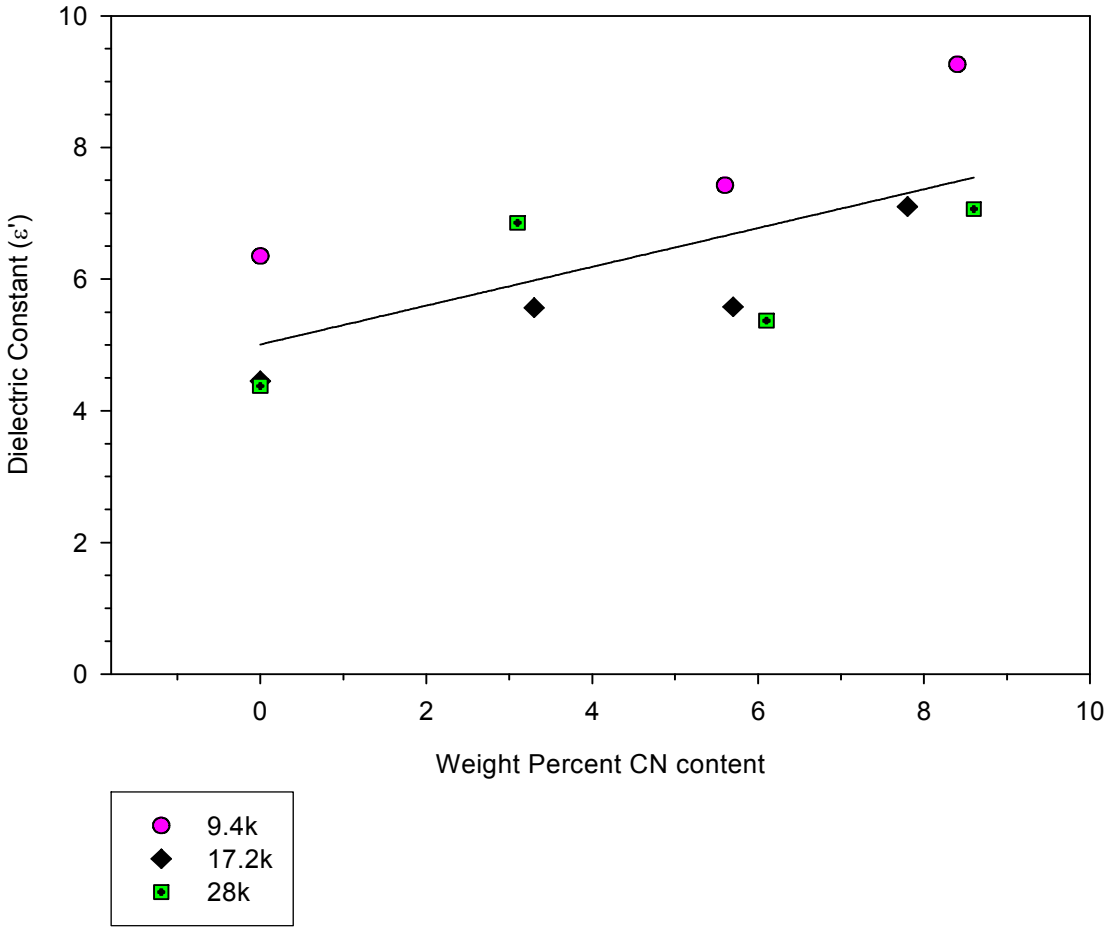

Figure 4.7: Cumulative plot of the dielectric constant of polymer films with varying molecular weight as well as varying weight % of CN-phenyl dipolar functionalities.

(The solid line indicates the linear trend line while the geometric symbols indicate the data points.)

Once the relation between the frequency and the dielectric values for the different CN-phenyl samples is established, the samples are tested to analyze the effect of temperature on the dipolar motion of the CN-PDMS polymer samples as a function of

frequency of measurement. Four samples are tested having 3.1 weight % CN-phenyl, 6.1 weight % and 8.6 weight % samples and a 0 weight % -phenyl. The experimental conditions used are the same as mentioned in section 3.3 of Chapter 3.

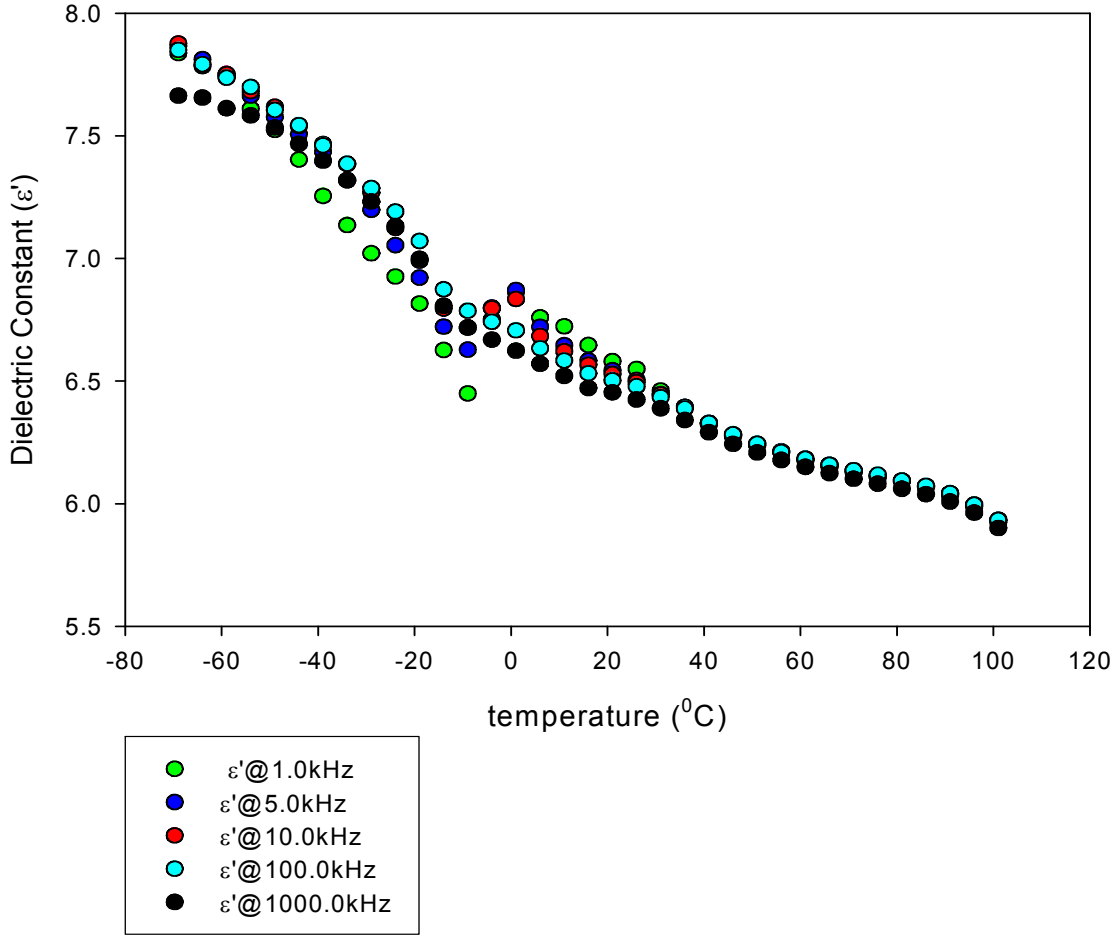

Figure 4.8: Dielectric constant of a control sample as a function of temperature and frequency.

The control sample shows similar trend for frequencies from 20 Hz to 1 MH showing that dielectric constant is independent of frequency in this range. The dielectric constant shows a steady decrease from ~ -44 º C to 100 º C. It reduces sharply around ~ - 36 º C to ~ - 20 º C. This transition is most likely due to the melting of the crystalline phase of the polymer blend .The melting temperature T_m of poly (dimethyl siloxane) is –44 º C to - 22º C as mentioned above in section 4.2 of Chapter 4.

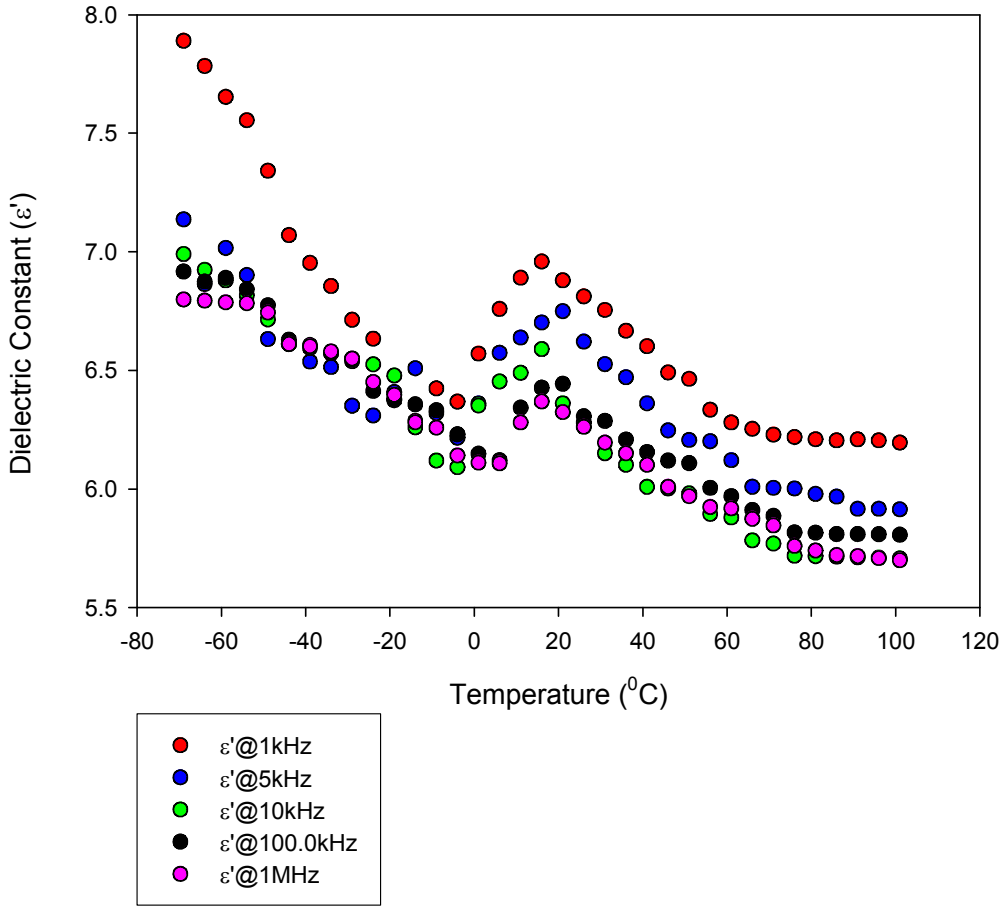

Figure 4.9: Dielectric Constant of CN-PDMS sample with 3.1 weight % CN-phenyl as a function of temperature and frequency

Figure 4.9 presents the dielectric constant of 3.1 weight % CN-phenyl. The dielectric constant shows a similar trend at every frequency. There is a steep decrease with the increase in the temperature from –80 º C to ~ 0 º C and further showing a steady increase in the dielectric value seen from 0 º C to 20 º C. The area under the peak is seen to decrease with increase in frequency. For instance, the magnitude of the peak for 1 kHz is greater than the magnitude of the peak at 1 MHz. This trend supports the theory of Dielectric Spectroscopy presented in the experimental section of Chapter 3, which states that as the frequency increases, the slower mechanism drops off. Thus at frequencies such as 100 Hz to 1kHz, all the dipoles tend to orient themselves and contribute towards the total charge on the surface of the sample which is then measured by the LCR meter. As the frequency increases, the dielectric constant value tends to decrease since the contribution to the total charge is only due to the faster mechanism such as the electronic polarization or atomic polarization.

A similar trend is observed for the 6.1 weight % CN-phenyl sample (Figure 4.10).The decrease in the dielectric value from –50 º C to around –20 º C can be attributed to melting of the CN-PDMS polymer blend.

It is observed that around room temperature the value of the dielectric constant for each of the samples from control to 8.6 weight % CN-phenyl samples are relative to the CN content, i.e. the 8.6 weight % sample shows higher value for the dielectric constant for the same frequency and same temperature range than the 6.1 % CN-phenyl and other lower CN-phenyl content samples (Figure 4.9).

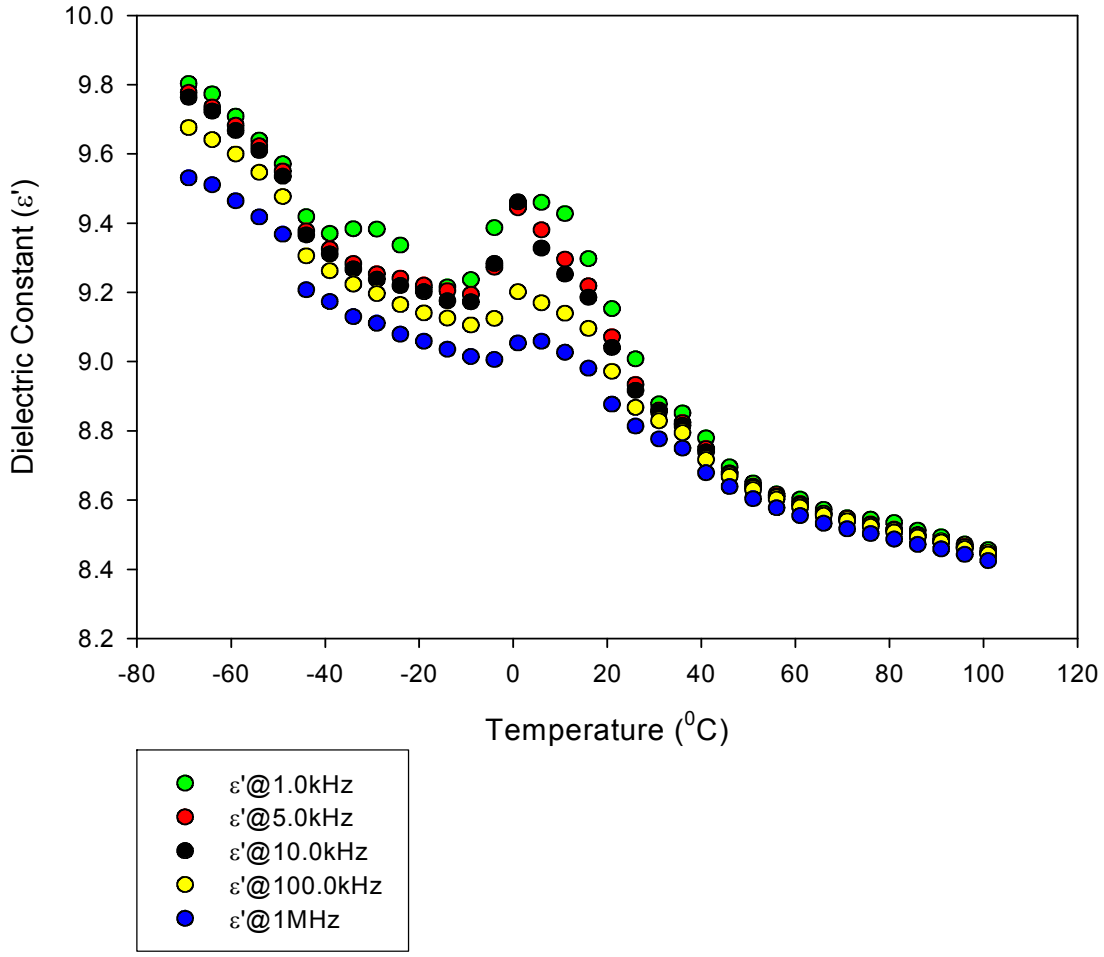

Figure 4.10: Dielectric Constant of CN-PDMS sample with 6.1 weight % CN-phenyl as a function of temperature and frequency.

In case of the 8.6 weight % CN-phenyl sample the Dielectric Spectroscopy shows a similar trend as seen in 6.1 and 3.3 weight % CN-phenyl samples. The dielectric value decreases with increase in the frequency as well as temperature from -80 º C to 0 º C. However the dielectric value is seen to be having an increasing trend for a lower

temperature range of –20 º C to ~ 20 º C. This behavior of the 8.6 % CN sample is possibly due to the higher weight % CN-phenyl content.

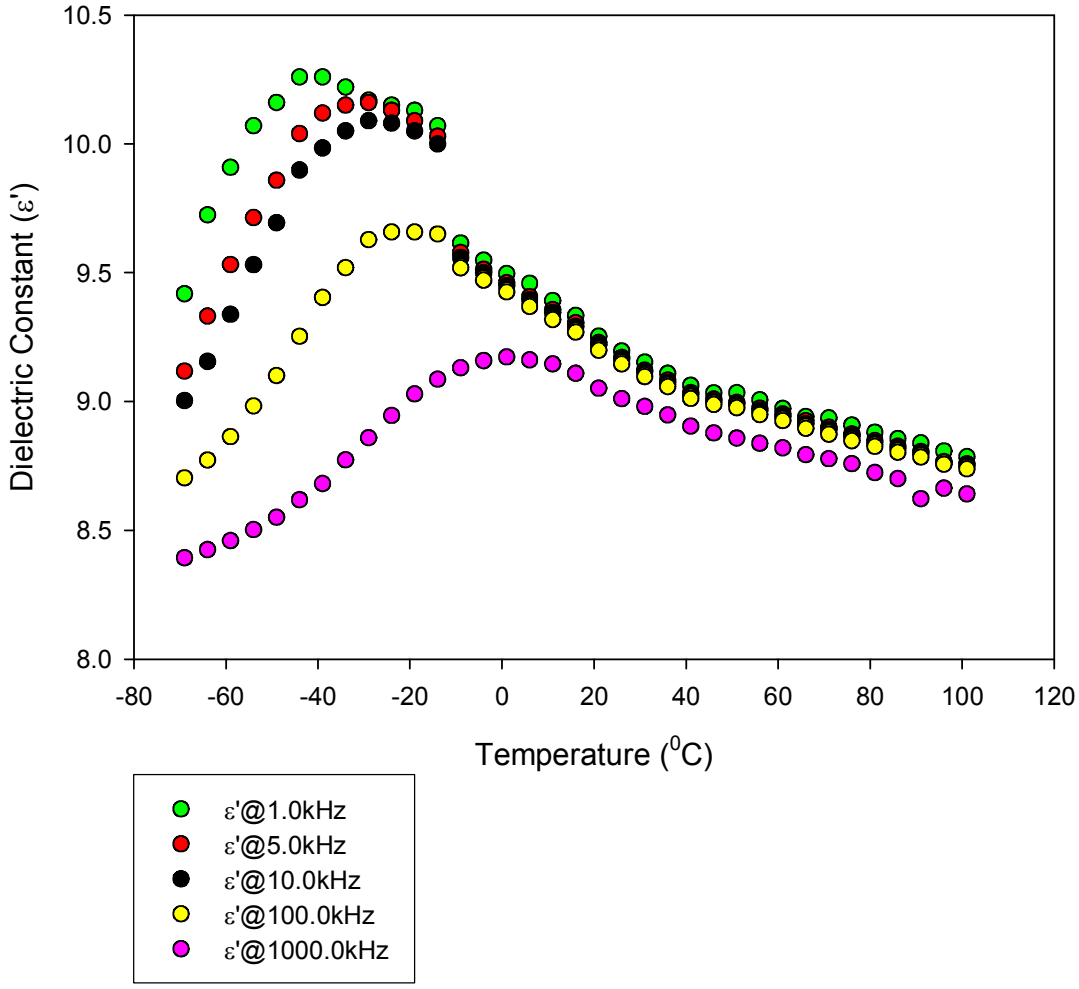

Figure 4.11: Dielectric Constant of CN-PDMS sample with 8.6 weight % CN-phenyl as a function of temperature and frequency

4.4 Strain Analysis

The electromechanical strain induced in the CN-PDMS polymer blend is measured in two configurations; strain induced along the length of the polymer and strain induced through the thickness of the polymer. In each of these strain measurements, a relationship between the dipolar functional elements and the magnitude and frequency of applied electric field is developed. This part of the study evaluates the driving mechanism of the polymer blend and analyzes the factors affecting this mechanism.

4.4.a Strain Induced Along The Length Of The Polymer

The electromechanical strain induced in the CN-PDMS polymer is measured using the experimental set-up shown in Figure 3.9, Chapter 3. The strain induced on application of the electric field is calculated using equation 27. It is observed that with the increase in the electric field, there is a non-linear (quadratic) increase in the strain induced along the length of the polymer. (Figure 4.13).This result indicates that the electromechanical strain induced in the polymer blend containing 8.6 weight % CN- phenyl moieties increases with the increase in the electric field. It is observed during the strain measurement that non-air side of the polymer seems to be active as compared to the air side. This is evident from the direction of the bending deformation. When a direct current electric field is applied along the length of the polymer sample such that the non-airside faced the positive electrode while the airside faced the neutral electrode as seen in part a of Figure 4.12, the sample bends towards the positive electrode. Further on switching the electrodes such that the non-

airside is now facing the neutral electrode as seen in part b of Figure 4.12, the sample bends towards the neutral electrode.

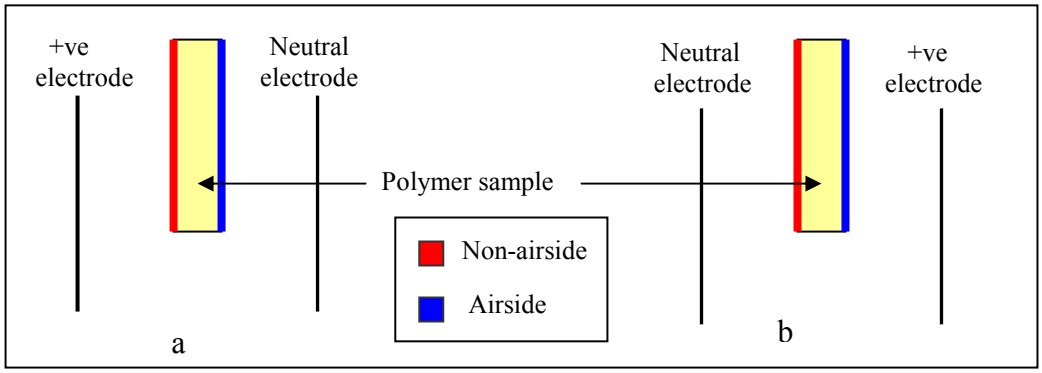

Figure 4.12: Arrangement of the polymer sample with side consideration.

This shows that the sample always bends towards the non-air side. The possible cause presented in section 4.1, where settling of the dipolar elements at the bottom of the Teflon dish would possibly make the non –air side more active than the airside. The source of the bending deformation when field is applied to the polymer is the contraction in the plane of the CN-PDMS polymer. It is observed that the dipolar functional elements in the polymer blend respond to the electric field by aligning along the direction of the electric field. The dipole alignment results in expansion in thickness of the non-airside, however in order to maintain a constant volume, the length of the non-airside decreases. This contraction in the length is constrained by the airside, the non-active side of the polymer blend. Thus the planar contraction is translated into bending displacement.

From Figure 4.13 it is seen that strain is related to the electric field by the following equation ($R^2 = 0.99$):

$$S = 0.4825\,E^2 \qquad (4.1)$$

Where S is the electromechanical strain induced in the polymer sample and is unit less (m/m) while E is the electric field applied across (MV/m). This equation shows quadratic nature of the electromechanical coupling between the strain and the field.

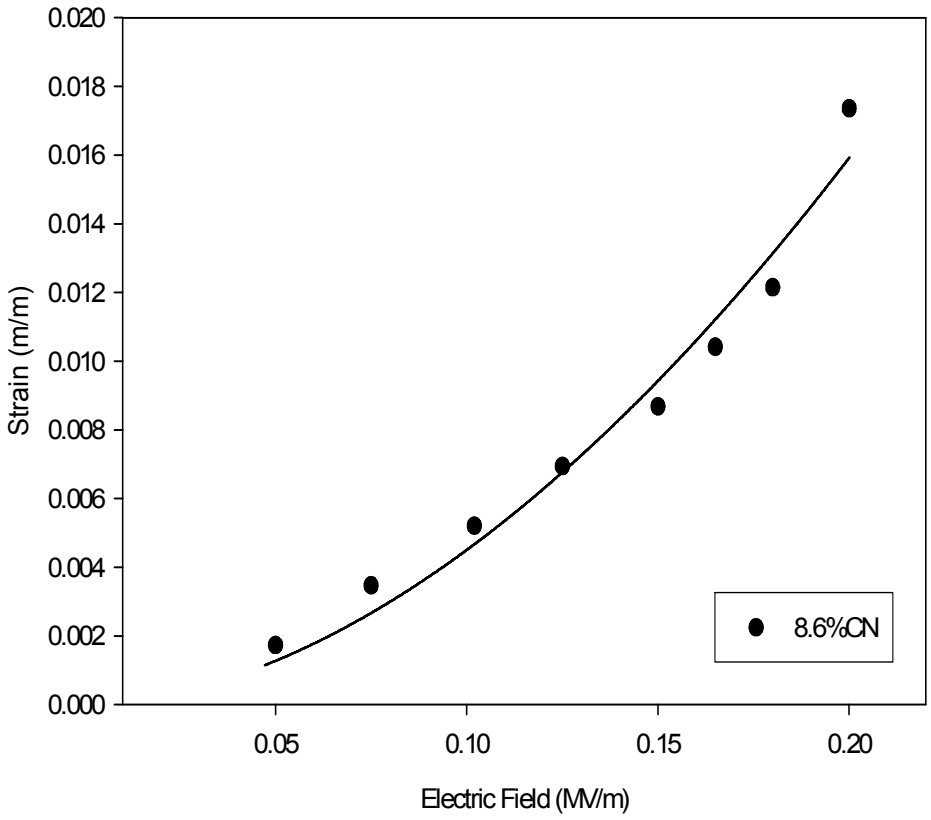

Figure 4.13: Electromechanical strain induced along the length of CN-PDMS sample as a function of electric field.

(The solid line indicates the trend of the induced strain, shown by the solid marks.)

A maximum of 1.75 % strain is induced along the length of the polymer blend for an electric field of 0.2 MV/m (Figure 4.13). From this plot it is seen that the percent-induced strain has a linear relationship with the square of the electric field ($R^2 = 0.996$). The electric field related electromechanical coupling coefficient is the denoted as M. The charge related electrostrictive coefficient Q is obtained from the following relationship:

$$S = 40.90 \cdot E^2 \tag{4.2}$$

For 8.6 weight % CN-phenyl containing sample the dielectric constant is 9.12 at 1kHz, thus M = 4090×10^{-16} (m^2/V^2) and Q is 93.83×10^6 (m^4/C^2).

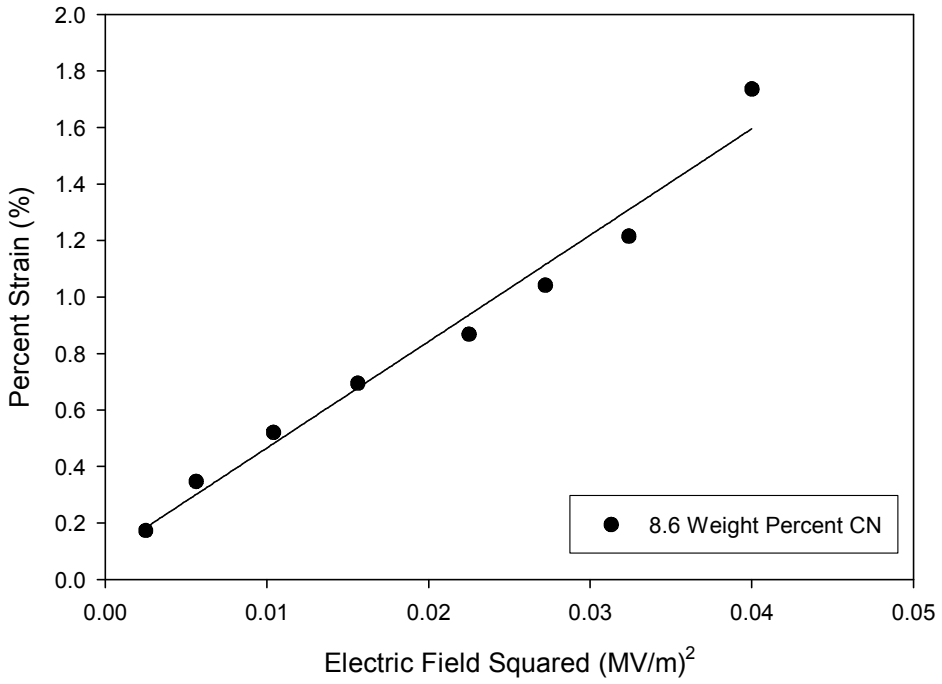

Figure 4.14: Percent strain in 8.6 weight % sample as a function of electric field squared.

(The solid line indicates the linear trend while the solid dots are the data points.)

In order to evaluate the strain rate of the CN-PDMS polymer blend, the strain induced along the length of the samples is analyzed as a function of time. Figure 4.15 shows a comparative plot for three samples having weight % CN-phenyl from 3.1 %, 5.6 % and 8.4 % and of the same molecular weight (9.4k). The sample actuation time was recorded and this test was used to evaluate the strain rate in each of the CN-PDMS sample. The time taken by the polymer samples to retract back from the maximum actuation stage is defined and is referred to as 'settling time '.

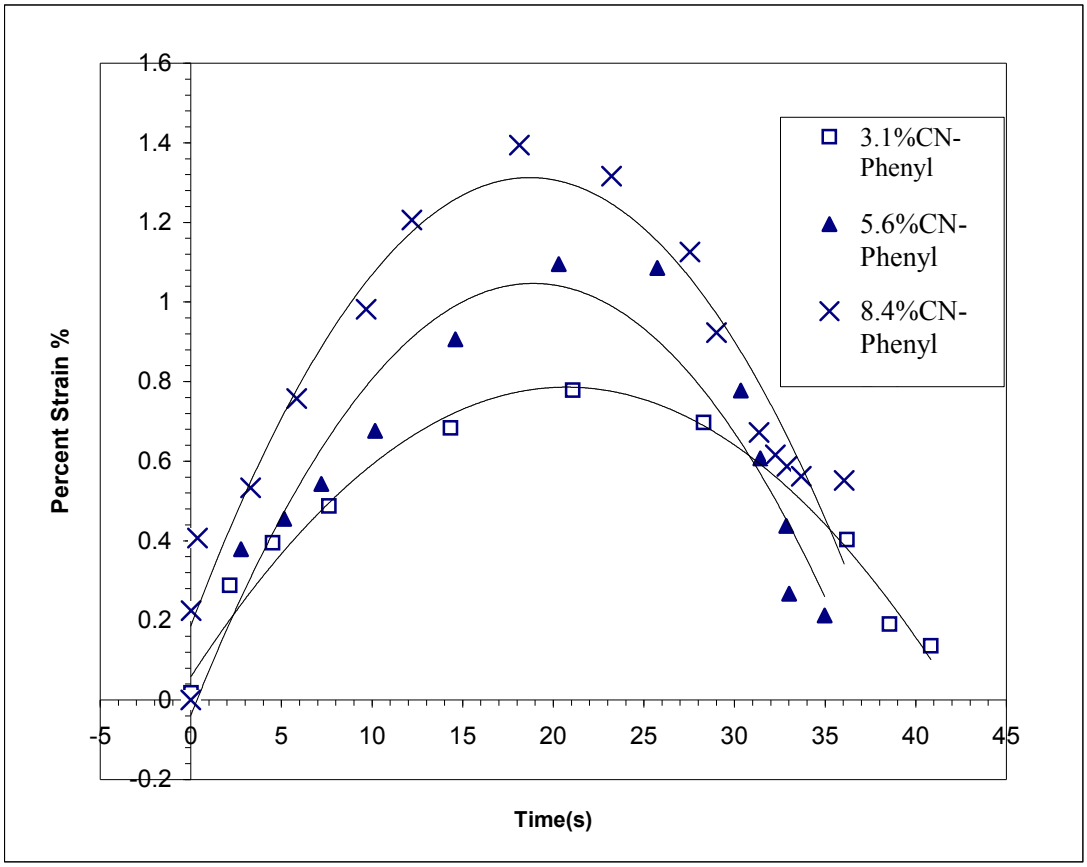

Figure 4.15: Comparative plot of the percent along the length of the polymer sample as a function of weight % CN-phenyl content of the polymers over the time of actuation.

(The solid lines indicate the trend of the strain rate while the solid symbols are the data points.)

Figure 4.15 shows that the lower CN-phenyl containing sample (3.1%) starts undergoing bending deformation at a later time relative to the higher CN-phenyl (8.4%) sample, which starts actuation as the electric field is applied. Also it is seen that for the same period of time and for the same electric field, the 8.4 weight % CN-phenyl sample produces highest deformation and thus the induced strain in the 8.4 % CN-phenyl sample is much higher than the strain induced in 3.1 % CN-phenyl sample. Table 2 presents the strain rate of the CN-PDMS sample presented in Figure 4.15.

Table 2: Percent electromechanical strain induced in the CN-PDMS polymer samples.

Weight Percent CN-phenyl content in the polymer blend (%)	**Electromechanical Strain rate**
8.4	0.0006[(m/m)/s], $R^2 = 0.989$
5.6	0.0005[(m/m)/s], $R^2 = 0.992$
3.1	0.0003[(m/m)/s], $R^2 = 0.992$

The higher strain rate is indicative of the higher dipolar polarization seen in 8.4 weight % CN-PDMS sample.

It is observed during this experiment that once a sample undergoes maximum actuation, it starts retracting back and the time taken by each of the three samples is different. For instance the 8.4 % CN-phenyl sample retracts back at a faster rate and has relatively small settling time. On the other hand the 3.1 % CN-phenyl sample remains in the actuated position for longer duration and also has higher settling time. The 3.1 % sample has a settling time of about 25 ~30 s as compared to a 8.4 % sample having settling

time of ~17 to 20 s. Thus from this experiment it can be concluded that the higher the percent of dipolar functional elements cross-linked to PDMS higher is the response time.

Using the camera software the velocity of the three different points along the CN-PDMS sample is measured. These three points are such that the first point is the free tip of the polymer strip, the second is the intermediate point, along the length of the strip, and the third point is just below where the polymer strip is held by the sample holder. The three points are as seen in Figure 4.16.

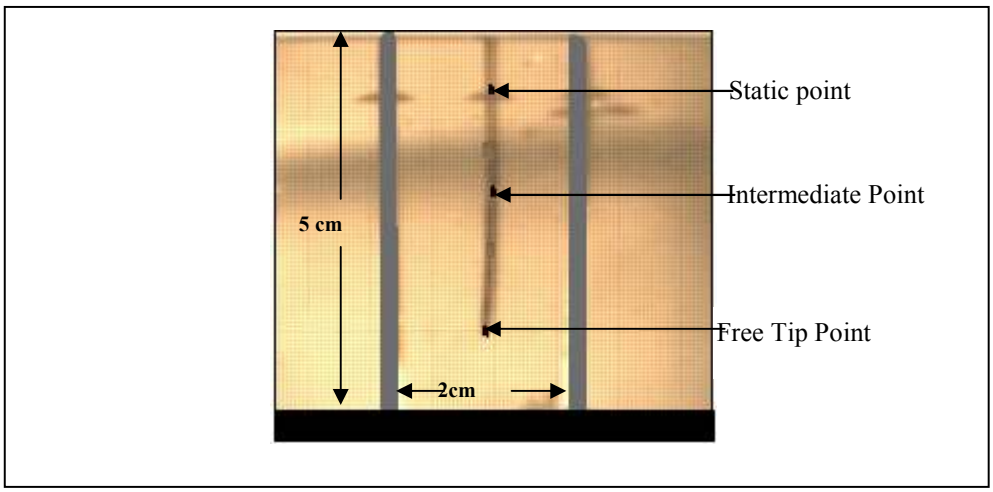

Figure 4.16: The three points along the length of the CN-PDMS sample suspended between two metal electrodes.

Once the bending deformation is captured by the camera, using the video analysis software the three points are marked along the suspended sample of CN-PDMS polymer (Figure 4.16). The software measures the displacement of each of the points and gives the velocity at which the free end and the other ends displaced. Figure 4.17 shows the

comparison between the velocities for each of the polymer sample having molecular weight of 9.4k.

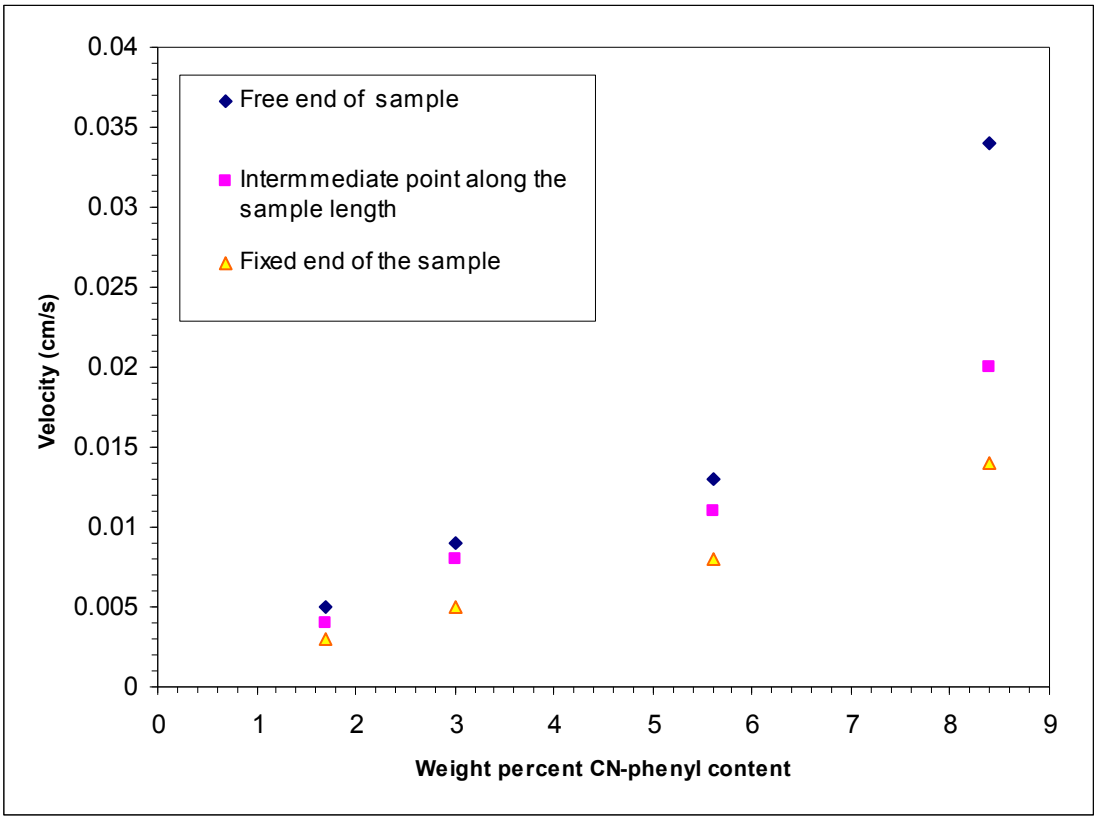

Figure 4.17: Velocity profile of the polymer films as a function of weight % CN- phenyl content.

From Figure 4.17, it is observed that the free tip has the maximum velocity compared to the intermediate and the fixed end. This plot also supports the assumption on constant curvature arc on application of uniform load. When the CN-PDMS samples are further analyzed, an interesting feature is observed; the sample tends to undergo bending deformation with increase in the field, then returns to the original position, however on immediately reapplying the field, the bending observed is more than in the first electric

field application. This effect seen in the CN-PDMS samples is referred as the ‘memory effect’ or ‘hysteresis’ because the sample remembers some part of the strain and on re-application of electric field the strain magnitude is enhanced. This memory effect is better followed in Figure 4.18. Figure 4.18 shows the data obtained for a 3.1 weight % CN-phenyl of length 4.1 cm suspended between two electrodes 2cm apart. The time interval between each field application is 25 s to 30 s. It is observed from this experiment that on application of electric field, the dipoles start aligning along the direction of the field due to polarization. Once the electric field is removed, the dipoles start to somewhat reorient randomly, but some dipoles do not lose their orientation completely; this is evident from the bending displacement obtained on re-application of the field for the second time. During the second or the consecutive field application, the orientation of the dipoles takes places for a lower value of electric field and actuation is faster as compared for the first field application. This phenomenon is also observed by Watanabe et al[65] where experiments performed on polyurethane show hysteresis effect on intermittent application of electric field.

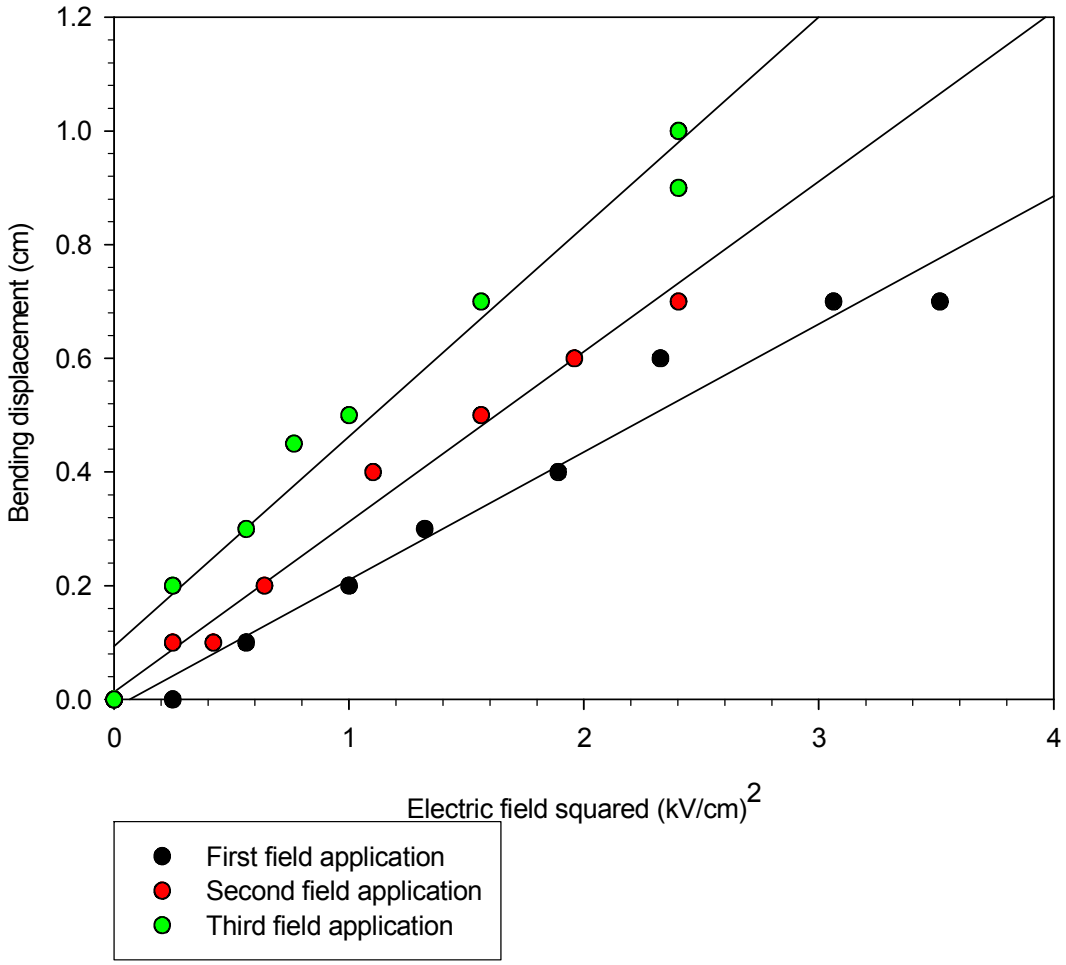

Figure 4.18: Memory effect shown by the polymer when electric fields are applied in sequence; an interval of 25 –35 seconds is allowed between each application.
(The solid line indicates the linear fit while the geometrical symbols represent the data points).

Table 3 gives the trend obtained for each of the three-field application and the displacement obtained for each case.

Table 3: Memory effect of CN-PDMS polymer sample.

Field Application (kV/cm) ^{2}	**Strain (cm/cm)**
First instance of field application	Strain = 0.585*field^2, R^2 = 0.908
Second instance of field application	Strain = 0. 665*field^2, R^2 = 0.952
Third instance of field application	Strain = 0.886*field^2, R^2 = 0.978

In the alternating current field analysis, two types of waveforms are used for better evaluation of the electromechanical strain developed along the length of the polymer samples. In Figure 4.19, the sample displacement from a single cycle of alternating current input has two cycles for every signal input cycle thereby showing it's trailing up with the signal applied to it. It is seen that for every single input cycle, there is a double cycle of the output displacement. This behavior further identifies the electrostrictive nature of the polymer sample. The output of the sample is not linear with the input, but on the contrary has a quadratic relationship with the input signal.

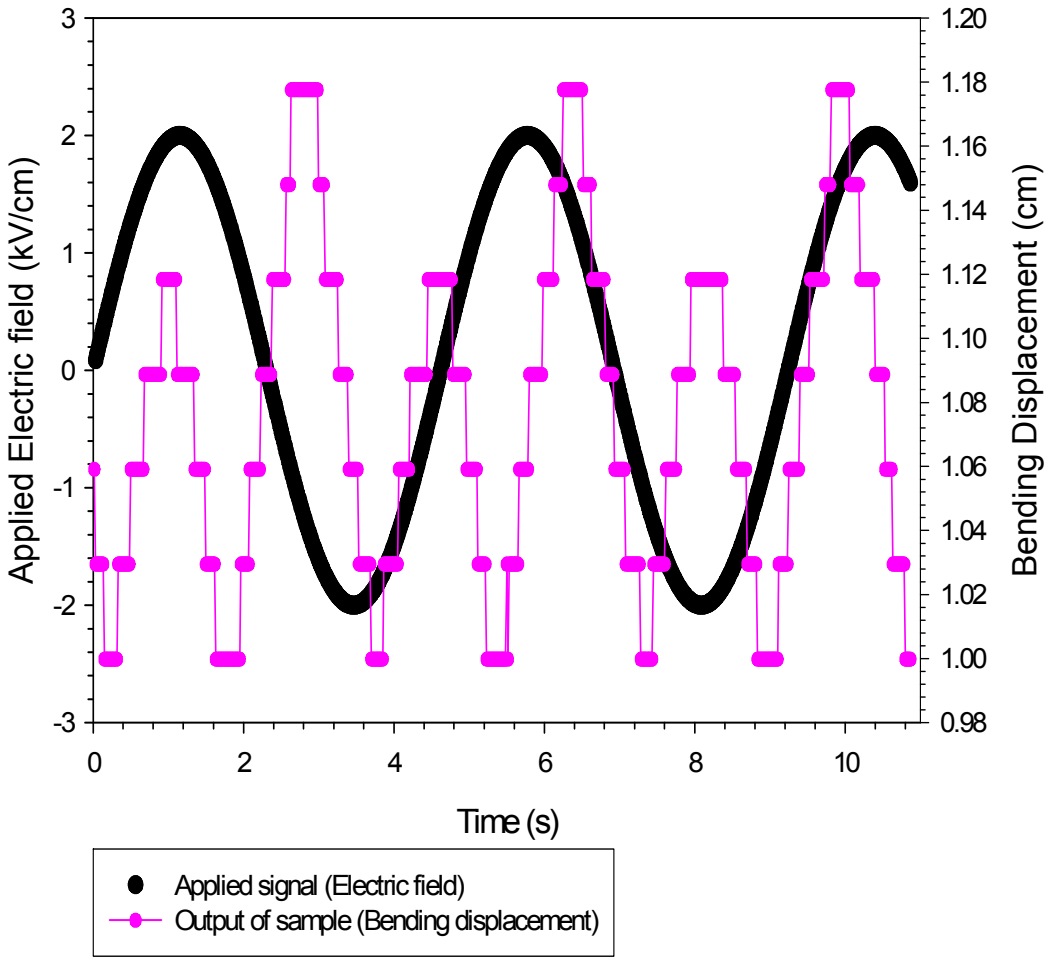

Figure 4.19: Polymer response upon applied alternating current field (sine wave).

When a square wave is applied to the same sample, a similar trailing behavior of the output displacement to the applied field of the sample is observed. This is seen in Figure 4.20. For every single input cycle a double output is obtained. However it is seen that unlike in the case of a single cycle of a sine wave, for the single cycle of a square wave the output displacement completes two cycles having same amplitude. This is

because in case of square wave, the dipoles have more time to orient themselves in the direction of the field. Since in square wave, electric field is held at the maximum value for more time unlike in the sine wave (Figure 4.20).

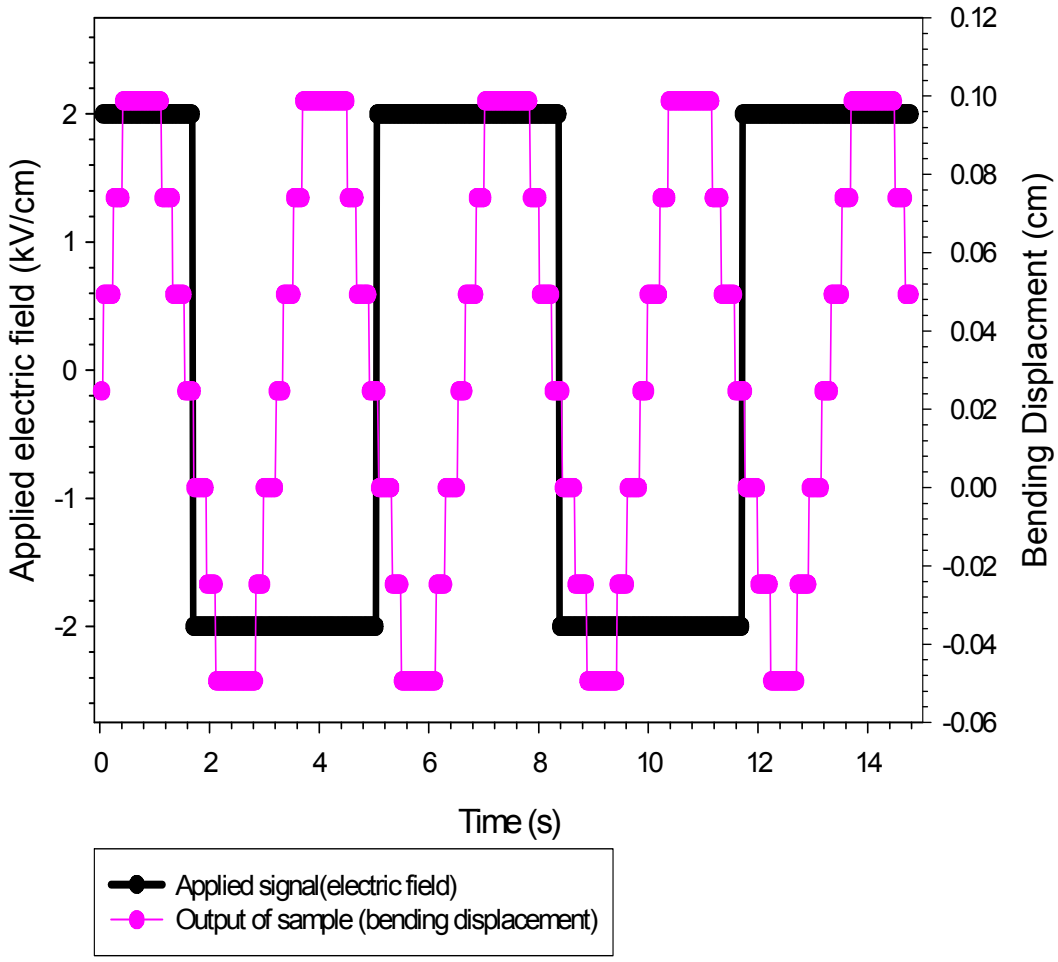

Figure 4.20: Polymer response upon applied alternating current field (square wave).

4.4.b Strain Induced Through The Thickness Of The Polymer

In order to analyze the thickness extensional electromechanical strain induced in the CN-PDMS samples, the samples are evaluated by painting the polymer with high purity silver paint on either sides and the experimental set-up seen in section 3.4 b is used. While performing this experiment, care is taken with respect to the side of the polymer which faces the fiber optic sensor of the Angstrom resolver. Each sample is tested for its air side and the non-air side to further confirm the settling of the dipoles when the CN-PDMS is processed.

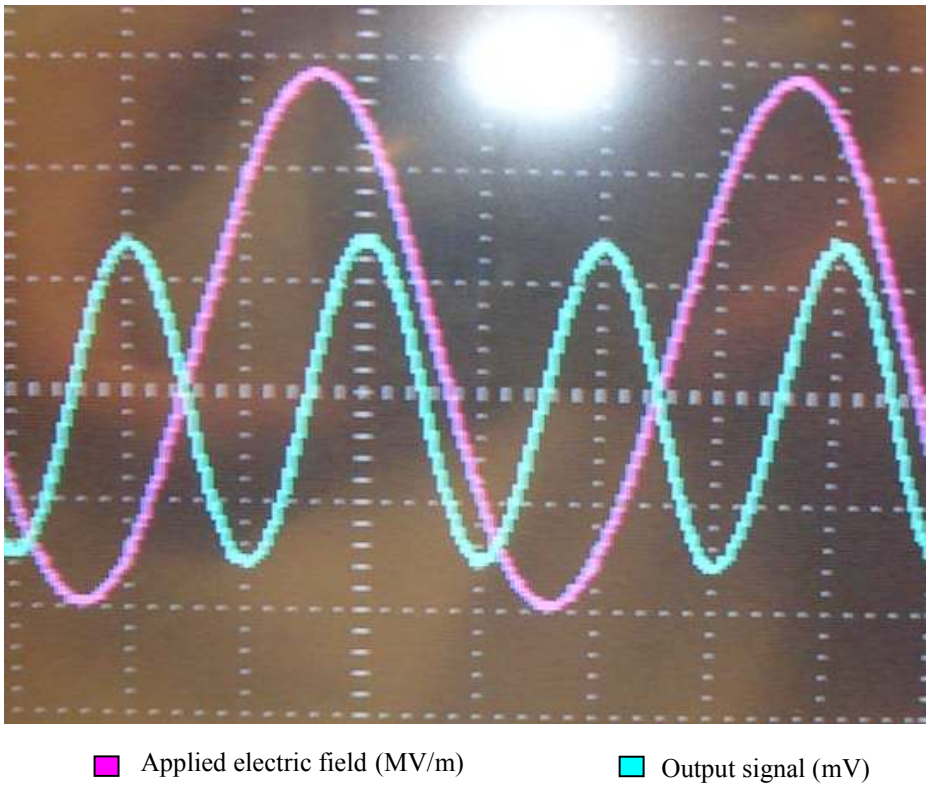

Figure 4.21: Snapshot of electromechanical strain induced through the thickness of the CN-PDMS sample.

Figure 4.21 is a snapshot of the output of the CN-PDMS sample when an alternating current electric field of known frequency is applied across the sample thickness. It is observed that the strain induced in the polymer has twice the frequency of the applied signal. Thus, showing a quadratic relationship with the electric field squared. This is further illustrated in Figure 4.22, which shows percent strain induced in 8.6 weight % CN-phenyl as a function of electric field squared. The strain induced in this polymer is related to electric field by the following equation

(R^2= 0.9779)

$$S = 0.2458E^2 \tag{4.3}$$

Where S is the percent strain developed in the polymer while E is the electric field in MV/m applied across the thickness of the polymer. The electrostrictive coefficient M is 0.2458 x 10^{-14} (m^2/V^2).

Similar trend is observed in all the CN-PDMS samples yielding the electrostrictive coefficient as displayed in Table 4. It is seen that as the weight % CN-phenyl content in the sample increases from 3.3 % to 8.6 %, the strain increases as seen by the increase in the electrostrictive coefficient M of the samples.

Table 4: Electrostrictive coefficients for the strain induced through the thickness of the CN-PDMS samples.

Weight percent CN-phenyl content (%)	Electrostrictictive Coefficient (m^2/ V^2)
8.6	25×10^{-16}
7.8	16.49×10^{-16}
6.1	13.77×10^{-16}
5.7	10.45×10^{-16}
3.3	6.68×10^{-16}
Control sample	0.2×10^{-16}

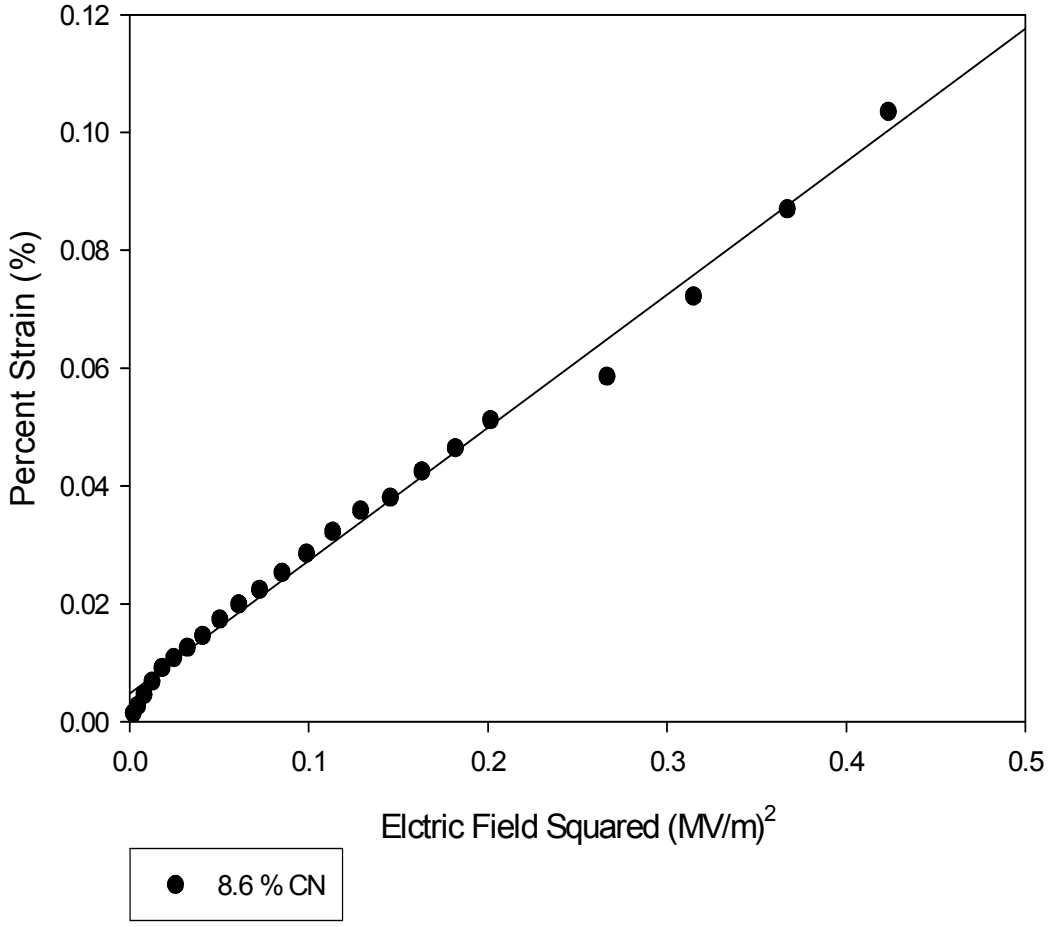

Figure 4.22: Electromechanical strain induced through the thickness of 8.6% CN-phenyl sample.

It is observed that once the fiber optic sensor is placed at the maximum position from the sample surface and the field is gradually increased, the distance between the sample and the fiber optic sensor tip tends to decrease. This implies increase in the thickness of the sample as field is increased. Increase in the thickness of the sample is due to the alignment of the dipoles along the direction of the electric field (Figure 4.23). In this figure, since one surface of the sample is held fixed to the holder using a double sided tape, the sample cannot show bending displacement as seen for the strain in length experiment. With the increase in electric field the dipoles start orienting with the electric field and the sample thickness increases (Figure 4.23 a and b).

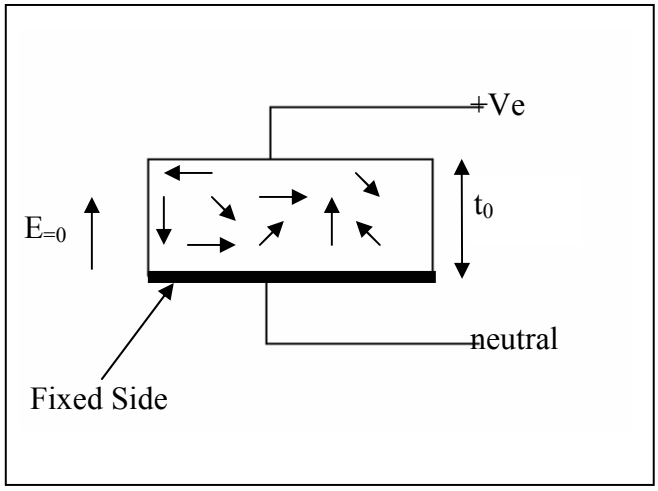

(a)

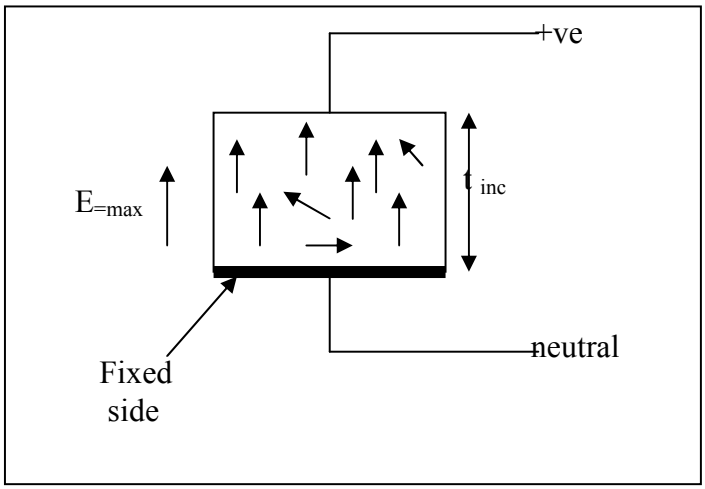

(b)

Figure 4.23: Electromechanical strain induced in CN-PDMS polymer through the thickness of the sample. (a) No electric field. (b) Application of electric field.

When the strain induced in CN-PDMS samples is plotted as a function of varying weight % CN-phenyl, it is observed that samples with higher dipolar content produce more strain than those with lesser dipole content, thus supporting the theory of electrostriction,

since the higher the dipolar content, the higher is the polarization and the strain induced in the polymer sample. (Figure. 4.24)

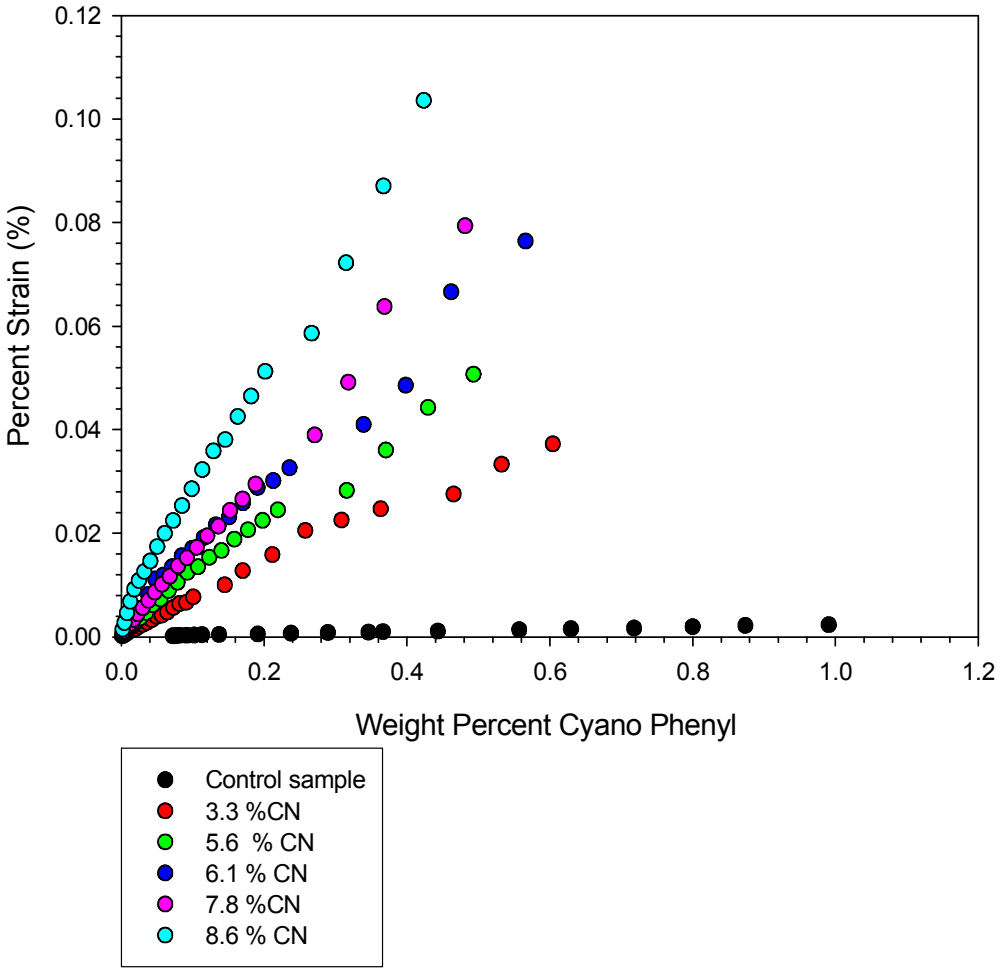

Figure 4.24: Comparative plot of percent strain induced in the sample as a function of varying CN-phenyl content.

Figure 4.24 shows that the control sample, which has no dipolar moieties present in it, shows some strain (0.0006%) developed in it. This is possibly related to the electrostatic

force acting on the polymer surface when placed under very high electric field. However when the strain in the control sample is compared with strain induced in other CN-phenyl samples, it is seen that the strain in control sample is extremely small and can thus be considered negligible. The % strain induced in the control sample is 0.0006% as compared to 0.035% in a 3.3 weight % CN-phenyl sample while 8.6 weight % CN-phenyl sample induces maximum % strain of 0.105.

Another important factor considered while performing this strain experiment is noting the side facing the fiber optic sensor. The non-air side of the CN-PDMS polymer is seen to be active in the length displacement. In order to confirm this, when non-airside is held fixed to the sample holder, less strain is induced as compared to when the non-airside is facing the fiber optic sensor. Table 5 shows that non-airside of the sample is more active as compared to the airside , also not all samples with their airside facing the sensor showed deformation thus yielding non-repetitive strain response, hence it is noted n/a in the table.

Table 5: Electrostrictive strain in CN-PDMS samples with side consideration.

Weight % CN-phenyl samples	**Electrostrictive coefficient Airside facing fiber optic sensor (m^2/V^2)**	**Electrostrictive coefficient Non-Airside facing fiber optic sensor (m^2/V^2)**
8.6	N/a	25×10^{-16}
7.8	10.2×10^{-16}	16.49×10^{-16}
6.1	N/a	13.77×10^{-16}
5.6	3.16×10^{-16}	10.45×10^{-16}
3.3	1.07×10^{-16}	6.68×10^{-16}
Control Sample	0.06×10^{-16}	0.2×10^{-16}

The repeatability of the strain induced through thickness is done by performing experiment on 3 samples having same CN-phenyl content as well as for same experimental conditions. Figure 4.25 presents the averaged values of the strain and their deviation from the standard value. Each value is the average value of strains obtained from 3 samples.

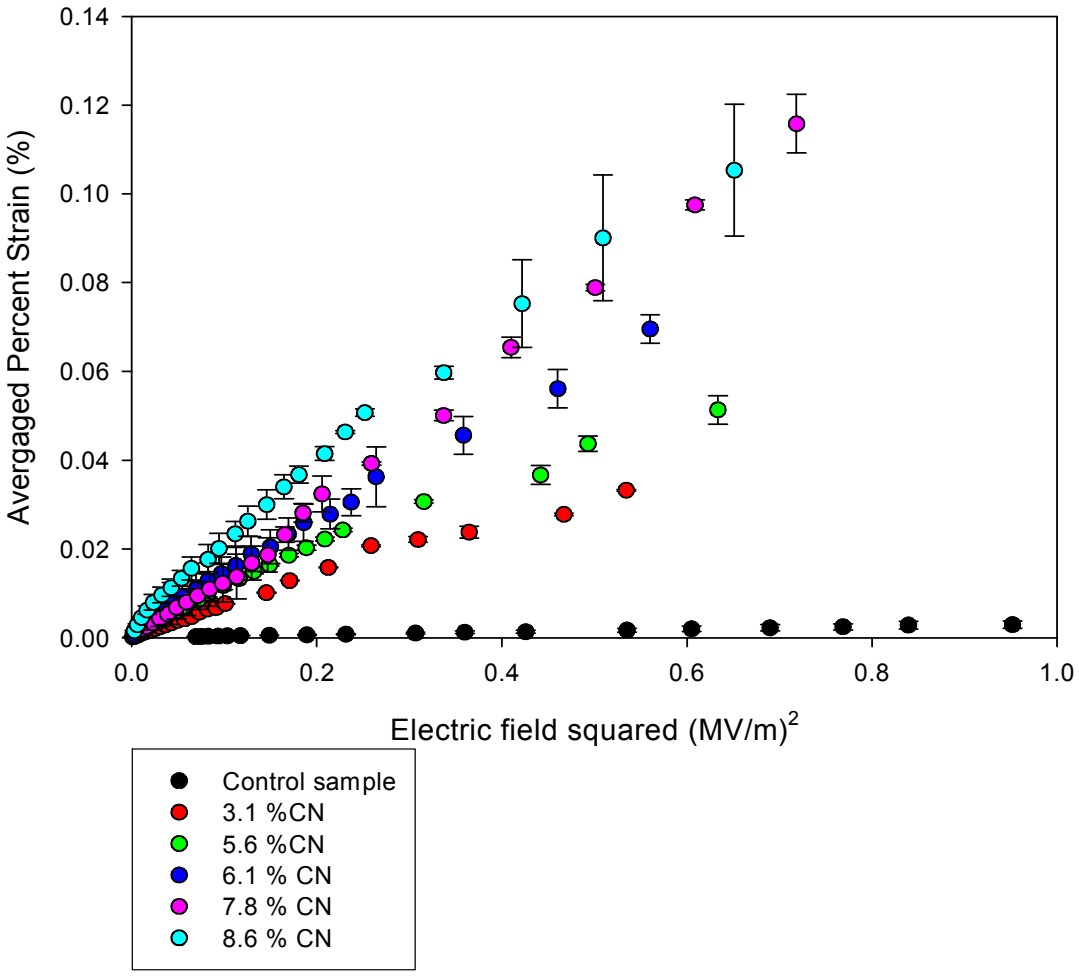

Figure 4.25: Averaged value of strain induced through the thickness of the samples and their standard deviation.

(The solid symbols are the data points while the vertical lines indicate the error bars.)

4.5 Load Current Analysis

The load current measurement is performed to obtain the current drawn by the CN-PDMS samples using the experimental set-up discussed in section 3.5.

Current for four values of input voltage are observed for a constant frequency. Figure 4.26 presents the load current exhibited by all the samples with cyano content varying from 3.3 to 8.6 weight % CN-phenyl. This experiment is performed on a control sample (0%) to compare the current drawn by each of the samples. It is observed from the experiment that as the dipolar concentration in the samples increases, the current taken up by the sample to actuate decreases. However for higher values of electric field such as 2 kV, the current drawn by the sample is fairly constant irrespective of the weight % concentration of the CN-phenyl in the PDMS.

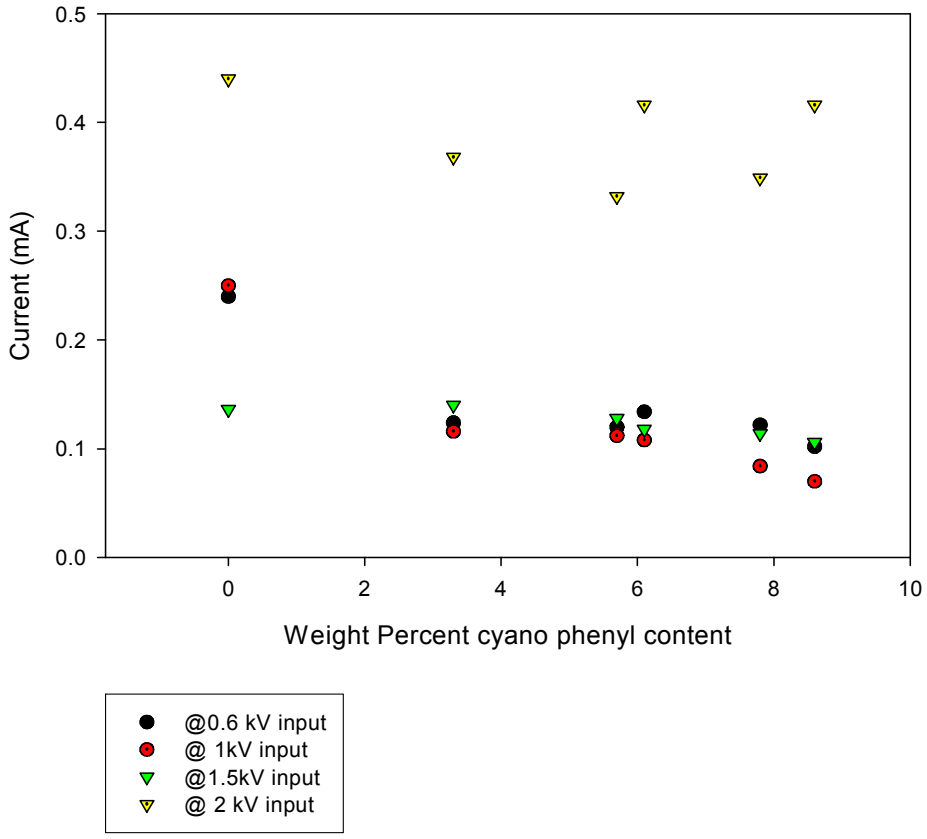

Figure 4.26: Current drawn by CN-PDMS samples for different applied voltage.

The CN-PDMS samples have very low capacitance thus draw extremely small amount of current in order to actuate. They act more like insulators and thus seem to be ideal candidates in applications such as prosthetic arms or nano-devices where current is a constraint. Unlike PZT where the load impedance is comprised of resistance and capacitance, in this study it is observed that CN-PDMS sample is more resistive and less capacitive.

4.6 Thermally Stimulated Current Analysis

Thermally stimulated current (TSDC) analysis is done on the CN-PDMS samples as a method to evaluate the charge storage and charge decay-related current in the samples. Four samples are analyzed using TSDC, each having different concentration of CN-phenyl from 3.3 % to 8.6 % and a control sample (0%) for comparison. Figure 4.27 shows the current spectra for the poled and the un-poled control sample. It is observed that around -48º C to -40 º C the charging current reduces sharply and then increases sharply. The temperature range where these peaks occur is the melting temperature of poly (dimethyl siloxane) and these peaks coincide with the peaks obtained in the dielectric spectroscopy done on the CN-PDMS samples. These peaks are observed for both the poled and the un-poled samples and may possibly be related to the melting of the crystalline phase of the polymer blend. However the magnitude of the charge current per unit area observed in the control sample is very low on the order of 0.9×10^{-9} A/m^2 when compared with other CN-PDMS samples having dipolar functionalities present in them.

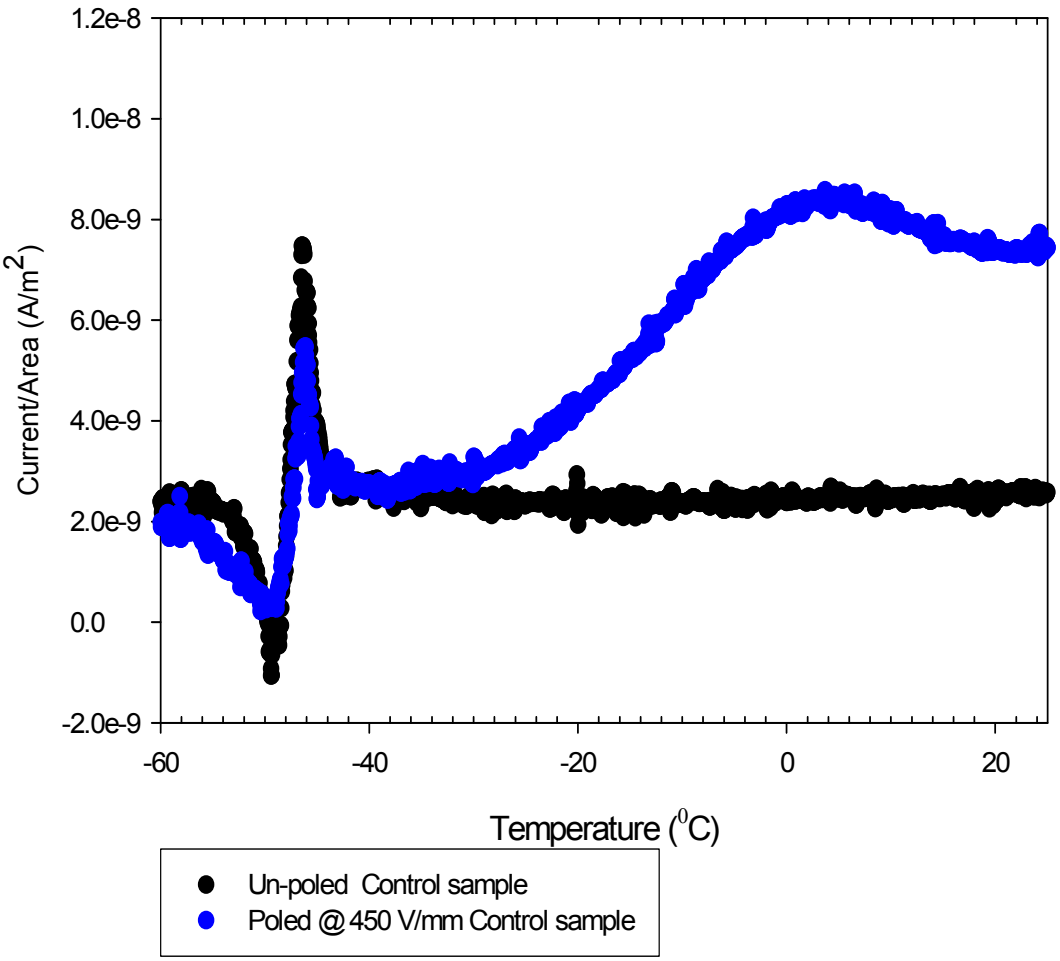

Figure 4.27: Charging current for poled and un-poled control sample.

When the TSDC is performed on a sample containing 3.3 weight % CN-phenyl, (Figure 4.28) the un poled sample does not show any peaks. After poling of the sample at E = 450V/mm, t_p = 5mins, the charging current shows a peak at –44 ° C; then as the temperature is further increased, the current rises steeply. The trend of the current with increase in the temperature can be possibly owing to the spontaneously generated current,

when there is a small difference between the contact potential of the two electrodes between which the sample is held[66]. Figure 4.29 is the charging current spectra for 8.6 % CN-phenyl. A peak is observed in the range of -50º C to -40º C.

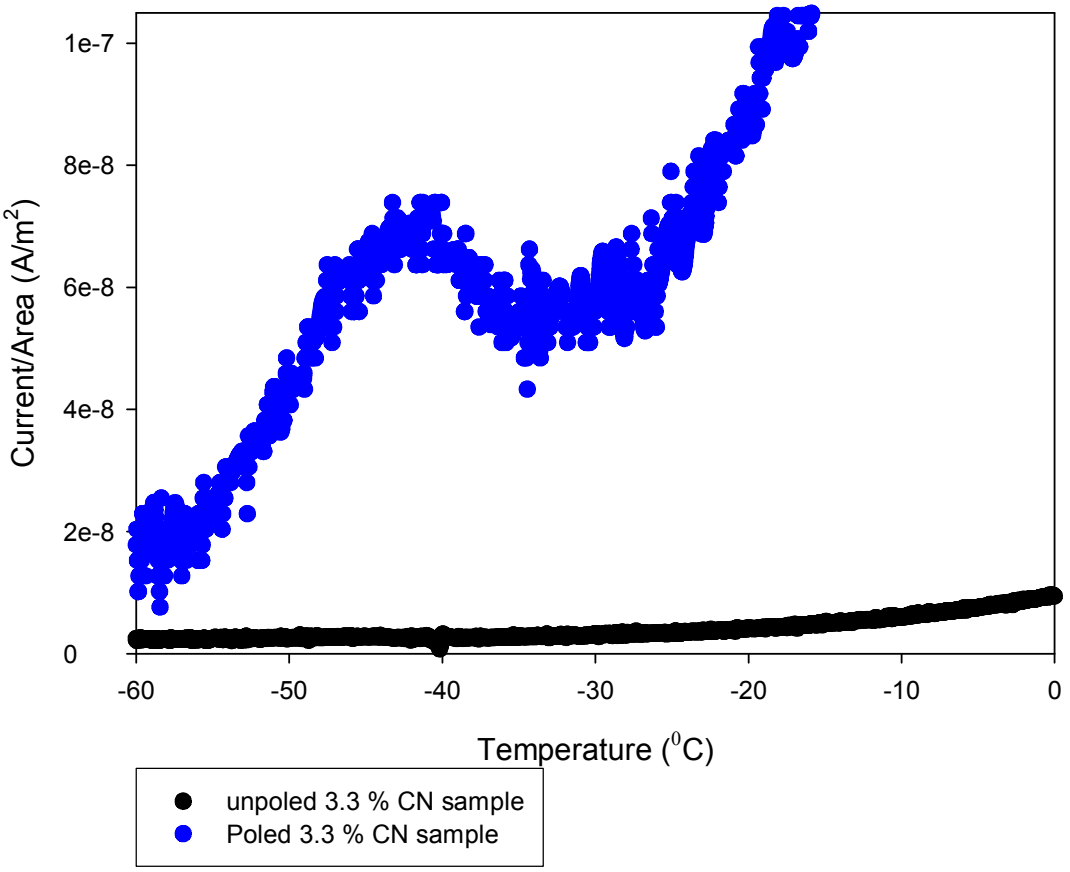

Figure 4.28: Charging current for poled and un-poled 3.3 % CN-phenyl containing sample.

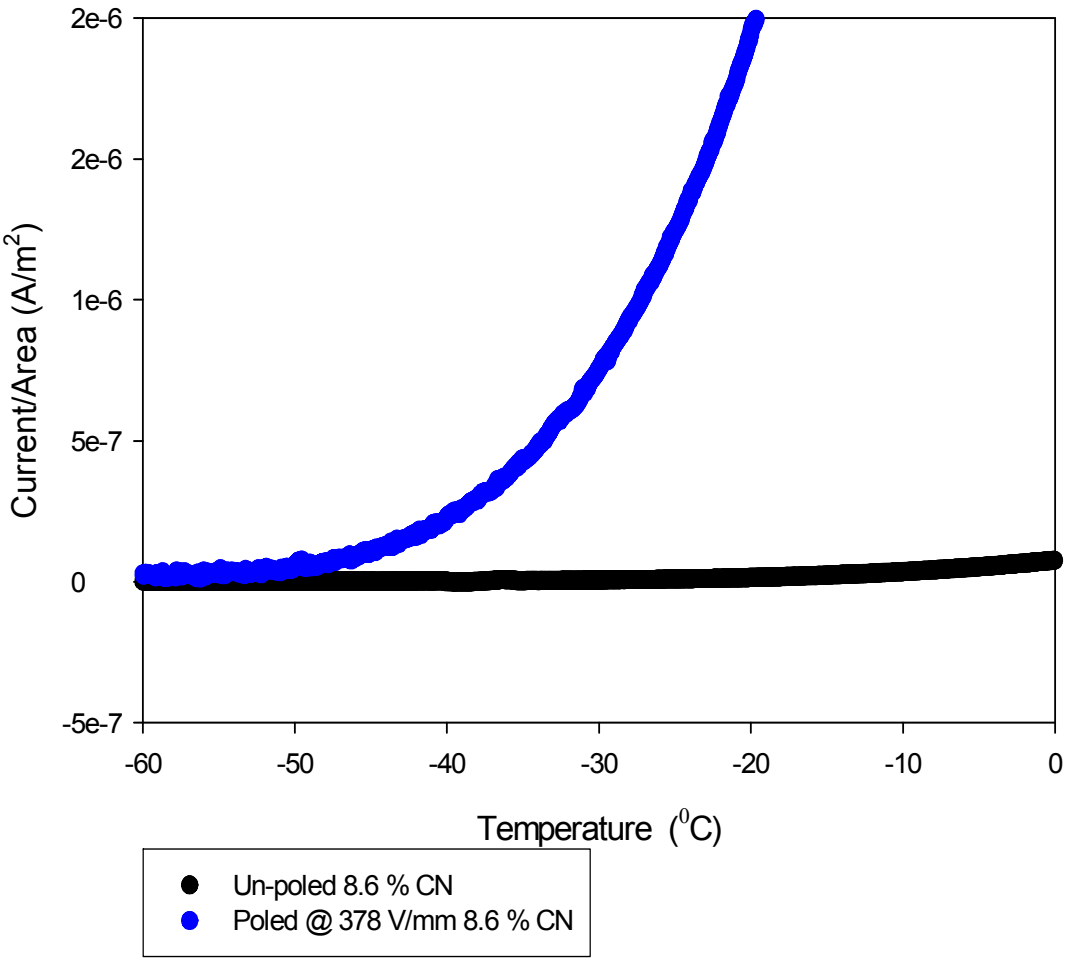

Figure 4.29: Charging current for poled and un-poled 8.6 % CN-phenyl containing sample.

Figure 4.30 compares the TSDC current spectra for samples with 0%, 3.3% and 8.6% CN-phenyl. It is seen that as the dipolar concentration increases, the activation energy increases in proportion. Thus samples with higher concentration of dipoles show

steeper current per unit area; also the charging current is seen for lower temperature.

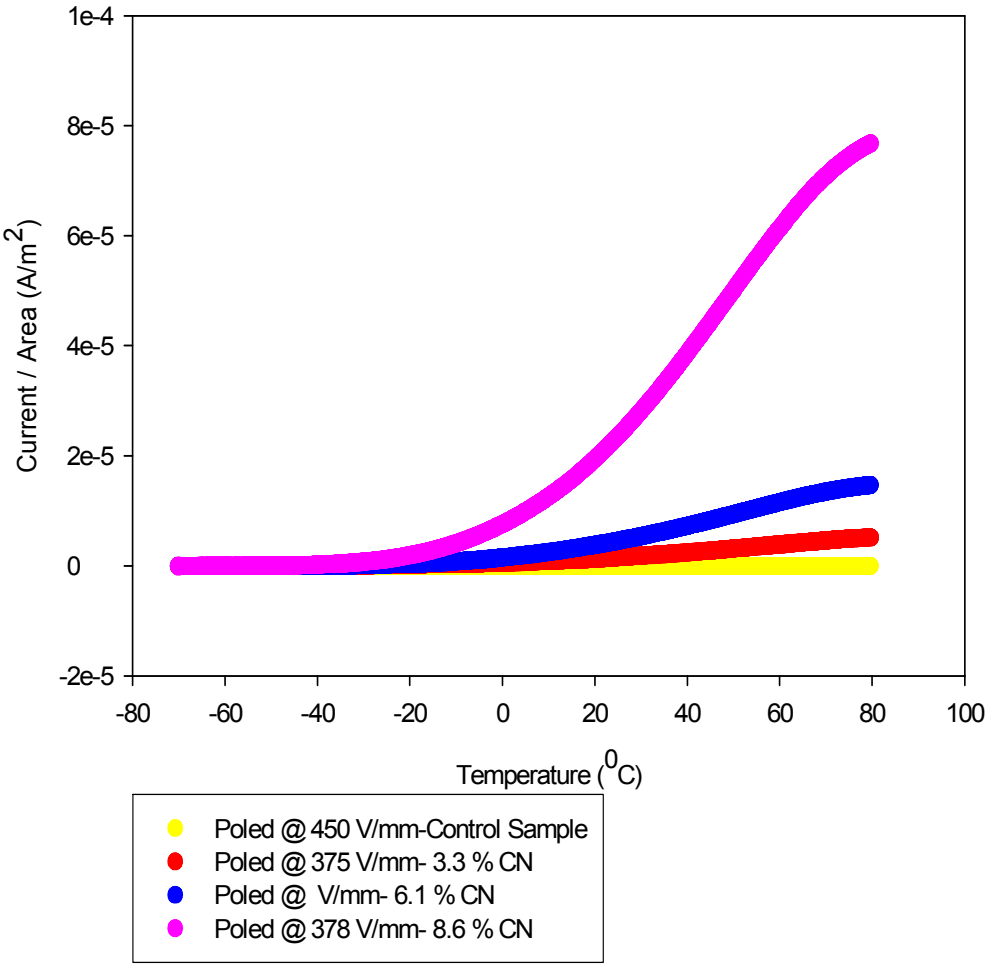

Figure 4.30: Comparative plot for the poled CN-PDMS samples.

CHAPTER 5 CONCLUSION

This study describes a method of taking advantage of a unique combination of properties offered by the hybridization of organic and inorganic components in a CN- PDMS system. A unique blend of PDMS cross-linked with dipolar cyano phenyl (CN) groups is presented. The main objective is to evaluate the physical behavior and the electromechanical performance of the resulting PDMS-based electrostrictive actuator. One of the key features is to relate variations at the molecular level to performance at the macroscale.

Poly (dimethyl siloxane) (PDMS) is chosen as the base polymer because it is a fairly transparent polymer having high elasticity and low stiffness. It is a polymer composed of an alternating backbone of silicon and oxygen atoms with two organic functionalities attached to each silicon atom. Owing to this unique molecular arrangement of PDMS, excellent physical properties of the CN-PDMS blend are expected, such as stability in harsh condition, wide temperature operability and resistance towards UV rays. Also PDMS allows cross-linking of several functional groups other than cyano phenyl, without compromising its base material properties.

Three different molecular weight (9.4 k, 17.2 k and 28 k) PDMS polymers are used to process the CN-PDMS blends. Evaluation of the physical properties of the CN-PDMS blend is done using Differential Scanning Calorimetery (DSC). The DSC results show that cross-linking of the functional moieties to PDMS does not detrimentally affect the PDMS

properties. This is seen from the melting temperature range obtained from the DSC results, where T_m remains in the range of –44 º C to –40 º C for all samples tested by DSC. Also, no other transitions are observed with addition of the polar CN-Phenyl moieties. Furthermore, the different molecular weights of PDMS used do not affect the characteristics of the CN-PDMS, confirming that molecular weight is not a variable that needs to be investigated further.

Using Dielectric Spectroscopy, the molecular motion of the CN-PDMS polymer is probed. Dielectric Spectroscopy establishes a point of reference on the performance of the polar component of the CN-PDMS blend, and possibly identifies the contributions towards the dielectric constant value of the material. It is observed that in the range of 20 Hz to 1 MHz, the control sample shows a fairly constant dielectric value from 4.6 to 4.0. It is also found that, as the weight percent dipolar content (% CN-Phenyl) in the polymer blend increases, the dielectric value at lower frequencies increases. The increase of dielectric constant with % CN-Phenyl illustrates the contribution of dipolar orientation at lower frequencies. The maximum dielectric constant is obtained for the sample containing maximum polar functionalities, where 8.6 weight % CN-Phenyl has a dielectric constant value of 9.12 as compared to 4.0 for 0 weight % CN-Phenyl.

Next, the electromechanical strain is evaluated for the various CN-PDMS blends. This is done by measuring electromechanical strain in two configurations; the strain induced along the length of the polymer and strain induced through the thickness of the polymer. In both strain analysis techniques, it is observed that the non-airside of the polymer blend is more active than the airside; meaning that a higher strain is observed on

the non-airside versus the airside. The possible cause for this difference is related to the processing method used for making the CN-PDMS blend. Since the CN-PDMS films are obtained by solution casting, a concentration gradient might cause the dipolar elements to settle at the bottom of the cast film, thus on curing giving a more active non-airside. In the strain yielded along the polymer length, it is observed that the strain obtained in the polymer is proportional to the square of the electric field (E^2), indicating an electrostrictive mechanism. Also the strain induced along the length of the polymer is governed by the dipolar concentration in the polymer. Higher strains are obtained as weight % CN-Phenyl is increased. A maximum strain of 1.74 % is yielded along the length for the 8.6 weight % CN-Phenyl. It is further found that higher weight % CN-Phenyl containing films undergo deformation at lower applied electric field (A 3.1 weight % CN-Phenyl sample shows displacement at 0.15 MV/m, whereas the 8.6 weight % CN-Phenyl displaces at 0.075 MV/m). Moreover, deformation occurs quicker on application of field for the higher weight % CN-Phenyl as compared to lower CN-Phenyl containing samples. Thus it can be concluded that increasing the dipolar concentration enhances both the strain value and the response time of the CN-PDMS sample, where a higher strain rate is yielded in higher CN-Phenyl containing samples (Strain rate of 8.6 weight % CN-Phenyl is 0.0006 m/m/s as compared to 3.1 weight % CN-Phenyl is 0.0003 m/m/s). These CN-PDMS samples show a memory effect as well. Higher values of strain are obtained for the same CN-PDMS sample on consecutive application of increasing electric field, thus showing the ability of the CN-PDMS polymer to remember the history from the previous field application.

For the alternating current analysis, it is observed that when a square wave is applied as the input, the output strain has double the frequency of the input, further supporting the theory of electrostriction. In the case of a sine wave, the frequency of the output strain is also twice that of the input. However the magnitude of the second cycle of the output is less than that of the first cycle, and this is because the sample displacement is gradual with application of field. The sample displaces a certain distance and retracts back, however it does not retract back the same distance. This behavior of the sample displacement is due to the nature of the input signal, which gradually translates from positive through zero to negative and thus yielding smaller amplitude for the consecutive cycle. This behavior of the displacement is possibly related to the orientation of the dipoles under the electric field. When the electric field value gradually becomes zero, the oriented dipoles do not loose their orientation immediately, moreover the dipoles retain some mobility, and thus not all dipoles retract completely. This is evident from the larger cycle followed by a smaller cycle (Figure 4.18). But in the case of square wave it is seen that input signal alternates between a positive value and a negative value with zero dc bias. Thus in this case the output follows the input as a function of E^2, but owing to just two transient values of the input signal the amplitude of each cycle of the output is the same. In the thickness configuration, the electrostrictive nature of the CN-PDMS blend is further supported. It is seen that the strain induced through the thickness of the polymer blend is governed by the dipoles present in the CN-PDMS blend. The orientation of the dipoles along the direction of the field results in an increase in the thickness of the CN-PDMS samples. Also, the strain yielded has quadratic relationship with the electric field. The

electrostrictive coefficients obtained for the CN-PDMS samples are seen to be proportional to the concentration of the CN in the blend (The electrostrictive coefficient obtained for 8.6 weight % CN-Phenyl sample is maximum and is 4090 x 10^{-16} m^2/V^2 while 3.1 weight % CN-Phenyl sample has a coefficient of 1759 x 10^{-16} m^2/V^2).

The load current measurements show that for lower values of electric field, samples with lower dipolar concentration show more current than the higher CN containing samples. When the input is increased to 2 kV, the current drawn by all the samples is fairly similar. However it is seen that the current drawn by the CN-PDMS samples for actuation is less in comparison to other electroactive materials such as CNT actuators and piezoelectric-ceramics, thus showing the smaller capacitive nature of the CN-PDMS blend.

The Thermally Stimulated Current (TSC) measurements show that the magnitude of the polarization current increases with increase in the dipolar concentration of the CN-PDMS blend. TSC for each case shows minor peaks in the current for a temperature range of -48º C to -40 º C, which can be related to the melting temperature of PDMS; this is then followed by a rise in the current, possibly related to dipolar relaxation.

A variety of electromechanical characterization techniques such as Differential Scanning Calorimetry, Dielectric Spectroscopy, Electromechanical strain analysis and Thermally Stimulated Current measurements indicate that the mechanism governing the induced strain in the CN-PDMS polymer is dipole-driven. The quadratic nature of the strain observed in both the length and thickness directions further supports the theory of electrostriction. Thus it can be concluded that the electrostrictive effect governs the mechanism in the CN-PDMS blends. It is observed in the electromechanical strain analysis

that in both length as well as thickness configuration, the CN-PDMS undergoes deformation. In case of the length configuration, the CN-PDMS polymer behaves analogous to a unimorph. The applied field is perpendicular to the length of the polymer; the dipoles within the sample begin to align along the direction of the field. This results into expansion in the thickness of the active side of the polymer sample, in order to maintain a constant volume, the length of the active side contracts. This contraction in length of the active side is constrained by the non-active side of the polymer. Thus translating the thickness expansion into bending deformation. This is evident from the bending deformation of the CN-PDMS sample under applied voltage, wherein bending is observed only on the non-airside of the polymer, which is the active side. The strain induced through thickness further confirms the expansion in the thickness of the active side. All the experimental techniques presented in the work show successful modification of the chemistry of poly (dimethyl siloxane) PDMS by cross-linking of the sample with polar cyano phenyl dipole (CN), yielding an electrostrictive polymer.

Future work will focus on: 1) evaluating the mechanical properties of the CN-PDMS blend; 2) analyzing the load current measurements in order to analyze the energy density of the CN-PDMS blend as an actuator; 3) developing more suitable electrodes. The electrodes used in this work are either non-contact metal electrodes or silver painted electrodes. These electrodes are not very compliant and thus might have resulted into constraining the displacement; and 4) characterizing PDMS cross-linked with other functional group such as fluoro or nitro, or clay inclusions, in order to further evaluate the nature of induced strain in the resulting polymer blend.

Literature Cited

(1) R.Lane, B.Craig. Materials that sense and response: An Introduction to Smart Materials. *The Amptiac Quaterly* 2003;7(2):9-14.

(2) M.Watanabe, T.Kato, M.Suzuki, Y.Hirako, H.Shirai, T.Hirai. Control of bending electrostriction in polyurethane films by doping with salt. *Journal Of Polymer Science* 2001;39:1061-1069.

(3) C.Melhuish, A.Adamatzky. Biologically Inspired Robots. 2001 16-27.

(4) M.Broadhurst, G.Davis. Piezo and Pyroelectric Properties. Topics in Mechanical Physics: Electrets. 1980:285-319.

(5) *www piezo com* 2005;Available at: URL: www.piezo.com.

(6) E.Fukada. History And Recent Progress in Piezoelectric Polymers. *IEEE transactions on ultrasonics, ferroelectrics and frequency control* 2000;47:1277-1289.

(7) D.Hanson, G.Pioggia, Y.Bar-Cohen, D.De Rossi. Android:application of EAP as artificial muscle in the entertainment industry. 2001 350-356.

(8) W.Zhou, W.Li, J.Mai. MEMS-fabricated ICPF microactuators for biological manipulation. 2003 337.

(9) T.Xu, J.Su, Q.Zhang. Electroactive-polymer-based MEMS for aerospace and medical applications. 2003 66-77.

(10) G.Atkinson, R.Pearson, Z.Ounaies, J.Harrison, C.Park, S.Dong, J.Midkiff. **Novel** Piezoelectric Polyimide MEMS. 2003.

(11) E.Smella. Conjugated polymer actuators for Biomedical Applications. *Advanced Materials* 2003;15:481-494.

(12) K.Newbury. Characterization, Modeling and Control of Ionic Polymer Transducers 2002.

(13) Y.Bar Cohen. Bionic humans using EAP as artificial muscles reality and challenges. *International Journal of Advanced Robotic Systems* 2004;1.

(14) S.Nasser, C.Thomas. Ionic polymer-metal composites. 2001 139-191.

(15) K.Newbury, D.Leo. Electromechanical modeling and Characterization of Ionic Polymer Benders. *Journal of Intelligent Material Systems and Structures* 2002;13:51-60.

(16) S.Nasser, Y.Wu. Tailoring actuation of ionic polymer-metal composite through cation combination. 2005.

(17) Y.Bar Cohen, S.Sherrit, S.Lih. Characterization of electromechanical properties of EAP materials. 2001 4329-4343.

(18) K.Mavallarappu. Feedback control of Ionic Polymer Actuators Virginia Polytechnic Institute and State University, VA.; 2001.

(19) J.Shaw. Polymers for electronic and photonic applications: Overview of polymers for electronic and photonic applications. 1993:1-59.

(20) J.Madden, P.Madden, I.Hunter. Conducting polymer actuators as engineering materials. 2002 176-190.

(21) R.Baughman. Conducting polymer artificial muscles. *Synthetic Muscles* 1996;78:339-353.

(22) K.Kaneto, M.Kaneko, Y.Minand, A.MacDiarmid. Artificial muscle: Electrochemical actuators using polyaniline films synthetic metals. *Synthetic Metals* 1998;71(2211):2212.

(23) R.Baughman, C.Cui, A.Zakhidov, Z.Iqbal, J.Barisci, G.Spinks, G.Wallace, A.Mazzoldi, D.De Rossi, A.Rinzler, O.Jaschinski, S.Roth, M.Kertesz. Carbon nanotube actuator 1999.

(24) Z.Ounaies. Advance Smart Materials. 2003. Ref Type: Data File

(25) S.Banda. Characterization of aligned Carbon nanotube/Polymer composite Virginia Commonwealth University; 2004.

(26) J.Madden, N.Vandesteeg, P.Anquetil, P.Madden, A.Takshi, R.Pytel, S.Lafontaine, P.Wieringa, I.Hunter. Artificial Muscle Technology: Physical Principles and Naval Prospects. *IEEE Journal of Oceanic Engineering* 2004;29:706-727.

(27) J.Barisci, G.Spinks, G.Wallace, J.Madeen, R.Baughman. Increased actuation rate of electromechanical carbon nanotube actuators using potential pulses with resistance control. 2003 549-555.

(28) J.Su, Q.Zhang, C.Kim, R.Ting, R.Capps. Effect of transitional phenomena on the electric field induced strain-electrostrictive response of a segmented polyurethane elastomer. *Journal of Applied Polymer Science* 1997;65:1363-1370.

(29) R.Pelrine, R.Kornbluh, G.Koffod. High strain actuator materials based on dielectric elastomers. *UNKNOWN* 2005.

(30) C.Ku, R.Liepins. Dielectric constant of polymers. Electrical Properties of Polymers: Chemical Principles. Hanser, 1989:21-56.

(31) G.Koffod. Dieletric Elastomer Actuators The Technical University of Denmark.; 2001.

(32) M.Zhenyl, J.Scheinbeim, J.Lee, B.Newman. High field electrostrictive response of polymers. *Journal Of Polymer Science Part B: Polymer Physics* 1994;32:2721-2731.

(33) R.Pelrine, R.Kornbluh, J.Joseph, R.Heydt, Q.Pei, S.Chiba. High field deformation of elastomeric dielectrics for actuators. *Material Science and Engineering* 2000;11:89-100.

(34) D.Hanson, V.White. Converging the capabilities of EAP artificial muscles and the requirements of Bio-Inspired Robotics. 2004 29-40.

(35) H.Kawai. The piezoelectricity of poly(vinylidene fluoride). *Japanese Journal of Applied Physics* 1969;8(975):976.

(36) A Lovinger. Ferroelectric Polymers. *Science* 1983;220(4602):1115-1121.

(37) G.Sessler. Piezoelectricity in polyvinylidenefluoride. *Journal of Acoustic Soc Am* 1981;70(6):1596-1608.

(38) G.T Davis. Piezoelectric and Pyroelectric Polymers. In: C.Wong, ed. Polymers for Electronic and Photonic Applications. Academic Press, 1993:435.

(39) J.Harrison, Z.Ounaies. Piezoelectric Polymers. 2002.

(40) Z.Cheng, V.Bharti, T.Xu, H.Xu, T.Mai, Q.Zhang. Electrostrictive poly (vinylidene fluoride trifluoroethylene) copolymer. *Sensors And Actuators Part A: Physics* 2005;90:138-147.

(41) Y.Shkel, J.Klingenberg. Electrostriction of polarizable materials: Comparision of models with experimental data. *Journal of Applied Physics* 1998;83:415-424.

(42) M.Watanabe, M.Yokoyama, T.Ueda, T.Kasazaki, M.Hirai, T.Hirai. Bending deformation of Monolayer Polyurethane film induced by an electric field. *Chemistry Letters* 1997;773-774.

(43) M.Watanabe, N.Wakimoto, H.Shirai, T.Hirai. Bending electrostriction and space charge distribution in polyurethane films. *Journal of Applied Physics* 2003;94:2494-2497.

(44) T.Ueda, T.Kasazaki, N.Kunitake, T.Hirai, J.Kyokane, K.Yoshino. Polyurethane elastomer actuator. *Synthetic Metals* 1997;85:1415-1416.

(45) R.Newnham, V.Sundar, R.Yimnirum, J.Su, Q.M.Zhang. Electrostriction in dielectric material. *Advances in Dielectric Ceramic materials* 2005;15-39.

(46) T.Hirai, H.Sadatoh, T.Ueda, T.Kasazaki, Y.Kurita, M.Hirai, S.Hayashi. Polyurethane elastomer actuator. *Die Angewandte Makromolekulare Chemie* 1996;240:221-229.

(47) Q.Zhang, J.Su, C.Kim. An experimental investigation of electro-mechanical responses in polyurethane elastomer. *Journal of Applied Physics* 1997;81:2770-2777.

(48) R.Pelrine, R.Kornbluh, J.Joseph. Electrostriction of polymer dielectrics with compliant electrodes as a means of actuation. *Sensors And Actuators* 1998;64:75-85.

(49) V.Bharti, X.Zhao, Q.Zhang, R.Romotowski, F.Tito, R.Ting. Ultrahigh field induced strain and polarization response in electron irradiated poly (vinylidene fluoride-trifluoroethylene) copolymer. *Material Research Innovation 2* 1998;(57):63.

(50) J.Li, N.Rao. Micromechanics of ferroelectric polymer-based electrostrictive composites. *Journal of the Mechanics and Physics of Solids* 2005;52:591-615.

(51) D.Damjovic. Ferroelectric, dielectric and piezoelectric properties of ferroelectric thin films and ceramics. 1998 Feb 10.

(52) W. Ren, G.Yang, B.Mukherjee, J. Szabo An interferometric measurement of the transverse Strain response of electroactive polymers. 2004 395-405.

(53) C.Andrieux, M.Farriol, I.Gallardo, J.Marquet. *Journal of Chemical Society* 2002;985-990.

(54) W.Lasek, M.Makosza. *[1H-NMR (CDCl3) δ (ppm)] 7 57 (Ar-H, d , 2H),6 95 (Ar-H, d, 2H), 6 02 (-CH2CH=CH2, m, 1H), 5 37 ((-CH2CH=CH2, dd, 2H), 4 59 (-OCH2CH=CH2, d, 2H)]* 1993;780-782.

(55) *www tainst com* 2005.

(56) *www psrc usm edu/macrog/dsc htm* 2005.

(57) H.Frohlich. Theory of Dielectrics. 2nd ed. Oxford Press, 1958

(58) J.Maxwell. A treatise on electricity and magnetism. Dover Publications, 1954

(59) W.Kingery, H.Bowen, D.Uhlmann. Introduction to ceramics. John Wiley & sons, 1976

(60) Q.Pei, O.Inganas. Electrochemical applications of the bending beam polypyrroles during Redox. *Journal of Physical Chemistry* 2005;9.

(61) W.Takashima, M.Kaucho, K.Kaneto, A.MacDiarmid. The electrochemical actuator using electrochemically-deposited poly-aniline film. *Synthetic Metals* 1995;71:2265-2266.

(62) T.Jordan, Z.Ounaies, J.Tripp, P.Tcheng. Electrical Properties and Power Considerations of a Piezoelectric Actuator. 2002 Feb. Report No.: A806473.

(63) *www thermal-analysis setaram com* 2005.

(64) M.Soutzidou, A.Panas, K.Viras. Differntial Scanning Calorimetery (DSC) and Raman Spectroscopy Study of Poly (dimethyl siloxane). *Journal of Polymer Science: Part B* 1998;36:2805-2810.

(65) M.Suzuki, Y.Hirako, H.Shirai, T.Hirai, M.Watanabe. Hysteresis in Bending Electrostriction of Polyurethane Films. *Journal of Applied Polymer Science* 2001;79:1121-1126.

(66) J.van Turnhout. Thermally Stimulated Discharge of Electrets. Topics in Applied Physics:Electrets. 1980.

VITA

Wrutu Parulkar was born on 30th March 1980 in Mumbai, India to Disha and Deepak Parulkar. In 1998 Wrutu completed high school from Sathaye College of Science and Arts, India. Wrutu graduated with Bachelor's of Engineering in Instrumentation & Controls field from Cummins College of Engineering for Women, Pune, India in 2002. Following her graduation she joined Johns Controls India as a Trainee Engineer, where she gained a brief industrial experience in Automation and Controls. In 2003 she was accepted in the Mechanical Engineering department at the Virginia commonwealth University, USA. She completed her Master's of Engineering at Virginia Commonwealth University, under the guidance of Dr. Zoubeida Ounaies.